Analysis of particulate matter and volatile organic compound emissions from 3D printing activity

Shirin Khaki MSc

Thesis Submitted for the MSc Degree

Supervisors:

Dr. Aoife Morrin, Dublin City University

Prof. Alan F. Smeaton, Dublin City University

School of Chemical Sciences

April 2022

School of Chemical Sciences

Declaration

I hereby certify that this material, which I now submit for assessment on the program of study leading to the award of MSc is entirely my own work, and that I have exercised reasonable care to ensure that the work is original, and does not to the best of my knowledge breach any law of copyright, and has not been taken from the work of others save and to the extent that such work has been cited and acknowledged within the text of my work.

Signed: Shirin Khaki 

ID NO: 19215664

Date: 28/04/2022

Table of Contents

List of Abbreviations v

LIST OF FIGURES VII

List of Tables x

List of Publications and Presentations xi

Acknowledgements xii

Abstract xiii

CHAPTER 1: 1

INDOOR AIR QUALITY IN DWELLINGS: A REVIEW ON STANDARDS, SOURCES, AND MONITORING TECHNOLOGIES IN THE LIGHT OF COVID-19 1

1.1 Introduction 2
1.1.1 Indoor air pollutants 3
1.1.1.2 Volatile organic compounds 3
1.1.1.3 Inorganic pollutants 5

1.2 Indoor air quality policy 6
1.2.2 Policies on air tightness and low-energy buildings 9

1.3 Indoor air pollution sources in the domestic setting 12
1.3.1 Traditional sources 13
1.3.2 Emerging sources on account of Covid-19 18
1.4.1 VOC sampling in indoor air 20
1.4.1.1 ISO guidelines for IAQ sampling 21
1.4.1.2 Passive sampling 22
1.4.2 VOC instrumental analysis 26
1.4.2.1 Liquid chromatography (LC) analysis of IAQ 26
1.4.2.2 Gas chromatography (GC) analysis of IAQ 29
1.4.2.3 Real-time instrumental analysis of IAQ 34
1.4.3 Sensing technologies for indoor air quality monitoring 35
1.4.4 PM sensing technologies for IAQ monitoring 41
1.4.4.1 PM mass (Pmass) 42
1.4.4.2 Particle number (Pnum) 43
1.4.4.3 Particle size distribution (Psd) 44
1.4.5 PM sensors for IAQ monitoring 47

1.5 Conclusions 49

CHAPTER 2: 51

MONITORING OF PARTICULATE MATTER EMISSIONS FROM 3D PRINTING ACTIVITY IN THE HOME SETTING 51

2.1. Introduction 52

2.2 Materials and methods 54

2.2.1 3D Printing domestic setting 54
2.2.2 3D Printing procedure 55

2.3 Particulate Matter Emission Monitoring 56
2.3.1 Results and discussion 58
2.3.1.1 PM emission profiles using recommended print settings 58
2.3.2 Impact of filament on PM emissions 60
2.3.2.1 Filament color 60
2.3.2.2 Filament brand 63
2.3.3 Impact of user-controlled print settings on PM emissions 64
2.3.3.1 Fan speed 64
2.3.3.2 Infill density 66
2.3.3.3 Extruder temperature 67

2.4 Assessing the usefulness of low-cost IAQ sensors for PM emission monitoringduring home 3D printing 69

2.5 Conclusions 71

CHAPTER 3: 73

MONITORING OF VOLATILE ORGANIC COMPOUNDS EMISSIONS FROM 3D PRINTING FILAMENTS 73

3.1 Introduction 74

3.2 Material and methods 77
3.2.1 3D printer and print chamber enclosure 77
3.2.2 Filament and printing object 78
3.2.3 Sampling procedure 79
3.2.4 GC-MS analysis 80
3.2.5 Data analysis 80
3.2.5.1 Chemometric analysis 81

3.3 Results & discussion 83
3.3.1 Method development 83
3.3.2 Colour studies 86
3.3.3 Brand studies 94
3.3.4 Temperature studies 102

3.4 Conclusions 106

CHAPTER 4: FUTURE PERSPECTIVES 109

References 112

Supplementary Information 158

List of Abbreviations

ABS	Acrylonitrile butadiene styrene
APS	Aerodynamic particle sizer
BDE	Bromo diphenyl ether
BTEX	Benzene, toluene, ethylbenzene, and xylene
CAR	Carboxen
CPC	Condensation particle counters
CSA	Colourimetric sensor arrays
CW	Carbowax
DI	Direct immersion
DNPH	Dinitrophenylhydrazine
DSA	Deposited surface area
DVB	Divinylbenzene
EBC	Energy in buildings and communities
EC	European Commission
E-nose	Electronic nose
EU	European Union
FDA	Food and drug administration
FDM	Fused deposition modeling
FID	Flame ionization technique
FMPS	Fast mobility particle sizer
FRs	Flame retardants
GC	Gas chromatography
HIPS	High-impact polystyrene
HS	Headspace
HPLC	High-performance liquid chromatography
HVAC	Heating ventilation and air conditioning
IAQ	Indoor air quality
IEA	International energy agency
ISO	International Organization for Standardization
IoT	Internet of Things
MS	Mass Spectrometry
NSAM	Nanoparticle surface area monitor
OP	Optical particle sensor

PA	Polyacrylate
PBB	Polybrominated biphenyl
PBDE	Polybrominated diphenyl ethers
PCA	Principal component analysis
PDA	Photodiode arrays
PDMS	Polydimethylsiloxane
PEG	Poly (ethylene glycol)
PEA	Polyester aluminium
Pmas	Particle mass
Pnum	Particle number
PSD	Particle size distribution
PTR	Proton transfer reaction
PVC	Poly(vinyl chloride)
PUF	Poly(urethane) foam
PM	Particulate matter
PLA	Poly(lactic acid)
QMB	Quartz crystal microbalance
RI	Retention index
ROHS	Restriction of hazardous substance
RP-HPLC	Reversed-phase high-pressure LC
RSD	Relative standard deviation
RT	Retention times
SPME	Solid-phase microextraction
SMPS	Scanning mobility particle sizer
SVOC	Semi-volatile organic compound
SMO	Semiconducting metal oxide
TD	Thermal desorption
TCD	Thermal conductivity detection
TIC	Total ion chromatogram
TOF	Time of flight
TVOC	Total volatile organic compounds
UFP	Ultra-fine particle
VOC	Volatile organic compound
VVOC	Very volatile organic compound
EPA	Environmental Protection Agency
WHO	World Health Organisation

List of Figures

Figure 2-1- PM0.3 profiles over time before, during, and after printing of a cube (20 × 20 × 20 mm) for (a) ABSB1b (bedplate-temperature: 80 °C; extruder temp: 245 °C, 0% fan, 20% infill) and (**b**) PLAB1b (bedplate temperature: 50 °C; extruder temp: 205 °C, 20% fan, 20% infill). 59

Figure 2-2-PM0.3 emission of a cube in different colors for (a) ABSB5 (bedplate temperature: 80 °C, extruder temp: 245 °C, 0% fan, 20% infill) and (b) PLAB8 (bedplate temperature: 50 °C, extruder temp: 205 °C, 20% fan, 20% infill).· 61

Figure 2-3- PM0.3 profiles for different brands for before, during, and after the printing of a cube for (a) ABSB1b, ABSB2b, ABSB3b, ABSB4b, ABSB5b (bedplate temp: 80 °C, extruder temp: 245 °C, 0% fan, 20% infill) and (b) PLAB1b, PLAB2b, PLAB3b, PLAB6b, PLAB7b, and PLAB8b) 64

Figure 2-4- PM0.3 profiles for different Fan densities over time for: (a)before, during, and after the printing of the test cube using PLAB8b (bedplate temp: 50 °C, extruder temp: 205 °C, 20% infill), (b) OTPM (left axis, scatterplot), and PMMAX emissions (right axis, scatter plot) 66

Figure 2-5- PM0.3 profiles for different infill densities over time (a) before, during, and after the printing of the test cube using ABSB5b filament with printing end time marked within blue dotted lines (bedplate temp: 80 °C, extruder temp: 245 °C, 0% fan), (b) $PM_{0.3}$ OT_{PM} (left axis, box 1(**b**) $PM_{0.3}$ OT_{PM} (left axis, box plot), and PM_{MAX} emissions (right axis, scatter plot) 67

Figure 2-6- PM0.3 profiles for different extruder temperatures before, during, and after printing of a cube for (a) ABSB1b (bed plate temp: 80 °C, 0% fan, 20% infill) and (b) PLAB1b (bed plate temp: 50 °C, 20% fan, 20% infill). 69

Figure 2-7- Comparison of PM2.5 emission profiles taken with the OPS and Cair sensors during the printing of the test cube using (a) ABSB5w, (b) ABSB5y, (c) ABSB5b, (d) PLAB8w, (e) PLAB8y, and (f) PLAB8b. Print conditions as stated in Figure 2. 70

Figure 3-1- VOC experimental setup 77

Figure 3-2- GC/MS data processing flow chart 82

Figure 3-3- Total ion chromatograms (TIC) after sampling in the printer chamber HS post-printing of the test

cube using filament PLAb1 for sampling times of (a) 5 (b) 10 (c) 15 and (d) 20 min. 84

Figure 3-4- Total ion chromatograms (TIC) after sampling in the printer chamber HS post-printing of the test cube using filament PLAB8b for n=4 replicates: (a) Rep 1,(b) Rep 2,(c) Rep 3, (d) Rep 4. The sampling procedure and analysis are as described in 3.2.5 and analysis are as described in 3.2.5 and 3.2.6. 86

Figure 3-5- Recovered abundances of butanoic acid, O-xylene, and TVOCs for a set of replicate analyses (n=4) from Figure 3.4. 86

Figure 3-6- PCA scores plot for replicate datasets (n=4) for ABS and PLA filaments containing black, white, and yellow pigments. Principal component 1 (PC1) and principal component 2 (PC2) summarised 43% of the variance of the overall dataset, with 25.5% being summarized by PC1 and 17.5% being summarized by PC2. 87

Figure 3-7- Heatmap showing the mean abundance of VOCs recovered (columns) from different ABS and PLA filaments (rows). Values were scaled and centred by their respective rows. 88

Figure 3-8- Stacked bar plot illustrating average abundances of the different compound classes recovered from black, white, and yellow ABS and PLA filaments (n=3). 90

Figure 3-9-Comparison of TVOC and PMmax emission profiles for different colors (a) ABS filament and (b) PLA filament. 91

Figure 3-10- Abundance values for frequently recovered aromatic hydrocarbons from ABS filaments (n=3). 92

Figure 3-11- Abundance values for frequently recovered acids from PLA filaments (n=3). 93

Figure 3-12- PCA scores plot for replicate datasets (n=4) for (a) 5 different brands of ABS filaments. PC 1 and PC2 summarized 41.7% of the variance of the overall dataset, with 22.9% being summarised by PC1 and 17.84% being summarised by PC2. (b) 6 different brands of PLA filaments. . PC 1 and PC2 summarised 45% of the variance of the overall dataset, with 26.8% being summarised by PC1 and 18.1% being summarised by PC2. 95

Figure 3-13- Heatmap showing the mean abundance of VOCs recovered (columns) from different ABS and PLA brands (rows). Values were scaled and centered by their respective rows. 96

Figure 3-14- Stacked bar plot illustrating average abundances of the different compound classes recovered from different brands of ABS and PLA. 98

Figure 3-15- Comparison of TVOC and PMmax emission profiles for different brands (a) ABS filament (b)

PLA filament. 99

Figure 3-16- Abundance values for frequently recovered aromatic hydrocarbons from different brands of ABS filaments (n=3). 100

Figure 3-17- Abundance values for frequently recovered acids from different brands of PLA filaments (n=3). 101

Figure 3-18- Stacked bar plot illustrating average abundances of the different compound classes recovered from different extruder temperatures when printing ABS and PLA. 103

Figure 3-19- Comparison of TVOC and PMmax emission profiles for different nozzle temperatures(a) ABS filament (b) PLA filament. 104

Figure 3-20- Abundance values for frequently recovered aromatic hydrocarbons from different extruder temperatures of ABS filaments (n=3). 105

Figure 3-21- Abundance values for frequently recovered acids from different extruder temperatures of PLA filaments (n=3). 106

List of Tables

Table 1-1- Various national and international IAQ guideline values 7

Table 2-1- Print settings used in PM studies 55

Table 2-2- A detailed list of tested filaments. 56

Table 3-1- Print settings used to print objects for VOC emission study. 78

Table 3-2. A detailed list of tested filaments 79

List of Publications and Presentations

Publications

Khaki, S.; Duffy, E.; Smeaton, A.F.; Morrin, A. Monitoring of Particulate Matter Emissions from 3D Printing Activity in the Home Setting. *Sensors* **2021**, *21*, 3247. https://doi.org/10.3390/s21093247

Acknowledgements

The work reported in this thesis was supported by Science Foundation Ireland (SFI) under Grant Number SFI/12/RC/2289_P2, co-funded by the European Regional Development Fund.

I would like to acknowledge my indebtedness and render my warmest thanks to my supervisors, Dr. Aoife Morrin and Prof. Alan F.Smeaton, who made this work possible. Their wakeless guidance, advice, and knowledge have been invaluable throughout all stages of the work.

I would also wish to express my gratitude to Mary Ross for her constant help and valuable suggestions while using the GC/MS and to all the technical staff at the chemistry school for their patience, cooperation, and dedication throughout the project.

Finally, my sincere thanks to my family, especially my sister, who encouraged me to start this journey in the first place and my mother for her support every step of the way. My friends Aicha, Roberta, Math, Melissa, and other friends and office mates deserve my thanks for who directly and indirectly provide me with inspiration, valuable suggestions, and of course, food during this research.

Shirin Khaki MSc

Title: Analysis of particulate matter and volatile organic compound emissions from 3D printing activity

Abstract

The indoor environment contributes significantly to human well-being, as most people spend about 90% of their time indoors. Many pollutants can arise in these settings from various sources, causing poor Indoor Air Quality (IAQ). These pollutants are usually a complex mixture of particulate matter (PM) and volatile organic compounds (VOCs). Airborne PMhas been highlighted as a critical indoor air pollutant. The damage caused by the inhalation and deposition of PM is closely associated with PM size. VOCs are organic carbon-containing compounds characterized by high vapour pressures at room temperature. Certain VOCs are considered carcinogenic, the health effects of which are linked with concentration levels and exposure times. Therefore, it is essential to study PM and VOCs emissions from sources in the domestic setting to understand their potential impacts on IAQ. Three-dimensional (3D) printers are an example of a new technology product that is becoming increasingly prevalent in the domestic and school settings, raising health and safety concerns for the users. Print filaments used in 3D printing are thermoplastic polymers extruded using high temperatures. Although chemistries of these filaments are diversifying, acrylonitrile butadiene styrene (ABS) and poly (lactic acid) (PLA) have remained dominant filaments on the market. In addition, there are various brands of these filaments available, and no regulation or testing requirements for their emissions currently exist. This thesis investigates the potential impact of 3D printing activity on IAQ concerning PM and VOC emissions in the domestic setting.

PM emissions were measured using an optical particle sensor (OPS) and low-cost air quality monitors. Size ranges of interest were from 0.3 μm to 10 μm. VOC emissions were sampled using solid-phase microextraction (SPME) in a closed chamber experimental setup and analysed using gas chromatography-mass spectrometry (GC-MS). This thesis presents significant impacts on PM and VOC emissions as a function of the filament material, brand, and colour used.

Given the growing use of 3D printing in indoor, non-ventilated settings, this research focuses on their emissions impact on IAQ, which could potentially induce adverse health effects. Accordingly, it is suggested that home users of 3D printers should be made aware of the potential impacts of their choices around print settings and filament types to make informed decisions around their printing materials and methods and ensure adequate ventilation and targeted emission control solutions.

Chapter 1:

Indoor air quality in dwellings: A review on standards, sources, and monitoring technologies in the light of Covid-19

1.1 Introduction

Indoor air quality (IAQ) is an essential determinant of population health and wellbeing[1,2], given that urban populations spend more than 90% of their daily lives in the indoor environment[3–5]. Apart from residential indoor environments, people can spend significant time in offices, schools and other educational institutes, and commercial and industrial buildings[6]. In addition, a growing body of research has demonstrated that human exposure to various airborne pollutants is often greater indoors than outdoors[7–10]. Research indicates that the concentration of air pollutants like benzene and other aromatic compounds in indoor environments could be at least twice as high as in outdoor environments[11,12]. IAQ has been a relatively recent topic of interest that has come to the fore in light of recent environmental issues such as building energy use, eco-construction materials and outdoor air quality[13].Finally, the outbreak of airborne viruses such as Covid-19 has brought the importance of IAQ to the fore, as people are confined in indoor spaces[14–16].

has a significant seasonal variance, which is to be the highest in the winter season[23–25].

On account of Covid-19, much of society has adapted to spending more time working in home-based offices[26,27]. However, there has also been a shift to the home setting for leisure activity in many instances, including exercising in home gyms instead of regular gyms. This increased time and activity level indoors converges with new home energy efficiency measures and increasingly efficient heating systems, potentially resulting in the build-up of pollutants in the domestic environment[28,29], leading to poorer IAQ and thus increasing the risk of indoor air pollution exposures[30–32]. In addition, a study has shown that the radon concentrations in energy- efficient houses exceed threshold values more frequently than in non-insulated dwellings over the same geogenic radon potential and building type[33].

1.1.1 Indoor air pollutants

1.1.1.1 Particulate matter

Aerosols refer to the suspension of particulates and liquid droplets in the air[34]. The particulates in indoor aerosols typically comprise particles ranging from sub-nanometre to several hundred- vapour diameters, which are classified as follows:

(i) coarse particles, $PM_{10.0}$, of diameter (>=10 μm),

(ii) fine particles, $PM_{2.5}$ of diameter (0.1-2.5 μm), and

(iii) ultrafine particles $PM_{0.1}$ (UFPs), of diameter (<0.1 μm)[35,36].

According to the US Environmental Protection Agency (EPA), particles less than 10 micrometres in diameter can get deep into your lungs. Some may even get into your bloodstream. Fine particles pose the greatest risk to health[37,38] . They potentially retain the longest in the lungs and have been associated with respiratory and cardiovascular diseases [38–40]. Domestic indoor PM of all sizes is generated through different activites such as cleaning, cooking and combustion sources , including heaters and gas stoves, cigarette smoking, and burning candles [41–44]

.

1.1.1.2 Volatile organic compounds

Volatile organic compounds (VOCs) are organic chemical compounds that have high vapour pressures at room temperature. They can be emitted directly from solids, surfaces, or precursor VOCs that react in air [45]. In indoor settings, they are often categorised according to their volatility as VVOCs, VOCs, and SVOCs (very volatile, volatile, and semi-volatile organic

compounds, respectively). The EPA reports that certain VOCs can be 2 to 5times more concentrated inside homes than in the outside air environmentResearch indicates that this elevated indoor concentration of VOCs is attributed to indoor pollution sources related to building or furniture emissions or anthropogenic activities [46,47].

Health is usually not acutely affected by short-term exposures to low concentrations and types of VOCs encountered in the indoor domestic environment. However, in the case of longer-term exposures, some common indoor VOCs, such as formaldehyde and benzene, are considered harmful risks to human health, potentially causing cancer [48]. Exposure to VOCs is incurred via inhalation, ingestion, and dermal contact [49].

Benzene, toluene, ethylbenzene and xylene (BTEX) are highly abundant VOCs and are frequently detected indoors [50–53]. BTEX ate from various sources, including building materials and furniture, heating and cooking systems, cleaning products and tobacco products [47,54,55]. Among BTEXs, the most critical compound from a public health perspective is benzene, classified in Group 1 of human carcinogens [56]. Ethylbenzene is included in Group 2 (possibly carcinogenic to humans), while toluene and xylene are in Group 3 (in this case, not enough data for a decision on carcinogenic effects) but, in any case, considered dangerous to health [57–59].

Total volatile organic compounds (TVOCs), a summation of all detected VOCs, are considered an essential indicator of air quality and are used as a metric in many countries. TVOCs are simpler to monitor than a host of specific VOCs, simplifying interpretation. However, there are no general agreements on compounds included in the TVOCs amount. Therefore, the nature of VOCs on which TVOCs are based is dependent on the monitoring technology used [60,61]. Consequently, it cannot be used quantitatively as a comparative metric for assessing IAQ. The European Commission (EC) has called for a new approach, indicating that the range of

compounds to be included in the TVOCs value has to be clearly defined to maximise its usefulness in evaluating IAQ [62].

1.1.1.3 Inorganic pollutants

Inorganic gases found in contaminated indoor air include nitrogen oxides (NO and NO_2), sulfur dioxide (SO_2), ozone (O_3), and carbon monoxide (CO). The two principal nitrogen oxides, NO and NO_2, are commonly detected in indoor air. NO is produced to larger extents from gas, wood, oil, kerosene, and coal-burning appliances such as stoves, ovens, and space and water heaters[63,64]. In homes, SO_2 can result from tobacco smoke, improperly or inadequately vented [64,65].

Photochemical reactions of oxygen mainly produce O_3, NO, and VOCs in the atmosphere. In the home setting, equipment such as laser printers and electrostatic air cleaners produce O_3 [66]. As well as being generated indoors, it can also come from outdoors, compromising IAQ [67]. Another indoor air pollutant, CO, is a toxic gas emitted due to incomplete combustion processes[31]. The primary sources of CO are tobacco smoke, defective cooking and heating devices, fireplaces, and outdoor air exchange, especially in dense traffic areas[63,68–70].

The Covid-19 pandemic has impacted air quality, both outdoors and indoors. Despite all the negative impacts of the pandemic, outdoor air quality improved temporarily in many parts of the world due to reductions in emissions of primary pollutants from major sources such as vehicular traffic and industries[71–73]. However, this reduction of ambient air pollution did not necessarily result in a similar trend in IAQ. The government's initial ‘stay home’ directives led to full-time occupancies of homes and increased aforementioned pollution-causing household activities such as cooking and cleaning, elevating the population’s exposure to home indoor air pollutants[74,75].

Since then, the domestic setting has readily evolved and facilitates full-time work in home-based offices and exercise in home gyms, potentially contributing more and new sources such as indoor pollutants [76]. Research studies also highlight that the airborne transmission of viruses is one of the most common modes of infection [77]. PM, a common pollutant in all indoor and outdoor environments, has contributed to both transmission and severity of Covid-19 health impacts [78–80].

1.2 Indoor air quality policy

1.2.1 National and international guidelines for homes

It is established that the combination of long-term exposure and anthropogenic indoor activities, even at low pollutant concentrations, degrade IAQ and pose risks to human health, Various European researchers and experts have prioritized airborne pollutants and individual VOCs for monitoring campaigns and proposed guideline values [81–84]. This research led to WHO IAQ guidelines for selected pollutants in 2010 [63], intended to be implemented in countries with no existing IAQ regulations [85]. However, as of 2022, these guidelines have not been updated, while outdoor air quality standards, on the other hand, are constantly being updated and strengthened.

Although there are no specific reference Directives on IAQ in European legislation, pre-legislative initiatives have multiplied over the years. Several European countries, including France, Finland, Austria, Belgium, Germany, and the Netherlands, have overcome the absence of European legislation and developed their guideline values [86–88]. Outside Europe, countries like Japan, China, the USA, and Canada have developed and adopted guideline values [89–92]. However, except for Belgium, Finland, and France, the recommended guideline values have no legal weighting, just offering guidance on IAQ based on expert evaluation [93].

Nonetheless, one primary goal is common to all of these guidelines: to protect public health from adverse effects of indoor air pollution and to eliminate or reduce exposure to those pollutants to the greatest extent possible [94].

A table of various national and international standards and guidelines for homes and public buildings is shown in Table 1.1. These IAQ guidelines for individual VOCs are stated in concentration (mg/m^3) for short and long-term exposures for those compounds considered the most hazardous by individual countries or international research bodies. It should be noted that the values in these guidelines are constantly being updated to protect the population from being over-exposed to them.

Table 1-1- Various national and international

Name	Country/ Organisation	Sampling & analysis approach	Threshold	Domestic sources
Carbon monoxide	WHO	Sampling: ISO 160000 Analysis: ISO 160000	30 mg/m^3 1h average 10 mg/m^3 8h average	Unvented kerosene and gas space heaters Leaking chimneys and furnaces Wood stoves and fireplaces Gas burners and supplementary heaters Tobacco smoke[95–97]
	Finland	Electrochemical cell or infrared analyzer	2 mg/m^3 8h average	
	France	/	10 mg/m^3 8h average	
	Germany	/	30 ppm 8h average	
	China	/	10 mg/m^3 1h average	
	USA	Sampling: passive diffusion or pump Analysis: ISO 160000	9 ppm 8h average	
Nitrogen dioxide	WHO	Sampling: passive diffusion or pump Analysis: ISO 160000	200 $\mu g/m^3$ 1h average	Tobacco smoke Gas, wood, oil, kerosene, and coal-burning Unfueled or poorly maintained appliances [5,98]
	France	Sampling: passive diffusion or pump Analysis: Spectrophotometry or ion chromatography	200 $\mu g/m^3$ 1h average	
	Germany	/	350 $\mu g/m^3$ 1h average	
	China	/		
	USA	Sampling: ISO 160000 Analysis: ISO 160000/	5600 $\mu g/m^3$ 8h average	
Benzene	WHO	Sampling: Passive sorbent tubes/ TD[1] Analysis: GC[2]	15 $\mu g/m^3$ 24h average	Building materials and furniture Heating and cooling systems PVC and rubber flooring Stored solvents[16,99–103]
	Finland		0.4 $\mu g/m^3$ 8h average	
	France	Sampling: ISO 160000 Analysis: ISO 160000	30 $\mu g/m^3$ short-term exposure	
	China	/	ng/m^3 1 hour average	
	USA	Sampling: multi sorbent cartridge and SUMMA[3] canister	3 mg/m^3 for exposure of >1 year	
Formaldehyde	WHO	Sampling: passive Analysis: HPLC[4]–U.V	g/m^3 30-minute exposure	Furniture and wooden products such as particleboard plywood
	Finland	Sampling: ISO 160000 Analysis: ISO 160000	g/m^3 long-term exposure	

	France	Sampling: active on a DNPH[5]coated silica gel Analysis: HPLC-U.V	g/m^3 short-term exposure	Insulating materials Textiles Do-it-yourself products such as paints, wallpapers, glues, adhesives, varnishes, and lacquers; Household cleaning products such as detergents, disinfectants, softeners, carpet cleaners, and shoe products; Electronic equipment, including computers and photocopiers; Other consumer items such as insecticides [5,52,104–108]
	Germany	/	g/m^3 short-term exposure	
	China	/	100 µg/m^3 1h exposure	
	USA	Sampling: active on a DNPH give number ref coated silica gel	100 µg/m^{3}1h exposure	
Styrene	WHO	Sampling: Passive sorbent tube/ TD Analysis: GC	µg/m^3 7 days exposure	Building materials, Consumer products, Tobacco smoke, Electronic equipment photocopiers, and laser printers [109,110]
	Finland	Sampling: ISO 160000 Analysis: ISO 160000	µg/m^3 annual exposure	
	Germany	/	300 µg/m^3 annual exposure	
	China	/		
	USA	Sampling: Multi sorbent cartridge and SUMMA canister	µg/m^{3}Annual exposure	
Toluene	Finland	Sampling: ISO 160000 Analysis: ISO 160000	g/m^3 long-term exposure	Consumer products such as synthetic fragrances and nail polish Do-it-yourself products such as paints, paint thinners, adhesives Cigarette smoke [54,58,111]
	France	Sampling: active - sorbent tube and solvent desorption Analysis: GC-FID[6] or GC-MS[7]	0 000 mg/m^3 short-term and long-term exposure	
	Germany	/	g/m^3 long-term exposure	
	China	/	0.2 mg/m^3 1-h average	
	USA	Sampling: multi sorbent cartridge and SUMMA canister		
Xylene	France	/	300 µg/m^3 long term exposure	Consumer products such as synthetic fragrances and varnish, shellac Paints, paint thinners, Rust preventives Cigarette smoke[54,112,113]
	Germany	/	g/m^3 long-term exposure	
	China	/	0.2 mg/m^3 1h average	
	USA	Sampling: multi sorbent cartridge and SUMMA canister	µg/m^3 annual exposure	
TVOCS	WHO	Sampling: ISO 160000 Analysis: ISO 160000	0.3 mg/m^3 8h average	
	Finland	Sampling: ISO 160000 Analysis: ISO 160000	200 µg/m^3 8h average	
	France	/		
	China	/	0.6 mg/m^3 8h average	
PM_{10}	WHO	Sampling: optical instruments based on light scattering, light absorption, or light extinction	50 µg/m^3 24h average	Occupants Cooking Tobacco combustion Combustion appliances Building materials and Furnishings Consumer products Cleaning activities Photocopiers and laser printers[5,37,42]
	Finland	Sampling: ISO 160000 Analysis: ISO 160000	< 20 µg/m^3 24h average	
	Germany	/	4 mg/m3 8h average	
	China	/	0.15 mg/m^3 24h average	
	USA	Sampling: pump/ size selective impactor	150 µg/m^3 24h average	

$PM_{2.5}$	WHO	Sampling: optical instruments based on light scattering, absorption or extinction	25 μg/m^3 24h average	Cleaning products Building materials,
	USA	Sampling: pump/ SMPS	35 μg/m^3 24h average	Consumer products such as candles Fuel-burning equipment such as furnaces, upholstered goods Activities such as cooking, sweeping and copy machines[5,43,114]

1 Thermal desorption; 2 Gas chromatography; 3 a stainless steel container that has had the internal surfaces specially passivated using a "Summa" process; 4 High-performance liquid chromatography; 5 Dinitrophenylhydrazine; 6 Flame ionization detection; 7- Mass spectrometry

Some agreements across these IAQ guidelines regarding focusing on certain VOCs and pollutants. Nevertheless, many values in guidelines differ from country to country, which may be partly due to differences in sampling and analysis procedures, different design principles, or the date that guidelines were established[85,115,116]. For example, Finnish air quality standards set the threshold at 4000 g/m^3 for long-term exposure to toluene. German standards set the limit at just 300 g/m^3. This heterogeneity in current regulation systems has led to a lack of comparability among European Union (EU) member states, both in terms of technical procedures and health evaluation, indicating a need for more comprehensive and integrated standards and policies to support regulatory measures.

1.2.2 Policies on air tightness and low-energy buildings

Since modern society needs to strengthen its efforts to cope with the challenge of climate change, it is recognized that buildings must be highly energy efficient. The necessary substantial reduction of heat losses through the building envelope requires a system of building codes to stipulate energy performance criteria and a widely applied regulatory policy tool for building energy efficiency [117]. The technical requirements of building codes cover different criteria, including thermal insulation as well as air conditioning systems,

ventilation, lighting efficiency, airtightness, and indoor and outdoor climatic conditions [118]. In EU Directives, the role played by energy efficiency buildings is clear and defined [91,119]. The most common normalized parameters include air exchange rate, specific leakage rate, and air permeability rate [120].

It should be noted that the regulatory approach varies depending on the country [121–123].For example, in countries like the UK and France, the regulations set limitations on the whole building permeability. In contrast, countries like Belgium and Finland set default values and recommendations.

Insufficient ventilation can lead to increased air humidity levels, resulting in an increased prevalence of dust mites and, in some cases, a high risk of mold growth [124]. Information on pollution sources in buildings, the model with the indoor hydrothermal condition, air quality, and thermal systems, and provide methods to optimize ventilation and air-conditioning. While there is no doubt that high IAQ and high energy efficiency can go hand in hand, open questions remain to foster widespread implementation in new and refurbished residential buildings.

The International Energy Agency (IEA) initiated the Annex 68 project to develop a fundamental basis for optimal design for good IAQ in highly energy-efficient residential buildings [125]. This project aims to gather existing data or provide new data on indoor pollutants and their properties and determine or perfect the tools to help designers and managers in achieving several objectives. These objectives include developing guidelines for design and control strategies for buildings with low energy consumption that will not compromise IAQ. These buildings would benefit from the latest advances in sensor and control technology, to identify methods to improve IAQ while ensuring minimum energy consumption for operations and identify and analyze relevant case studies to examine and optimize performance [125].

A growing body of scientific evidence has shown that indoor pollutants can differ in airtight homes compared to less thermally insulated homes. For example, the IAQ of energy-efficient dwellings to conventional buildings in France was studied and showed higher concentrations of VOCs such as terpenes and hex-aldehydes present in more energy-efficient buildings, possibly related to poor air exchange of the VOCs potentially stemming from the wood or wood-based insulation products [126]. In other research done in Spain, the co-dependence was established between airtightness and a low air change rate associated with high indoor CO_2 concentrations[84]. Good indoor air quality is crucial for achieving a healthy and comfortable indoor climate. This issue is critical for public non-residential buildings such are nurseries, hospitals, and schools to avoid sick building syndrome. When improving energy efficiency through maintenance and refurbishment, combining thermal insulation of the building envelope with the air-tightening of the envelope is recommended. The reason for this is the influence of airtightness on energy efficiency, thermal comfort, indoor air quality, and moisture condensation. Research presented in this paper investigates the correlation between a building's airtightness and levels of CO_2, relative humidity, and temperature as basic parameters for determining indoor thermal comfort. Presented results were obtained by measuring all the above-stated parameters in classrooms and faculties. All observed buildings are different in their age and building technology; during measurements, meteorological parameters were also observed and the number of occupants in classrooms and the size of the classroom itself[127]. Studies done in recently retrofitted residences in Finland and Lithuania have shown that while heating energy consumption decreased by averages of 24% and 49%, respectively, after energy retrofitting, there was a significant elevation in measured BTEX concentrations in residential buildings that underwent this energy retrofits[30], due to recent renovation involving the use of building materials, such as paints and varnishes. Comparative studies of conventional and

energy-efficient houses in North America, Switzerland, Austria, Ireland, and the Czech Republic showed that radon levels in energy-efficient buildings also tended to be higher[128–132], potentially linked to reduced air exchange rates, a consequence of refurbishment aimed at energy-saving[33,133]. Thus implementing building codes or other policies meant to save energy poses a threat to IAQ if they are not coupled with a revision of ventilation regulations[134].

Several essential metrics and measurement techniques described here are available to help understand and reduce indoor air pollution. However, greater integration is needed to ensure that IAQ plays a clear and critical role in energy efficiency interventions[32,135]. Energy efficiency and IAQ must not conflict but must be complementary. While energy efficiency measures are likely to provide a net benefit in terms of energy savings and warmer homes, care should be taken to mitigate against reductions in air quality when installing interventions that increase the airtightness of homes[133].

1.3 Indoor air pollution sources in the domestic setting

A host of sources generate indoor air pollutants in homes. Due to this range of sources and chemical reactions and the wide variation in building types and uses, the composition, and thus toxicity, indoor--emitted PM and VOCs are dynamic and complex[136–138]. In addition, certain sources (e.g. furnishings, building materials) passively generate pollutants at a relatively stable rate. In contrast, other sources generate active contributions, such as smoking and cleaning [139]. All pollution sources can generally be categorized into six groups: (1) building materials, (2) ventilation and air exchange, (3) heating systems, (4) occupant activities such as cooking and cleaning, gadgets, (5) human presence which contributes bio-effluents and (6) Electronic devices[47,140,141]. The following sections will describe the research on

these sources as traditional and emerging sources noted on the pandemic.

1.3.1 Traditional sources

Depending on the building type and age, it has been reported that building materials alone represent approximately 40% of indoor VOC sources[142]. The constant presence of organic acids indoors in buildings occupied or not suggests that building materials may be sources of these compounds[142–144]. Materials common to the domestic environment, such as solvents and paints, adhesives, and coatings and coverings on walls, ceilings, and floors, emit significant VOCs due to their large surface areas and permanent exposure to the indoor air atmosphere[77,78]. The abundant species in the adhesive are 2-methyl-hexane, heptane, and toluene[145]. At the same time, common VOCs emitted from wall paintings are ethylene glycol, toluene, and xylene. Furniture, textiles, household fabrics, and paints are other primary sources of indoor air pollutants, causing up to 10-20% of TVOCs in different indoor environments[80]. Building materials such as paints, thermal insulation, carpets, and other floor coverings, furniture, and electronic equipment are common stationary sources of VOCs in residential spaces[142,143].

Also contributing to IAQ is the exchange rate of outdoor air with indoor air. This is directly related to the airtightness of a dwelling. For example, the number of external façades and their exposure to wind and window-opening behavior impact air exchange and thus the IAQ. These factors govern how much outdoor air circulates indoors and the level at which indoor air pollutants can build up. In addition, outdoor air can negatively impact indoor air pollution where primary sources of some pollutants, e.g., NO and O_3, in homes are, in fact, outdoor

sources such as traffic and air ventilation systems[8,73,82].

Heating systems in the home also influence IAQ. They can be classified into five categories: gas, central heating, solid fuel, biomass, and others (e.g., sawdust, electricity, etc.). In homes with gas heaters, mean indoor NO_2 concentrations were an average of 7.2 ppb higher in homes than in those without a gas heater[146,147]. The presence of a gas heater had an even more significant impact during the winter months. Solid fuels consisting primarily of coal for residential heating are common in many places, including within European and North American countries[148,149], despite being known for their negative influence on IAQ. The combustion of coal, for example, is a source of SO_2 and oxides of nitrogen (NOx). These and other pollutants are adsorbed or absorbed into PM, which can further concentrate and increase its toxicity[56,148]. As such, the latest WHO IAQ guidelines strongly recommend against the residential use of coal[150][145]. Using biomasses for domestic heating, already considered a relevant pollution source in the outdoor atmosphere, can also heavily affect IAQ, even when using technologically advanced appliances such as thermos-stoves and airtight fireplaces[151]. This is due to the inefficient burning of these fuels generating large amounts of PM, CO, and hydrocarbons[152,153]. In several regions of the world, residential combustion of solid fuels (biomass and coal) for heating has been shown to contribute to total outdoor $PM_{2.5}$ emissions, including Europe (13–21% in 2010, central Europe is the highest)[148]. To protect peoples' health, policy-makers in regions with relatively high levels of outdoor air pollution from household heating-related combustion have provided incentives to switch from solid fuel combustion for heating to gas- or electricity-based heating, one successful example of which is Sweden[149,154].

Cooking combustion processes such as gas stove cooking represents one of the most prevalent temporal sources of air pollution in the indoor environment. Cooking aerosols contain large

amounts of $PM_{2.5}$ and $PM_{10.0}$ and a wide range of VOCs, including formaldehyde, acetaldehyde, acrolein, benzene, toluene, and xylene [47,155,156]. Cooking also releases large amounts of NOx, nitrous acid (HONO), and more complex oxidized organic molecules, such as sorbic and lactic acid[138,157]. The quantities and nature of these emitted VOCs are highly dependent on the cooking type, such as frying, roasting, grilling, boiling, and broiling, as well as ingredients, fuel types, temperature, and extraction/ventilation equipment [158,159]. When it comes to cooking, we need to distinguish between emissions caused by the fuel type and those caused by the cooking process itself. For example, sunflower oil has been shown to produce high aldehyde emissions when heated than oils with lower unsaturated fatty acid content (e.g., rapeseed oil) regardless of the cooking method or food type [160–162].

NO_2 and CO are primary pollutants produced from combustion. Measurements showed the concentration of NO_2 in the kitchen and the living room on the stove type used in the kitchen: the concentration of NO_2 in homes with gas stoves was higher than in homes with electric stoves[163–165]. Kitchens with gas stoves were the most polluted compared to electric stoves. The highest NO_2 levels in the kitchen were observed during winter when natural ventilation is also reduced[166–168].

Consumer products for cleaning, polishing, indoor fragrances, or personal care and cosmetic products are also relevant to indoor air pollution. These products release a host of VOCs that reside in the air or settle in airborne PM and on surfaces. Cleaning with these products is a significant human activity that influences indoor air by emitting many VOCs, among which xylene and ethylene, and formaldehyde are common[108,169–171]. Cleaning with bleach produces reactively chlorinated and nitrogenated compounds, which can detrimentally impact indoor air quality and human health[172,173]. Several chlorinated VOCs, including chloroform ($CHCl_3$) and carbon tetrachloride (CCl_4), have been measured in indoor air

following bleach use[174,175]. In addition, Bleach-related Cl radicals can react with other indoor VOCs to yield corrosive hydrogen chloride (HCl), which can subsequently condense to form secondary organic aerosols[174]. While the increased use of disinfectants has been essential in the battle against Covid-19, continuous use and overuse of these disinfectants could have short- and long-term adverse effects on human health, aquatic ecosystems, and terrestrial environments[176].

In addition, it has been proved that commonly used consumer products, including air fresheners, laundry products, personal care products, scented candles, etc., are significant sources of VOC in households[177–179]. As a result, different VOCs are emitted from these products. The US Food and Drug Administration (FDA) has classified at least 42 as toxic or hazardous[180,181]. Fewer than 3% of fragrance formulations of the VOCs within these products were disclosed on product labels or material safety data sheets, partly because consumer products are not required to disclose all ingredients[178,182]. However, it is well-known that many fragranced products emit terpenes such as limonene and α-pinene[183–185]. In addition, terpenes react with O_3 to generate a range of secondary pollutants, including formaldehyde, acetaldehyde, secondary organic aerosols, and UFPs[186–188], whose levels within indoor air should be minimized.

Ingestion of organic chemicals from building materials and consumer goods containing any form of chlorinated FR can provide a potential path to exposure [189], as they have been proven to be a chlorinated source of VOCs[190–192]. Some FR materials may also contain inhalable particles associated with health effects, e.g., polymeric foam insulation[193].

Humans themselves are a source of pollution indoors through their activities and natural emissions from the body. The chemicals that constitute human skin oils can be classified as wax esters, fatty acids, and squalene, which readily react with ozone and form secondary

aerosols[194,195]. Skin cells, or epithelial cells, are frequently reported as airborne biological components in indoor environments[196]. These cells are often reported as dust microflora in indoor environments, both in air and from surfaces. The skin cells are often overlooked as a significant agent that may impact the quality of living space[196]. Breath is also a significant source of VOCs, including alcohols, hydrocarbons, aldehydes, and ketones[197,198]. In addition to common VOCs, breath emissions from different subjects have highly individual characteristics[199]. The concentration rate of human-generated pollutants in an indoor environment is determined by several factors, including the volume of the space, the air exchange rate, the number of people indoors, and individual habits such as diet, which impact exhaled VOC composition[197]. For instance, many VOCs are present in food and drinks, contributing to the VOCs from exhaled breath[200,201].

During the Covid-19 pandemic, the magnitude of some of the sources mentioned above intensified, with people spending extended time at home. For example, in the early stages of Covid-19, increased cleaning and viral disinfection caused elevated indoor pollutants[202,203]. However, as the pandemic continued, certain activities have evolved in homes. Practices that will likely be maintained beyond the pandemic and their impacts on IAQ are discussed below.

1.3.2 Emerging sources on account of Covid-19

Printers, computers, laptops, and other electronic equipment are all standard pieces of equipment in the office environment. Moreover with many traditionally office-based people working from home due to the pandemic, concerns about the levels of potentially harmful pollutants from electronic equipment have grown. Computers do emit a range of VOCs[204,205], although in most cases, their emission rates are low and less significant than other indoor and outdoor sources. For laptops, the chemical composition of emissions includes alcohols, carboxylates, and ketones[206,207]. Some studies indicate that many VOCs, including formaldehyde and O_3, are emitted from photocopiers and laser printers[208,209]. The type and quantity of substances emitted are determined by the toner and paper used, the equipment age, and the maintenance history[210]. VOC emissions from printers (and copiers) include styrene, toluene, xylenes, and alkylbenzenes[211]. PMs are also emitted, and again, the size and emission rate vary among brands and models[210–212]. By comparing PM emission rates from printing to other indoor human activities, it has been shown that PM emitted from laser printers could reach comparable levels to those generated by indoor incense burning[213]. As with all emissions, depending on the ventilation rate for a room, PM emitted by a laser printer disperses within a few minutes or can reside for up to several hours[214].

With fitness centers closing due to Covid-19 restrictions worldwide, many people began using their homes as gyms, generating another potential source of indoor air pollution. Studies have shown that physical exercise intensity influences IAQ, as high CO_2, VOCs, CO, PMs, and CH_2O are generated during exercise[215,216]. Various studies have looked at indoor air quality in the gym environment. For example, CO_2 concentrations are dependent on exercise intensity levels; e.g., CO_2 was higher in high-intensity classes than in yoga classes. Exposure to PM in fitness centers and gyms during classes is estimated to be about 6-fold higher than rest times,

mainly associated with increased activity and particle resuspension[217–219]. Furthermore, higher amounts of $PM_{10.0}$ and CO inhaled by clients in these classes were observed and attributed to increased respiratory ventilation and more significant PM re-suspension caused by the vigorous activity of the high-intensity interval training [216]. Considering that physical training with high intensity is being practiced frequently nowadays in home gyms, attention should be paid to this activity as a potential source of indoor air pollution, mainly where high-intensity exercise is being performed, and domestic pollutants could be airborne[219,220].

As well as home office equipment, there has been a recent upsurge in the deployment of 3D printers in a domestic setting by hobbyists and families in recent years. Although Covid-19 has not driven this trend, its timing has broadly coincided. 3D printers, especially in the home setting, are important to consider as an emerging source of interest. There are currently no regulations or requirements for enclosures or built-in filtration systems for these devices[221]. However, it is well-understood that thermal processing of polymeric filaments used as printing materials leads to the formation of VOCs and PMs[222–224]. These emissions depend highly on print filament type and the print parameters used. For example, acrylonitrile butadiene styrene (ABS) thermoplastic filaments, which require a high temperature to melt, produced more emissions than filaments made of the biomaterial polylactic acid (PLA), which melt at a lower temperature[225–227]. Invitro cell experiments have evidenced the adverse health effects of exposure to 3D printing-induced PMs[228]. These studies showed that PLA-emitted PM elicited higher toxic response levels than ABS-emitted particles at comparable mass doses[227,229]. However, there are considerable discrepancies in the reported composition of the VOC mixture emitted during 3D printing. Abundant VOCs reported include aliphatic aldehydes (C6 – C10), lactide, 2-butanone, styrene, caprolactam, and ethylbenzene[226,230–232].

Furthermore, diverse flame retardants, cyclic ethers, and esters of acrylic acid and palmitic acid have also been detected[233–235]. Of these, acetaldehyde and styrene are classified as potential carcinogens. Like PMs, VOCs emitted from 3D printing depend highly on filament manufacture and the color used[236,237].

1.4 Review on monitoring strategies of indoor air pollutants

Monitoring the nature of and the concentrations of pollutants in our indoor home air is important to identify potential sources of concern and monitor the effectiveness of any mitigating measures taken to minimize pollutant levels[238–240]. In general, monitoring indoor air pollutants will give us a greater quantitative understanding of their levels and patterns and will provide evidence for guidelines and future legislation in the area. To monitor IAQ, there are 2 main strategies employed: (1) discrete sampling of the air and using offline instrumental laboratory methods to analyze the collected samples, and (2) deploying sensors directly that are capable of continuous monitoring of pollutants of interest. For research purposes, the first strategy is typically employed by using instrumental techniques such as mass spectrometry; we can identify and profile the VOCs present with exceptional sensitivity. The second method lends itself to monitoring by the homeowners themselves to track overall air quality in real-time TVOCs, CO_2, and PM monitoring[43,241].

1.4.1 VOC sampling in indoor air

Air sampling is the process of capturing contaminants in a known volume of air. The airborne contaminants are measured and compared against the volume of air. The results are a concentration, usually milligrams per cubic meter (mg/m^3) or parts per million (ppm). Many environmental parameters need to be considered when assessing the air quality in an indoor

environment. Any investigation of IAQ requires a clear definition of the measurement objectives and a strategy for actions required to meet those objectives. The choice of analytical methods depends upon the agents that need to be measured and the purpose of the study. Conditions during indoor sampling should always be recorded to fully interpret the analytical data, including location within the room, air exchange rates, distance from vents, occupancy, and activities occurring during sampling[242]. Two methods for indoor air analysis are passive and active sampling. Passive sampling involves deploying a sorbent material at a particular location in a room for a fixed duration. The sampler itself is taken and brought for analysis. Active samplers involve using a pump to draw the air through a sorbent bed. Because of the active nature of this technique, sampling times are typically much shorter than for passive sampling. An active sampler can obtain readings over a short timescale (s) with the average of several data points taken over a longer timescale (min or h). In contrast, passive samplers provide a time-integrated pollutant concentration over the entire exposure period. Finally, it should be noted that the simultaneous deployment of passive and active samplers has become a good practice, as both methods have advantages, improving the data quality[243,244].

1.4.1.1 ISO guidelines for IAQ sampling

The ISO 16000 series deals with indoor air measurements. This standard applies to indoor environments such as dwellings, public buildings such as schools, hospitals, restaurants, and theatres, and workrooms and workspaces in buildings that are not subject to health and safety inspections regarding air pollutants. Standards of the ISO 16000 series specify the determination of the following indoor air pollutants: VOCs, SVOCs, individual organic compounds, i.e. polychlorinated biphenyl, polychlorinated dibenzofurans, FRs, plasticizers and amines, and carcinogens like asbestos and formaldehyde. This standard consists of the

following parts, under the general title Indoor air: “General aspects of sampling strategy”, “determination and sampling” and “measurement and storage strategies” for the pollutants as mentioned earlier[245,246]. ISO 16000 also describes general considerations about the duration, period, and location of sampling of indoor air pollutants and recommends parallel measurements of concentrations of outdoor air pollutants[242].

1.4.1.2 Passive sampling

Passive, also termed ‘diffusive’, samplers rely on unassisted molecular diffusion of gases to a sorbent medium[247]. This method provides a convenient, cost-effective method for sampling VOCs and a good option for extended duration sampling (e.g., typically >8 h). It can target heavy molecular weight compounds for subsequent isotopic analysis; for example[248,249]. Due to their basic requirements, they are the most common sampling approach used for sampling indoor air environments in general[250].

Passive samplers comprise a sorbent material to adsorb target VOCs of interest. Sorbents that have been used for indoor air sampling include porous carbon (e.g., Carboxy, Carbosieve), graphitized carbon black (e.g., Carbograph, carbon pack, Carbotrap), porous polymers (e.g., Tenax, PoraPak, Chromosorb, Amberlite resins) as well as inorganic solids such as quartz wool and molecular sieves[251,252]. The boiling point of targeted compounds is the critical factor when selecting a sorbent type. Weak sorbents, such as porous polymers, are used when working with VOCs and SVOCs, whose boiling point is above 100 °C. For VVOCs with boiling points between 30 °C and 100 °C, a medium-strength sorbent, such as a graphitized carbon black, should be utilized; however, if the boiling point falls in the range –48 °C to 30 °C, a strong sorbent, such as a carbon molecular sieve can be adapted[253]. Sorbents can be used singly or

in multi-sorbent packings. Multi-sorbent packing increases sorbent strength to facilitate a wider range of volatility[254].

The development of passive samplers has been increasing over the last few decades, with significant improvements relating to the range of analytes that can be sampled based on new sorbent chemistries and the decreasing cost of these devices[255]. Among recently commercialized passive samplers, polyurethane foam (PUF) disks are a promising approach validated and used in several studies[256].

In terms of geometries, conventional passive sampling approaches include (1) axial samplers, offering options for thermal desorption or solvent extraction for subsequent analysis, and (2) radial samplers that use TD tubes and typically require TD-GC-MS analysis[257]. The specific sorbent is fitted between a cap and a fine-mesh gauze, regulating the airflow through tube[242]. Generally speaking, compounds compatible with axial sampling range in volatility from vinyl chloride (using a strong carbonized molecular sieve sorbent such as Unicarb^{TM}) to SVOCs such as n-C16 and above (using a weak sorbent such as Tenax)[258,259]. Standard sorbent tubes can be used in passive mode for short-term monitoring (1–8 h) of ppm levels of VOCs and longer-term environmental monitoring (3 days to 4 weeks) of indoor or outdoor air[257,260].

Passive samplers with radial symmetries have been made available in more recent years. They employ a coaxial system in which a cylindrical adsorbing cartridge is housed inside a cylindrical diffusive barrier[261]. A larger diffusive surface and the short distance between the diffusive barrier and adsorbing surface result in a much higher effective sampling rate than their axial counterparts. Because of this, radial samplers are often used for short-term deployment (4 h to 1 week) and are not always suited to sampling high-concentration atmospheres[257,262].

Although simple to execute, passive sampling procedures can be time-consuming and multi-staged to include sampling, extraction, and analysis, leading to loss of analyte. To integrate activities such as sampling, extraction, and analyte enrichment, novel microextraction techniques have been recently introduced. They are less time and labour-consuming [257,258] and more sensitive due to enrichment and can provide quantitative results[265]. By definition, microextraction means that all modes of these techniques require sampling using small volumes of extraction medium under strictly defined extraction conditions[266]. SPME typically comprises a fused silica coating with a specified adsorbent. The SPME sampling and analysis process is composed of two steps: (i) partitioning of analytes between the extraction phase and the sample matrix during sampling and (ii) desorption of concentrated extract into an analytical instrumentb[265]. SPME can be performed in the headspace (HS) and direct immersion (DI). In HS-SPME, the fiber is exposed to an HS to be sampled [267,268]. In DI-SPME, the fiber is exposed to the sample matrix itself. The analytes partition directly from the sample to the fiber extracting phase[269]. Frequently used commercially available fiber coatings are polydimethylsiloxane (PDMS), polyacrylate (PA), Carboxy (CAR; a carbon molecular sieve), DVB, and Carbowax (CW; polyethylene glycol), the variety of which is constantly growing with increasing numbers of applications[270–272]. Fibers are available in various coating combinations, blends or copolymers, and fiber assemblies[263,273]. The miniaturization and portability of SPME devices greatly facilitate on-site passive samplers' implementation. When coupled with portable analytical instruments such as portable GC-MS, on-site analysis can also be performed[264,274].

Numerous applications for passive devices are described here to sample VOCs in indoor air. They have been used in various indoor environments, including homes, offices, classrooms, etc. For example, in one study, axial sampler tubes with different sorbents (Tenax TA,

Carbopack, activated charcoal) were used to assess indoor air VOC concentrations for 1-7 days [275]. Targeted VOCs included chlorinated ethenes, ethane, methanes, aromatic and aliphatic hydrocarbons. The 10 VOCs tested showed differences in passive sampler performance attributable to the properties of the chemicals. However, the different samplers are not equally susceptible to bias and variability for all compounds. Poor retention for the long-duration samples has been observed for the sampler with Carbotrap, which is the weaker sorbent[248].

Using radial tubes with activated charcoal another study sampled domestic VOCs in 100 Romanian houses in radial tubes. Using TD-GC-MS for sample analysis, limonene, heptane, and carbon tetrachloride were identified as predominant pollutants attributed to recent renovation works and floor coverings [276]. Perception of indoor air quality (PIAQ) was evaluated in French dwellings. This survey was combined with in-field assessment measurements of VOCs. Measurements were conducted using radial samplers (containing Carbograph, sampling time: 7 days). Using GC-MS-FID, VOCs detected included aromatic hydrocarbons, aliphatic hydrocarbons, chlorinated hydrocarbons, and glycol ethers. The results indicated a correlation between perceived IAQ and some of the measured VOCs, including acrolein, benzene, and styrene. A PUF passive sampler and an active sampler were co-located in 37 indoor spaces, including green renovated and non-renovated low-income housing units, campus dormitories, detached homes, and office space, to measure the levels of phthalates, fragrance chemicals, and FRs[277]. The results showed good agreement (R^2=0.88) between active and passive sampling methods for characterizing the relative abundance of each chemical, where the measured active sampler concentrations and passive sampler masses were significantly positively correlated for14 for 21 chemicals. Concentrations of hexanal, acetaldehyde, and formaldehyde in three different rooms of an office environment were

sampled using a 15 min deployment of SPME (PDMS–DVB) fibers, followed by GC-MS analysis[278]. For both hexanal and acetaldehyde, the concentrations were below the limit of quantification for this extraction time. However, the formaldehyde concentration was determined in two sampling points but low enough to meet French regulation limits. Aromatic amines, a group of SVOCs, were targeted for sampling in a flat and an office[279]. Active adsorption tubes and passive SPME (DVB/CAR/PDMS) sampling were used and compared. Analyses were via GC-MS. Benzylamine, 3-aminophenol, and 4-aminophenol were detected on the active samplers but not detected using the SPME method.

1.4.2 VOC instrumental analysis

Chromatography is a key separation technique in VOC analysis. It enables the separation and subsequent qualitative and quantitative analysis of complex mixtures, as long as samples are volatile or soluble in a suitable solvent[33]. Although analytical chromatographic techniques differ, they are all based on partitioning sample components between two phases, one stationary and one mobile phase[280]. The most common chromatography types based on the physical state of the mobile phase include LC and GC[281]. The principles of these techniques are briefly described in the following section. However, given that the review focuses on VOCs, the emphasis will be on GC as the key analytical method.

1.4.2.1 Liquid chromatography (LC) analysis of IAQ

LC includes column and planar types and is characterized by a liquid mobile phase. Column-based LC uses a column packed with a stationary phase, a porous medium of granular silica or polymer material. A sample is injected into a mobile phase at high pressure to transport the sample onto and through the column. When the sample is injected, the compounds separate

over time-based on their relative affinity to the stationary and mobile phases. During a chromatographic run, the composition of the mobile phase can be kept constant (isocratic) or modified (e.g., by increasing the content of the organic solvent in a mixture throughout the run) using a gradient profile. The elution strength of the mobile phase can be varied throughout the separation in gradient elution, allowing good control over run time and quality of separation. However, a special pump is required to flow the mobile phase in a gradual elution [282]. Reversed-phase high-pressure LC (RP-HPLC) is the most commonly used form of LC. RP-HPLC has a nonpolar stationary phase, e.g., modified silica, and a moderately polar aqueous mobile phase. This technique is particularly useful for low or non-volatile organic compounds, which cannot be handled with GC, making them amenable to a wide range of applications, such as pharmaceuticals and food analysis[283].

UV detection is most common in detectors, often utilizing UV-photodiode arrays (PDA) based on low initial cost, ease of use, and robustness. MS detection has become increasingly common as a detector for compound identification[284,285]. Although GC is the more popular approach for analyzing volatiles in indoor air, LC has found value for analyzing certain species, e.g. carbonyls, as they have been used widely in many household products like paints, varnishes, waxes, solvents, detergents, or cleaning products. An RP-HPLC method was reported for analyzing eight carbonyl compounds from the indoor environment of an office[286]. The study looked to identify and quantify 7 aldehydes (acetaldehyde, propionaldehyde, acrolein, butyraldehyde, crotonaldehyde, n-pentanaldehyde, and benzaldehyde) and one ketone (acetone). 2,4-DNPH passive samplers were used for sampling in this work. The main sources of these detected carbonyls included the building materials, paints, laminate, wooden varnished, wood ceilings, and particle-board present within this indoor environment.

1.4.2.2 Gas chromatography (GC) analysis of IAQ

GC, as stated, is a far more common technique for analyzing VOCs in indoor air. It separates volatile components of a sample depending on differences in partitioning modes between a carrier mobile gas phase and a column-based stationary phase. Hydrogen, helium, argon, or nitrogen are used as carrier gases, with helium being most preferred because of its efficiency and safety. These stationary phases are available in different types: non-polar, mid-polar, and polar like methyl silicone, methyl phenyl silicone, methyl cyano propyl silicone, methyl trifluoro propyl silicone, etc. Highly polar phases like polyethylene glycol (PEG), known as wax columns, are also available for polar sample separations. Non-polar phases are more thermally stable compared to polar phases[287].

After injection of the sample into the GC inlet, the sample mixture is first vaporized, if not already in the gas phase. For trace concentration samples, the whole sample is transferred onto the column by the carrier gas in what is known as a spitless mode. Only a portion of the sample is transferred to the column for high concentration samples in split mode. In the column, the components of the vaporized sample partition between the liquid stationary phase coating on the column and the carrier gas. Since the partitioning process depends on the sample components' boiling points and the polarity of the stationary phase, the column retention times (Rt) will be different for each sample component. Once the components elute from the column, they travel into the detector, which responds quantitatively to the components and converts them into an electrical signal. Common detector types used in GC include FID, thermal conductivity detection (TCD), and MS[288].

FID, a common GC detector, uses a flame to ionize organic compounds containing carbon following the separation of the components in the column. The resulting ions are collected

over time and measured by a current converted into a voltage[289]. FID has good sensitivity and detection range and is a universal detector for organic compounds[290,291]. However, it responds poorly to highly halogenated hydrocarbon gases, i.e., vinyl chloride and tetrachloroethylene. It is also destructive, so it cannot be connected directly to other GC detectors; however, an FID can still be used with another detector if part of the carrier gas stream is split between the FID and the other detector[292].

The TCD, also known as a Katharometer, is a bulk property detector and a chemical-specific detector commonly used in GC. TCD works by having two parallel tubes containing gas and heating coils. Gases are analyzed by comparing the heat loss rate from the heating coils to the gas. Normally one tube holds a reference gas, and the sample from the column is passed through the other[293,294]. TCD is a good general-purpose detector for initial investigations with an unknown sample. It responds to all compounds, thanks to the fact that all compounds, organic and inorganic, have a different thermal conductivity from helium. The TCD is also used to analyze permanent and inorganic gases (for example, argon, oxygen, NO, CO_2, CO, SO) because it responds to all these substances, unlike the FID, which cannot detect compounds that do not contain carbon-hydrogen bonds[295,296]. A disadvantage of TCD is that it is less sensitive than the other detector and has a larger dead volume; therefore, it will not provide as good a resolution as the FID. However, combined with thick film columns and correspondingly larger sample volumes, the overall detection limit can be similar to an FID.MS is amongst the most powerful GC detectors. Unlike others, it can perform both highly sensitive quantitative and qualitative analyses. For example, it supersedes the classical detectors described above due to its unsurpassed capability for structural analysis[297]. When coupled to GC, it ionizes the gaseous eluted compounds from the column, separates the ions in

vacuum based on their mass-to-charge ratio and measures ion intensity[298,299]. Peak retention times and mass spectra are obtained, which are used to identify the compounds[300,301]. Although MS can provide highly quantitative and structural information on compounds within samples, a high level of skilled expertise is required to interpret spectra and assign structures. Even at that, not all compounds can always be identified with high certainty[62].

For VOC profiling in indoor environments, both FID and MS are frequently employed as detectors[302]. The monitoring of VOCs in the indoor air of 9 homes was accomplished using an active sampling approach using sorbent tubes packed with Tenax, followed by GC-FID analysis[303]. 12 target VOCs, benzene, toluene, ethylbenzene, xylene, styrene, benzyl alcohol, and d-limonene, were selected as compounds of interest because they are known to be emitted in high abundances from products widely used at homes like cleaning and personal care products. The most abundant detected VOC in all dwellings was d-limonene (mean: 231 $\mu g/m^3$; maximum: 611 $\mu g/m^3$). All the other targeted compounds were monitored at concentration levels 1-2 orders of magnitude lower. They were generally comparable with those previously reported. In another study, GC-FID was used for analyzing BTEX concentrations in beauty salons[304]. Sampling was via charcoal active sorbent tubes. The concentration of most BTEXs in this environment was lower than guideline values, with only benzene concentrations being higher than recommended levels by Health Canada[305]. In another study, the exposure levels to BTEXs within dwellings in residential, roadside, industrial, and agricultural (rural) areas in an Indian city were assessed again via sampling with activated charcoal tubes followed by GC-FID analysis. The samples were taken fo once a week over a year, and toluene was found to be the most abundant pollutant in roadside and agricultural area homes.

GC-MS has also been used mostly for untargeted analysis of VOCs. For example, the range of VOCs emitted from five edible oils (canola, soybean, peanut, corn, and lard) was studied using GC-MS using an active sampling method with Tenax[306]. The results indicated that the total concentrations of VOCs emitted from soybean oil increased significantly from 8.5 to 75.5 mg m^{-3} when the cooking temperature was increased from 130 to 270 °C. Aldehydes were the most abundant VOCs species detected, accounting for 42.1%–74.6% in the temperature range 130–270 °C. GC-MS has also been used to study the VOC emission profile from 3D printers using different print filament materials in indoor settings [233]. VOCs detected in this study in the most significant quantities included caprolactam from nylon-based filaments, styrene from ABS and high-impact polystyrene (HIPS), and lactide from PLA filaments. GC-MS was used to profile indoor VOCs and aldehyde contamination status in energy-efficient homes in another indoor air application. Passive samplers for VOCs (carbon molecular sieves) and targeted passive samplers for aldehydes (DNPH-impregnated silica gel) were used to collect samples in 169 homes[307]. Energy renovation and the absence of mechanical ventilation were associated with higher indoor levels of formaldehyde, toluene, and butane for homes in the study built between the 1950s and 1990s, as they had higher TVOCs and formaldehyde concentrations than homes built during other periods.

An emerging trend in GC analysis is multidimensional GC (GC×GC), where two columns with different polarities (1D and 2D columns) are connected in series by a modulator. The modulator is used to periodically transfer fractions of analytes from the 1D column effluent to the 2D column. Analytes that cannot be separated in the 1D column due to a similar physiochemical property have the opportunity for separation in the 2D column based on differences in other properties. For example, GC×GC has advantages, such as higher chemical resolution, higher peak capacity and structured chromatograms with organic classes regularly distributed. The

addition of an MS detector to GC×GC provides increased capability to identify minor components, thus enabling various data processing methods, including target analysis, the group- type analysis, and nontarget analysis.

Coupling mass spectrometers (GC-MS/MS) in series with GC provides another technique with many advantages for analyzing target compounds in complex mixtures. The targeted compound is selectively ionized. Its characteristic ions are separated from most of the mixture in the first MS. The selected primary ions are then decomposed by collision. From the resulting products, the final mass analyzer selects secondary ions characteristic of the targeted compound[308][302]. GC- MS/MS is well-suited to identify unknown volatile components using the mass fragmentation patterns and transitions associated with the unknown analysis.

A thermal desorption and quantification method by GC-MS/MS was developed recently and used to simultaneously quantify SVOCs (50 pesticides, 16 PAHs, 22 PCBs, seven phthalates, and five alkylphenols) in indoor air. Indoor air was collected on Tenax-TA passive samplers exposed for 15 days in 10 different homes. This method permits the determination of >100 pollutants in a single run, including those requiring a derivatization step, with very low quantification and detection limits that were not traceable using GC-MS[309].

Even though MS is a very popular GC detector in the case of complex samples, a multi-detector approach can permit more reliable identification of a broader spectrum of VOCs[310,311]. A multidetector GC obtains supplementary chromatographic data from the additional detector(s) in a single chromatographic run. This confirms the obtained results and has other benefits such as higher throughput, time, and labor savings[312]. The GC-FID-MS system is the most common multi-detector system: MS delivers data for component identification, and FID is used due to its wide quantitation response range for the quantitative

analysis and higher sensitivity[313]. GC-FID-MS was used in a study to characterize wood-

based material emissions in an indoor environment[314]. VOC sampling was performed using Carbotrap cartridges deployed passively for at least 72 h. A quantitative inventory of VOCs emitted by these wood-based products was proposed. Terpenes and carbonyl-based VOCs were the main identified and quantified species.

1.4.2.3 Real-time instrumental analysis of IAQ

There is a great advantage in deploying real-time instrumental techniques in the analysis of indoor air, especially given its dynamic nature. Proton transfer reaction mass spectrometry (PTR-MS) is an established method for the rapid and direct online monitoring of VOCs characterized by short response times and high sensitivity[10,315]. Moreover, technological developments, particularly the introduction of a time-of-flight (TOF) mass analyzer (PTR-TOF-MS), has significantly improved sensitivity and have resulted in ultra-trace level detection limits, pushing the boundaries of real-time analysis applications[315,316]. The GC RCP (Reducing Compound Photometer) is yet another real-time analyzer equipped with a uniquely designed hybrid U.V photometer. This analyzer is the ideal solution for measuring trace amounts of hydrogen, carbon monoxide, and select hydrocarbons.

In a controlled experimental setup using a PTR-TOF-MS, emissions from boiling, charbroiling, shallow frying, and deep-frying of various vegetables and meats and emissions from vegetable oils heated to different temperatures were investigated[317]. The results showed that emissions from boiling vegetables were dominated by methanol. In addition, significant amounts of dimethyl sulfide were emitted from cruciferous vegetables. Emissions from shallow frying, deep frying, and charbroiling were dominated by aldehydes of differing relative compositions depending on the oil used. SPME-GC-TOF-MS was used to obtain emission profiles of volatiles concerning temperature and the duration of 3D printing with PLA filaments. A CAR/PDMS SPME fiber was used for sampling[231]. The concentration of volatiles steadily

increased until the end of printing, with the most abundant VOCs released during the printing process being lactide (145 min), acetaldehyde (45 min), acetic acid (61 min), 2-butanone (73min), and the $(C3H3O)^+$ fragment (55 min). This is significant since acetaldehyde is considered a potential occupational carcinogen. However, its maximum concentration (~0.3 mg/m^3) remained below the threshold limit for occupational exposure of 45 mg/m^3.

1.4.3 Sensing technologies for indoor air quality monitoring

Real-time sensors are attractive for indoor environment monitoring, particularly in the home. Several low-cost consumer devices have been driven by standard sensor technology that can address this. Chemical and gas sensors have become an indispensable part of our technology-driven society. They can be found in pharmaceutical, food, biomedical, environmental, and security monitoring applications, to highlight a few[318]. Advantages of the established gas sensors on the market today include low cost of manufacturing, short response times, simple miniaturized designs, and good analytical performance in terms of sensitivity, selectivity, range, linearity, etc [319]. Coupled with recent advancements in mobile technologies, the Internet of Things (IoT), and machine learning, these sensors offer a low-cost solution for the real-time monitoring of IAQ[320]. A commercial example of an IAQ monitoring device is Eirdata, which provides real-time monitoring capability for CO_2, TVOCs, radon, and PM and calculates virus transmission and mold growth risks, helping consumers optimize IAQ[321].

The gas sensor plays a pivotal role in all environmental sensing, including indoor air monitoring[322,323]. Gas sensors are categorized mainly by their transduction principle, e.g., semiconductor, optical, electrochemical, and thermometric. During the past few decades, semiconductor metal oxide (SMO) gas sensors have become a robust technology for domestic, commercial, and industrial gas sensing applications[324–326]. SMO-based sensors are electrical conductivity sensors that detect target VOCs or other gases based on redox reactions. When the target gas absorbs onto a responsive SMO sensing film, it causes a change in electrical resistance, from which the concentration of that targeted gas can be determined[327,328]. Despite the simplicity of SMO measurements for use as gas sensors, the detection mechanism is complex and not yet fully understood. This complexity is due to the various parameters that affect the function of the solid-state gas sensors. These include the adsorption ability, electrophysical, and chemical properties, catalytic activity, thermodynamic stability, and the adsorption/desorption properties of the surface. SMO sensors have been successfully commercialized due to high sensitivity, fast response times, low maintenance and fabrication costs, and good portability[329]. However, SMOs ' selectivity, stability, and durability are less than ideal. The primary concern is selectivity, which is currently being addressed using sensor array structures[330,331]. When sensor arrays are used, collected data can be analyzed using post-processing techniques such as neural networks to understand the nature of the adsorbed gas response[329,332].

Several SMO sensor approaches in the research literature are related to IAQ monitoring. For example, to evaluate the performance of one SMO material for an air monitoring system, odorous pollution in an indoor environment was studied using the SMO of interest and compared to GC-MS analysis[333]. The sensing element of the sensor contains a metal

oxide semiconductor layer formed on an alumina substrate and an integrated heater. Active multi-sorbent bed sampling tubes for GC-MS analysis were also deployed. Samples were collected over 14 days. High aromatic hydrocarbons, alcohols, aldehydes, and carboxylic acids were detected. The detection range of the SMO and the GC-MS workflow demonstrated a good correlation (R^2=0.7466). In another comparative study, VOC monitoring was conducted in an office environment using SMOs with four gas-sensitive layers for three weeks[334]. Different analytical systems accompanied the tests (GC-MS, mobile GC-PID, and GC-RCP). The results showed quantitative agreement between analytical systems and the SMO gas sensors. Absolute concentrations obtained from the SMO sensors and the analytical systems are similar. Some offsets between the different analytical systems were noted. However, they were not higher than expected for trace gas measurements, even using high-cost lab analysis.

Electronic noses (E-noses), comprising sensor arrays and pattern recognition algorithms, are considered a potential way to balance the trade-off between cost and accuracy for daily IAQ monitoring[335]. E-noses do not detect individual VOCs but provide an olfactory signature (fingerprint) of the analyzed air. As well as SMO-based E-noses, a large diversity in E-nose sensor transduction exists, including acoustic, e.g. quartz crystal microbalance (QMB), calorimetric, and optical transduction has been developed over the years [336,337]. Among E-nose types, SMO sensors are the most widely used due to their capability of detecting organics and inorganics, high reproducibility (precision), and low manufacturing cost [338]. However, E-nose technology can suffer from sensor drift, poor selectivity, and environmental sensitivity (e.g., to humidity changes or interferents)[339,340].

The possibility of utilizing an SMO E-nose to detect and identify the genus of fungi in contaminated building materials were recently investigated, which involved performing the

analysis of the air in the vicinity of fungi potentially found in residential buildings[341]. The E-nose consisted of 8 SMO sensors. Analysis was also conducted using SPME-GC-MS. The studies indicated that the E-nose enabled distinguishing between the non-contaminated and contaminated samples, providing a basis for further developing fungi detection techniques based on this approach. A simple E-nose architecture was recently designed for evaluating indoors based on an array of SMOs. The sensor unit includes four sensors measuring air quality parameters such as CO_2, CO, $PM_{10.0}$, NO_2, temperature, and humidity[342]. The results showed the feasibility of these E-noses to detect CO and NO_2 at concentrations lower than IAQ threshold values, making them potentially suitable for integrating with heating ventilation, and air conditioning (HVAC) systems. In another report, an E-nose consisting of 5 SMO sensors mounted on an electronic board circuit was placed in an experimental room of 40 m^3 to understand its ability to monitor the typical indoor air VOC concentrations[343]. Performance was assessed in the presence of 5 VOCs, including toluene, xylene, acetaldehyde, acetone, and formaldehyde. To validate sensor responses, passive sampling and GC-FID were used. Only two showed a good correlation between the five sensors' analyzer measurements for injected VOC concentrations and decay. In addition, higher pollutant concentrations led to sensor saturation and convoluted responses, inducing lower correlations in sensor signals with analytical instruments.

Colorimetric sensors are optical sensors that have recently begun to be revisited as an analytical technique for the targeted identification of VOCs[344,345]. A typical colorimetric sensor consists of a color-responsive recognition element coupled with signal transduction and processing technology. The transduction and the processing elements can be simple optical sensors such as cell phone cameras, webcams, or scanners. Even in wearables, these small sensor devices have started to make inroads in the personal protection and environmental sensing markets. They have broad applicability as qualitative diagnostic sensors for compound

identification and discriminating components in complex matrices. Arrays of these sensors, referred to as colorimetric sensor arrays (CSAs), can enable pattern recognition. Arrays have been developed to detect target analytes using functionalized materials[346]. Analyte identification is based on a CSA response by performing chemometric image analysis on before and after images to look for the extent and pattern of color change[347]. This approach differs from conventional E-nose technology. It generally relies on the weaker and less specific intermolecular interaction, giving CSAs an advantage - the ability to exploit the chemical characteristics of target analytes rather than their physical properties, resulting in selective and discriminatory effects responses towards a wide range of VOCs [348–350]. However, from a practical perspective, one of the major shortcomings of CSAs is their inability to deliver a component-by-component analysis for mixtures of VOCs.

A colorimetric sensor for detecting an important indoor air pollutant, formaldehyde, was developed with an active sampling system[351]. The sensor was based on coating a silica substrate with a chemical mixture of hydroxylamine sulfate and thymol blue in a solvent mixture containing methanol-water and glycerol to give a color indicator that shows a distinct and selective color change upon interaction with formaldehyde. Colour responses were monitored using a webcam. The sensor showed high sensitivity to formaldehyde (30 ppb) and accuracy over a 0-750 ppb dynamic range with a response time of 2 min. It was not subject to humidity or interferences in air, making it suitable for continuous formaldehyde monitoring in indoor air. A recent colorimetric sensor platform was reported to characterize VOC emissions from heated cooking oils (sunflower, rapeseed, olive, and groundnut oils)[352].

array targeted VOCs commonly found in cooking oil emissions (aldehydes, ketones, and carboxylic acids) by incorporating pararosaniline, 4,4-azodianiline, and pH indicators sensing materials. These sensor responses suggested that heating sunflower oil produced higher volatile aldehydes than the other cooking oils under investigation, which GC-MS analysis validated. Another colorimetric method was recently reported for rapidly detecting trimethylamine. To develop these sensors, several dyes previously found to be broadly cross-reactive (i.e., in discriminating among toxic chemicals, 31 oxidants and 18 common organic solvents) 16 were optimized; these included acid and base-treated pH indicators, Lewis acids, redox-sensitive dyes, and chromogens, and solvatochromic dyes were formulated and printed within immobilization chemistries. Data acquisition was made in various ways - using a flatbed scanner and a mobile phone camera. Principal component analysis (PCA), hierarchical cluster analysis, and support vector machine analysis showed excellent sensor discriminatory power over a wide range of concentrations of triethylamine with error rates
<1%, indicating the robustness of the designed CSA. A field study was carried out where another CSA was deployed as a VOC detector to understand emission sources from day-to-day household activities[160]. The sensor array comprised pH indicators and aniline dyes. Pararosaniline and N, N-dimethyl-4,4'-azodianiline dyes were mixed with two acids (sulfuric or p-toluene sulfonic acid) in different ratios dissolved in a plasticizer and dissolved in sol-gel. When deployed in several households, the sensor response was shown to correlate with occupant activity (cooking and cleaning) and the building year of the house, highlighting the potential for these easy-to-use sensor arrays to provide real-time data to inform home occupants on temporal ventilation needs.

The Covid-19 pandemic has accelerated the public interest in monitoring home IAQ. It has driven the launch of several low-cost, miniaturized indoor air quality sensors capable of real-

time monitoring onto the market[353,354]. Therefore, there is still considerable scope for developing a more cost-effective, accurate, and reliable IAQ monitoring system. For example, suppose the quality of the measurements can be improved. In that case, sensors could become a game-changer in monitoring outdoor and indoor air pollution, personal exposure and health assessment, citizen science, and air pollution assessment in developing countries.

1.4.4 PM sensing technologies for IAQ monitoring

There are several instruments for measuring different characteristics of PM. The most critical measurements of particles are particle concentration and size. A particle size analyzer can determine the behavior of the particle in the air. In contrast, particle concentration measurements are important to standardize emission limits, guaranteeing air quality standards. These instruments vary in precision, accuracy, sensitivity (detection limits), time resolution, and cost. This section will give special attention to technologies for measuring particle concentration.

Indoor PM events are frequently time and space-specific, brief, intermittent, and highly variable[186], meaning that high spatial and temporal resolution measurements are necessary to understand the controls and influences on PM. High temporal resolution measurements are common practice, with any "real-time" measurement instrument providing sufficient resolution in most cases; however, spatially varying measurements are less common, with campaigns rarely deploying multiple sensors within a single indoor environment[136,355].

In concentration methods, the PM concentration is generally measured using four main metrics: particle mass (Pmass), particle number (Pnum), particle size distribution (Psd), and particle surface area. These instruments are based on different measuring principles and can be gravimetric, optical microbalance, or electrical. The following section defines these metrics

and briefly outlines some measurement techniques used to quantify the different PM parameters.

1.4.4.1 PM mass (Pmass)

PM mass (Pmass) is the most used metric to measure PM. Pmass concentration is the total mass of particles per unit volume ($\mu g/m^3$). Mass concentrations can be classified per specified size range, e.g., $PM_{10.0}$, and $PM_{2.5}$, defined as measurements including all $PM_{10.0}$ or $PM_{2.5}$ μm and smaller, respectively.

Pmass is measured using gravimetric and optical methods. This principle of gravimetric sampling consists of pulling air through a filter using a pump. The measured pump flow multiplied by the sampling time provides the sampled air volume. The weight difference of the filter before and after the sampling period provides the mass of particles sampled from the air. Dividing the sampled particle mass by the air volume results in the Pmass concentration. With this principle, a time-averaged mass concentration is obtained for sampling[356]. This technique is applied as a reference method by the US EPA[357]. Passive samplers have also been developed and are lighter (1–5 g), smaller (1.5–5 cm), and less noisy than pump-operated samplers[356]. However, they must be deployed for longer times. Once a sample has been collected and weighed, it can be further characterized using microscopy. The Pnum, Psize, shape, and structure of particles collected can be studied[358,359].

Optical methods are real-time and based on interactions of PM with light. They are based on the principle of measuring scattering, absorption, and extinction (the sum of scattering and absorption) to determine the Pmass of an aerosol. Scattering laser photometers can measure the intensity of scattered light in one or more directions using a photometer detector. The combined intensity of scattered light is proportional to the PM concentration within the optical

volume[360,361]. These photometer sensors can obtain real-time measurements with a frequency

of 1s and measure particles from ~40–100 nm upward in size. Measurement efficiencies are significantly lower at the smaller particle sizes. Therefore, optical Pmass sensors are often co-located with gravimetric samplers for calibration[362]. When choosing an appropriate Pmass sensor, there can be significant trade-offs as gravimetric sample analysis is labor-intensive and cannot be used to measure UFPs due to their low mass. Optical measurement efficiencies vary depending on the PM's optical properties and therefore do not provide absolute Pmass concentrations[363].

1.4.4.2 Particle number (Pnum)

Particle number (Pnum) concentration is the total number of particles per unit of air volume. Number-based measurements count all particles, regardless of how big or small they are. These measurements give us valuable insight into ambient and indoor air quality since they suggest the relative impact of specific pollution sources on a given location.

Pnum is also measured using optical and current methods. Optical particle counters (OPCs) work similarly to a scattering laser photometer with a diode laser shining on the optical volume. A photodetector measures the scattered flash. Unlike photometers, only one particle is illuminated at once. OPCs use a light source, usually a diode laser, to light a sample of particles at a given angle. Scattering laser photometers measure the intensity of scattered light in one or more directions using a photometer detector; the combined intensity of scattered light is directly proportional to Pmass concentration within the optical volume[364]. The size of the particle is proportional to the intensity of the flash and electrical current generated. Therefore, particles can be sized based on the amplitude of the current generated. OPCs are light, portable, rugged, and quiet; however, their main limitation is their inability to count particles < 300

nm[355,365]. To overcome this, PM can be grown by condensing vapors and then counted using a Condensation Particle Counter (CPC). Particles are grown by creating vapor from a working fluid (usually butanol, isopropyl alcohol, or water) that condenses onto the particles to grow in size and can be optically counted [366,367]. Once grown, the particles pass through the focal point of the laser beam and are individually counted. However, it should be noted that miniaturized CPCs are susceptible to counting errors when multiple particles are located together in the optical detection region, which is a common occurrence for concentrations >250,000 particles/cm^3 [368–370].

1.4.4.3 Particle size distribution (Psd)

Particle size distributions tell us how large or small the particles are in a given area. This data gives insight into the health hazards posed by pollution and the potential sources of pollution in a certain area (i.e., local and upwind).

Psd information can be obtained from scanning mobility particle sizer (SMPS), fast mobility particle sizer (FMPS), OPCs, aerodynamic particle sizer (APS), and passive air samplers[360]. SMPS is often the equipment of choice when conducting fundamental aerosol research, environmental and climate, printer emission, and inhalation and exposure studies. It is considered the most precise instrument for measuring Psd[371,372]. It is an electrostatic classifier connected in line with a CPC. In this system, the electrostatic classifier selects particles of a given size, and the CPC counts these particles. The FMPS differs from the SMPS by using an electrostatic classifier and multiple low-noise electrometers to measure Pnum and Psd in 5–600 nm. It has a 1s sampling frequency, making it suitable for measuring the temporal change in aerosol processes. However, the SMPS measures smaller particles ranging from a few nanometers to 1 μm, with higher accuracy than the FMPS[373].

APS sensors use particles' inertia to determine their size. Aerosol flows through a constricted nozzle to accelerate it. The particles in the aerosol then pass through two laser beams separated by 200 μm. The time difference detected between the two scattered light pulses determines aerodynamic diameter[374]. The SMPS with a range of 1–1000 nm is often paired with an APS (with a range of 0.5–20 μm) when Pnum and Psd >1000 nm are also of interest in studies[355].

PM monitoring is of interest in the domestic setting regarding human activities as a source. For example, understanding PM emissions during cooking processes have been studied widely. For instance, Pmass and Psd were tracked during cooking processes in one study using an OPC. Active gravimetric sampling was used to determine calibration factors[375]. The OPC used was able to detect $PM_{2.5}$ concentrations between 0.1 $\mu g/m^3$ - and 100 mg/m^3 at a sampling frequency of 6 s. The obtained data showed that the PM emission rate varies over time as a meal is cooked and is caused by various frying factors such as oil or fat, the pan temperature, and the pan type. When determining $PM_{2.5}$ exposure using an OPC, its measurements should be accompanied by those from a gravimetric sampler to provide a scale for OPC's measurements. In another example, an OPC was used to assess the efficacy of a commercial air purifier in a household environment concerning its capacity to reduce PM concentration[376]. Pmass concentrations ($PM_{10.0}$, $PM_{2.5}$) and Pnum in 7 size-fractions between 0.3 and 10 μm were measured. The measurements were carried out in a room of an apartment of about 40 m^3 for 24 h. The OPC results showed that the tested air purifier significantly reduced $PM_{10.0}$ and $PM_{2.5}$ by about 90% and 80%. In addition, a butanol-based CPC and an FMPS were used in another study to assess secondary UFP emissions from floor cleaning products in indoor conditions[377]. Pnum concentrations and Psd were measured simultaneously during simulated cleaning events. The CPC measured the number concentration of particles down to 4 nm in diameter with 1 s sampling time. The FMPS measured the Psd range 5.6-560 nm, with a similar sampling time. Ten out of twenty cleaning products were recognized as emitting products as a generation of

particles in their nucleation range (about 10nm) was measured. The emission factor of the emitting products ranged between 1.5 ×109 part/m^2 and 1.1 ×1011 part/m^2 and then led to a total Pnum concentration comparable to other well-investigated indoor sources when cleaning the entire floor area of a typical dwelling.

UFP and PM size dynamics emitted from candles have been studied within a home setting[378].

The study used an SMPS equipped with a classifier and a DMA, a combination that created a

Psd quantification range of 2.5-64 nm. A second portable CPC with a lower cut-off of 10 nm was deployed to validate SMPS measurements > 10 nm. Single candles burnt in living rooms with mostly open interior doors could be expected to Pnum in order of magnitude of 300-400 m^{-3} which would also exceed average background concentrations of <10 000 cm^{-3} [378]. The physical properties of indoor PM were measured in an apartment located in an urban background site in Prague[379]. An SMPS measured the Pnum distribution (14.6–850 nm). Larger particles were measured by an APS (0.54–18 μm). The total Pnum max was 9.38 × 10^4, 2.89× 10^4, 2.25 × $10^{5,}$ and 1.57 × 10^6 particles/cm^3 detected after vacuum cleaning, smoking, incense burning, and cooking (frying) activities, respectively.

PM represents many components whose identity and source are poorly understood. Thus, as new measurement technology emerges, it must be adapted to maximize the existing measurement platforms' information-gathering capacity and utility. In addition, the development of accurate, real-time instruments opens the door to measurements with better spatial resolution and coverage, with higher reliability and operational simplicity. However, developing particle measurement strategies and systems for indoor application is substantially different from those encountered with VOC monitoring. Also, with PM measurements, it is important to understand the Pnum, Pmass, Psd, and chemical composition of each particle [380].

Moreover, These sensors can also be affected by humidity and temperature, and the same set

of sensors can perform inconsistent yield[381,382]. These issues make developing sufficiently sensitive sensors when measuring over a large range of concentrations and size ranges of PM more challenging.

1.4.5 PM sensors for IAQ monitoring

Low-cost, portable sensors capable of measuring high temporal PM concentrations have been at the forefront of meeting the rapid increase in public awareness and interest in PM and IAQ, particularly recently due to Covid-19. These sensors are based on the light scattering principle. The cost of these sensors can be up to 300 times lower than the standard/reference PM monitoring instrumentation. In addition, the broad deployment of these sensors in homes has become feasible[383]. This, amongst other things, has created an awareness of IAQ and enabled homeowners to understand PM sources and levels in their domestic environments[384].

Based on the light scattering principle, PM sensors use a focused beam of visible or infrared light through an aerosol, and a photodetector monitors the intensity of the PM scattered light in a selected direction. PM sensors are classified into volume scattering devices and optical particle counters (OPCs). The light is scattered from the ensemble of particles in the former. The photodetector provides a single digital or analog output. The output reading is converted to a Pmass concentration for different size ranges. OPCs count and estimate the sizes of individual particles, and the readings are converted to a Pmass concentration based on the assumption that the particles are spherical and of consistent bulk density. OPCs are limited in size ranges. They can detect as particles <0.3 μm cannot scatter light sufficiently, while PM
>10 μm is not easy to draw into the sensor[385,386].

The utility of a low-cost wireless sensor network to measure PM levels in households using cookstoves was demonstrated to provide insights into the Spatio-temporal distribution of

indoor air pollution[363]. In this case, multiple low-cost PM sensors were deployed to obtain $PM_{2.5}$ concentrations. A laser photometer was also used, recording reference measurements to evaluate sensor performance (R^2=0.713). The obtained data demonstrated low spatial variability within the kitchen due to its small size, poor ventilation, and high Pmass concentrations similar to those found in the kitchen in the adjoining rooms due to insufficient ventilation from open doors and windows. The results indicated the importance of Spatio-temporal measurements, which provided insights into the effects of multiple factors such as the household layout and ventilation characteristics.

Another $PM_{2.5}$ sensor was used to collect real-time $PM_{2.5}$ concentrations simultaneously at 15 indoor and one outdoor sites in a single apartment[387]. Deployed sensors measured particle numbers of three particle size ranges, i.e., 0.3–1.0 μm, 1.0–2.5 μm, and 2.5–10 μm, providing Pmass concentrations for $PM_{1.0}$, $PM_{2.5}$, and $PM_{10.0}$. It was found that indoor PM predominantly originated from outdoor infiltration and cooking emissions.

The performance of 6 commercialized optical PM sensors designed for home use was assessed by comparing their output to reference $PM_{2.5}$ and PM_{10} measurements from 21 common residential sources[388]. Sensors selected for testing met the following criteria: (1) capable of measuring $PM_{2.5}$; (2) report Pmass concentrations; (3) display real-time data. Reference measurements were obtained with a professional-grade aerosol photometer. All sensors had semi-quantitative responses (within a factor of two compared to reference measurements) to

sources like vacuuming, combustion products, and cooking but had low or no reactions to sources for which emitted Pmass was in PM < 0.25 μm, including candle burning and cooking without frying or grilling.

Three other $PM_{2.5}$ sensors were evaluated in an occupied, non-smoking residence over 12 months to assess the sensors, the built-in calibrations, and the need for additional data to achieve high accuracy for long deployments[389]. Sensors were deployed in the living room. A light-scattering nephelometer reference instrument with time-resolved and filter-based measurements was also deployed and operated for about a week each month. Two of the sensors exhibited high R^2 values against the reference instrument at the beginning and end of the measurement year, showing good potential for use in scientific research. However, only one of the three sensors exhibited high accuracy without any post-processing or additional measurements, indicating the need for calibration of each of the sensors before the data can be used to evaluate residential exposures.

Improving the portability and reducing the cost of sensors for measuring gaseous pollutants and PM without sacrificing selectivity and sensitivity is currently the main challenge in IAQ. Sensor networks can offer unique environmental analysis opportunities if appropriate infrastructure is in place. For example, portable computing devices such as smartphones or tablets can form interactive, participatory sensor networks that could facilitate public and professional users to collect, analyze, and share a wide range of data.

1.5 Conclusions

IAQ has been largely ignored up to now. However, as we spend plenty of time indoors, especially in the pandemic era of COVID-19, it is vital to monitor the air quality we breathe

every day. Undoubtedly, low-cost sensors can enhance indoor air pollution monitoring by enabling mass deployment density and closely assessing the occupants' exposure levels. Due to their limited robustness and repeatability and the lack of widely accepted protocols for their testing and utilization, the technology does not appear mature enough to be used on a mass scale for regulatory or compliance purposes[390,391]. However, analytical, and laboratory-based machines are still the mainstream equipment applied to IAQ research

Chapter 2:

Monitoring of particulate matter emissions from 3D printing activity in the home setting

2.1. Introduction

There is an increasing interest in indoor air quality (IAQ). It is well-established that a wide range of indoor pollution sources, activities, and ventilation conditions can adversely affect health[55,392]. Airborne particulate matter (PM) has been highlighted as a critical pollutant in indoor air[393]. The damage caused by the inhalation and deposition of PM in the human respiratory tract is closely associated with PM size. Significant deposition fractions in the lungs are characteristic of submicron and ultrafine particles ($\leq$ 1 μm and $\leq$ 0.1 μm diameter, respectively)[389,394]. Indoor air pollutants in the domestic setting are linked to various sources, including building materials, soft furnishings, and occupants' activities such as cooking and cleaning[138]. Beyond traditional sources, deploying devices and new technologies in the domestic setting can require an impact assessment on IAQ[395]. Three-dimensional (3D) printers are one example of a technology product becoming increasingly prevalent in the domestic setting. Although initially intended for the rapid prototyping of commercial products in the industry, the progressive decrease in cost and ease of operation has led to a wide adaptation by the consumer market[221,396]. This upsurge in the deployment of 3D printers raises a significant health and safety concern for home users in terms of IAQ, especially given that low-cost 3D printers have no requirement for enclosures or built-in filtration or air cleaning systems[397].

Most home-based 3D printers are based on fused deposition modeling (FDM). The FDM printing process works by heating a filament material in an extrusion nozzle head to a temperature above the filament melting point, extruding onto a printer bed. It solidifies and forms a solid bond with the previous layer[233,398–400]. Although options for filament materials to use for FDM printing are widening, acrylonitrile butadiene styrene (ABS) and polylactic acid (PLA) have remained dominant filament materials. ABS is non-biodegradable and typically printed at 240–260 °C. PLA is a biodegradable plastic mainly derived from natural

sources and printed at lower temperatures, typically 200 to 220 °C. ABS has better mechanical strength and higher impact resistance than PLA and therefore tends to be better suited to printing goods that require resistance to pressure[224]. Published research has demonstrated that the thermal degradation of filaments in FDM printing releases sub-micron and ultrafine particles[222,223]. The filament type used primarily influences PM emissions from 3D printing[236,401]. In recent reports, printing with ABS filament resulted in 3 to 4 times higher emissions than printing with PLA, attributed to the higher extruder temperatures applied for melting ABS filament. Several studies have found that more significant amounts of smaller particles (less than <100 nm diameter) are emitted from ABS filaments than PLA[235,402,403]. Other studies have investigated the effects of filament color on PM emission. Significant differences have been noted and attributed to the different additives and pigments used[400,404].

Print settings such as extrusion and bedplate temperatures have also been investigated. Higher extrusion temperatures generally lead to higher PM emissions and a decrease in PM size, regardless of filament type[404]. Several papers have discussed that undisclosed additive in ABS result in the release of volatile semi-volatile compounds at extrusion temperatures. The nucleation and condensation of these compounds result in new particle formation and consequently higher PM emissions[227,405]. Other studies have reported that bedplate temperature can also impact PM emissions. The condensation of vapor emitted from bedplates at elevated temperatures increases the PM emission rate[227,233]. However, the effect has been determined to be relatively minor.

Many of the studies cited above were conducted in closed testing environments, including acrylic or stainless steel chambers[406,407]. However, there is little literature reporting the measurement of PM emissions from home 3D printers in real domestic indoor environments that demonstrate the direct impact on IAQ in the home and the potential for 3D printing to

increase PM exposure for the home user. This study aims to bridge the gap between 3D printing PM emission studies typically carried out in controlled laboratory environments in closed chambers and the real environment of an open setup used for 3D printing in a typical domestic setting. In this work, PM emissions were monitored over time during a 3D printing activity in a living room of a domestic house. PM emission profiles were collected using an optical particle counter during 3D printing with different filament types, colors, brands, and print settings to understand the impact of these factors on the resulting PM emission. Finally, a low-cost home-use IAQ sensor was investigated as a potentially affordable means for home users of 3D printers to monitor printer PM emissions.

2.2 Materials and methods

2.2.1 3D Printing domestic setting

To assess PM emission from 3D printing activity, printing was carried out in a family-sized living room in a domestic setting. No print enclosure was used. The room was 3.1 m × 5.5 m × 2.4 m in dimensions, or 41 m^3, with one door and two windows. During printing, ventilation was controlled whereby doors, double-glazed windows, and mechanical ventilation wereshut. The room temperature and humidity were kept at 18–20 °C and 50–60%, respectively. Air

exchange rates were not measured for this study; however, they should not be less than 0.3 l/s/m^2 for a domestic dwelling[94].

2.2.2 3D Printing procedure

The 3D printer employed in this study was a desktop home printer, Creality Ender-3 (www.l3D.ie). This fused deposition modeling (FDM) motorized printer has a single extruder nozzle, a heating bedplate (235 mm × 235 mm), an active cooling fan, and a hot-end fan. The cooling fan is located next to the extruder nozzle, operating consistently at a user-defined speed to cool the extruded filament during active printing. The hot-end fan is directed onto the motor to maintain its temperature.

A 3D cube test piece was printed for all studies (20 mm × 20 mm × 20 mm) using a gcode file, with a print duration between 27 and 36 min, depending on filament type and print settings. A range of print parameters was investigated (Table 2.1) for their impact on measured PM emissions. Certain settings were maintained constant throughout the study, as specified in Table 2.1. As a control for monitoring PM emissions arising from the printer itself, a blank print of the cube was carried out without filament and is termed a null print.

Table 2-1- Print settings used in PM studies

Print Settings	Value
Print speed (mm/s) *	50
Filament diameter (mm) *	1.75
Bed temperature (°C) *	80 (ABS) 50 (PLA)
Filament colour	white, yellow, black
Cooling fan speed (%)	0, 20, 40, 60, 80, 100
Infill density (%)	0, 20, 50, 80, 100
Extruder temperature (°C)	235-255 (ABS) 200-220(PLA)

*fixed parameters

ABS and PLA filaments were used in this study. Several different brands of black filament

materials were purchased from Two additional filament colors (white and yellow) for a single ABS and PLA brand were purchased. A summary of the filament materials investigated is presented in Table 2.2.

Table 2-2- A detailed list of tested filaments.

Filament	Brand	Color	Code
ABS	1	Black	ABSB1b
ABS	2	Black	ABSB2b
ABS	3	Black	ABSB3b
ABS	4	Black	ABSB4b
ABS	5	Black	ABSB5b
ABS	5	White	ABSB5w
ABS	5	Yellow	ABSB5y
PLA	1	Black	PLAB1b
PLA	2	Black	PLAB2b
PLA	3	Black	PLAB3b
PLA	4	Black	PLAB6b
PLA	5	Black	PLAB7b
PLA	6	Black	PLAB8b
PLA	6	White	PLAB8w
PLA	6	Yellow	PLAB8y

2.3 Particulate Matter Emission Monitoring

PM emission data were collected continuously using an optical particle counter/sizer (OPS) sensor (PC-4000, GrayWolf sensing solutions, Ireland) before, during, and after the 3D printing of the cube test piece. After each print was run, the room was ventilated until $PM_{0.3}$ returned to baseline (<10,000/ft^3) before starting the next print.

The OPS sensor used to monitor PM during 3D printing measured particle size ranges based on 6 custom binning channels, which were calibrated at 0.3, 0.3–0.5, 0.5–1.0, 1.0–2.5, 2.5–5, and 5–10 μm with a flow rate of 0.1 ft^3/min. The sampling interval was 90 s. The OPS sensor was placed 1 m directly across from the printer nozzle head, in line with the ISO 16000-1 recommendation[404]. Unless otherwise specified, all PM emission profile data reported in this paper are taken from a 0.3 μm channel, which provides a concentration of PM with a diameter of 0.3 μm ($PM_{0.3}$) passing over the sensor as a function of time. PM concentrations measured for the other channels, 0.3–0.5 μm ($PM_{0.5}$), 0.5–1.0 μm ($PM_{1.0}$), and 1.0–2.5 μm ($PM_{2.5}$), are given in the SI for reference. This study did not present responses from the other channels, 2.5–5 μm ($PM_{5.0}$) and 5–10 μm ($PM_{10.0}$).

A Cair sensor (NuWave, Ireland) was used as a low-cost home IAQ sensor to track PM emissions. This sensor measures PM from 2 channels 1–2.5 μm ($PM_{2.5}$) and 3–10 μm ($PM_{10.0}$). The flow rate of these sensors has not been disclosed. The sampling interval was 90 s, and the Cair sensor was placed 1 m directly across from the printer nozzle head, in the same position as the OPS sensor.

Three replicate prints were carried out for all tested print conditions. The averaged data for these replicate prints are plotted in all figures to describe the typical print profile. To visualize the repeatability of the PM emission profiles, a set of replicates for a specified set of print conditions is shown in Figure S1.

2.3.1 Results and discussion

2.3.1.1 PM emission profiles using recommended print settings

The $PM_{0.3}$ emission profile at all stages of printing the test cube was monitored using the OPS sensor for both ABS and PLA filaments using filament-specific recommended settings (Figure 1a,b).In the first instance, $PM_{0.3}$ was monitored to establish the background level (Region 1). As an additional control, null prints (no filament) were carried out under the same settings as the filament used. However, no significant emissions beyond baseline levels were observed. This trend was the same for other PM sizes measured by the OPS sensor, and these data are presented in Figure S2. The printing process was initiated with the heating of the bedplate (Region 2). In the case of ABS, the bed heating started at 30 min and was heated to 80 °C over 3 min. For PLA, the bed was heated to a lower temperature of 50°C over 90 s. Bedplate heating did not significantly impact PM emission background levels for either filament. However, there may be a minor impact on the ABS filament emissions observed in Figure 1a. This observed increase in PM emission, if confirmed, is negligible and may be an artifact related to the timescale of the data sampling interval (90 s). The extruder heater was switched on (Region 3). PM emissions increased steadily for both ABS and PLA filaments. Finally, the extruder temperature was programmed to increase the recommended temperature for both ABS (245 °C).

Moreover, PLA (205 °C) is related to the filaments' different melting points [408]. It can be seen that even before printing, the heating of the extruder resulted in a significant increase in $PM_{0.3}$ for both filaments. The time point where this occurs is the onset time for an observed elevation PM emission above the baseline level (OT_{PM}) in this study.

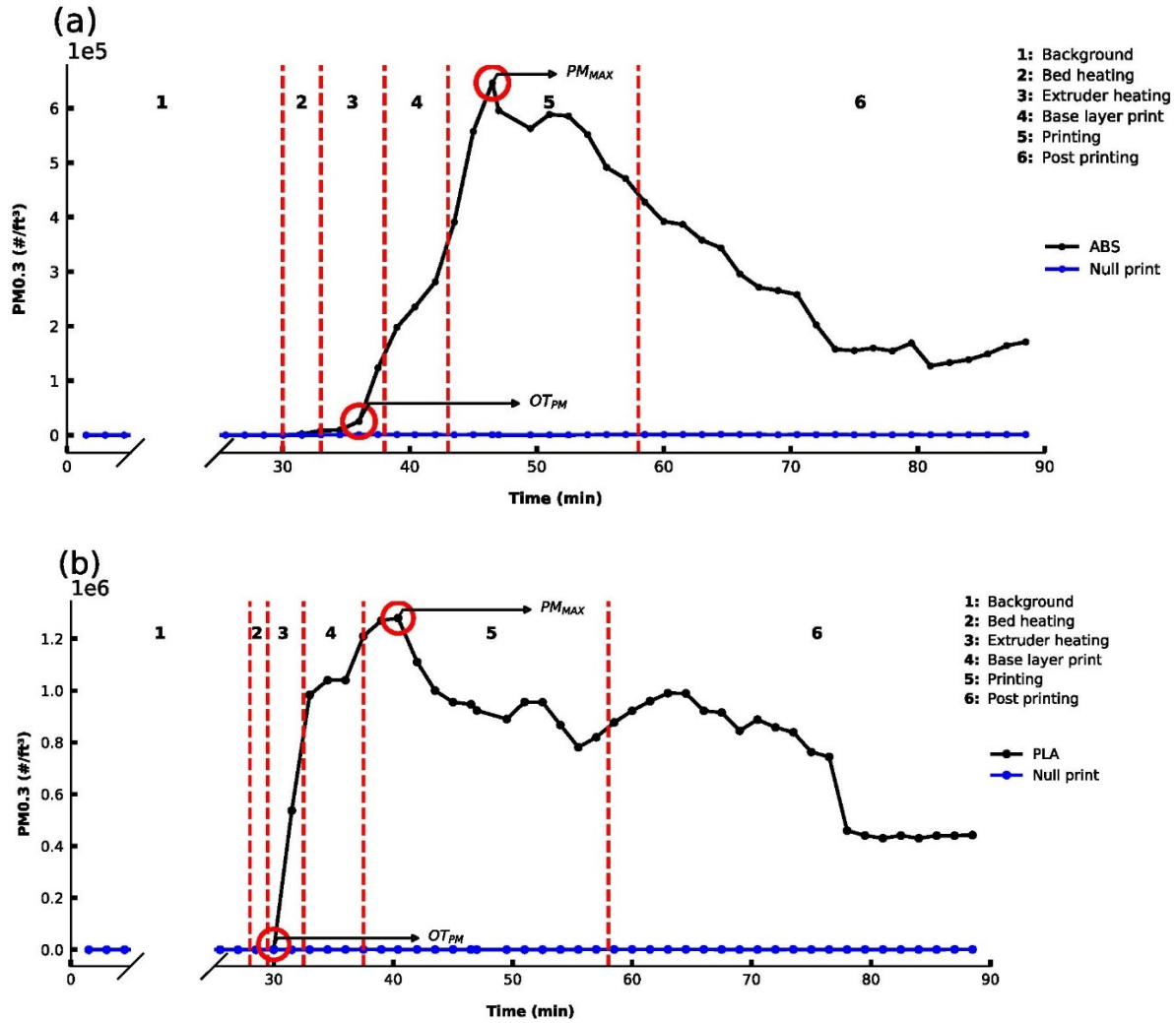

Figure 1-1- PM0.3 profiles over time before, during, and after printing of a cube (20 × 20 × 20 mm) for (a) ABSB1b (bedplate-temperature: 80 °C; extruder temp: 245 °C, 0% fan, 20% infill) and (**b**) PLAB1b (bedplate temperature: 50 °C; extruder temp: 205 °C, 20% fan, 20% infill).

The print process commences with a base layer print in region 4 (Figure 2.1). The base layer is 100% infilled and printed slower than subsequent layers to allow the filament to cool and adhere to the bed. It serves as the foundation layer for the object to be printed—the PM emission increases during the base layer print for ABS and PLA. Following Region 4, the bulk printing of the object is initiated at a pre-specified infill density (20%), and shortly after this initiation, the PM emission reaches a maximum emission (referred to as PM_{MAX}). The time point for PM_{MAX} is likely a result of a lag effect whereby it is the printing of the base layer that results in higher extrusion per area, leading to the PM_{MAX} occurring in region 5. The repeatability of this effect is also seen in Figure S2, where the same effect was observed for

PM emission profiles for other PM size ranges. The bridging effect causes this high emission during the base layer print. This arises from how the base layer is deposited through an initial outer 2D square frame followed by extruded filament lines bridging across the frame. This results in a high initial surface area of the structure, leading to a large amount of exposed heated filament, from which the PM emission occurs.

After the base layer print, bulk printing is carried out at the user-specified infill density (20%). Lower amounts of extruded filament are exposed per area than the base layer print during the bulk print, leading to the observed decay in PM emissions. The systematic decrease continues for the rest of the print and continues to decay post-printing (Region 6). The sharp decrease in $PM_{0.3}$ for PLA in Region 6 at approximately 80 min is unknown. However, the general trend within this region, which is post-print, is for the PM emission to decay. It is noted that the PM emission stabilizes at a level significantly higher than the background approximately 20 min after the print finishes. Indeed, it was observed that the decay back to baseline only occurred when ventilation was provided to the room by way of opening a window or door. Depending on the print carried out, this ventilation time ranged between 30 min and 4 h.

2.3.2 Impact of filament on PM emissions

2.3.2.1 Filament color

To investigate the impact of filament color on PM, the test cube was printed in different colors for both ABS (ABSB5b, ABSB5w, ABSB5y) and PLA (PLAB8b, PLAB8w, PLAB8y) and $PM_{0.3}$ emissions were monitored (Figure 2.2 a,b). It can be seen that the filament color

dramatically impacts $PM_{0.3}$ emission profiles for both filament types. Interestingly, the trend observed was different for different filament types. However, it is important to note that this study's ABS and PLA filaments were sourced from different brands.

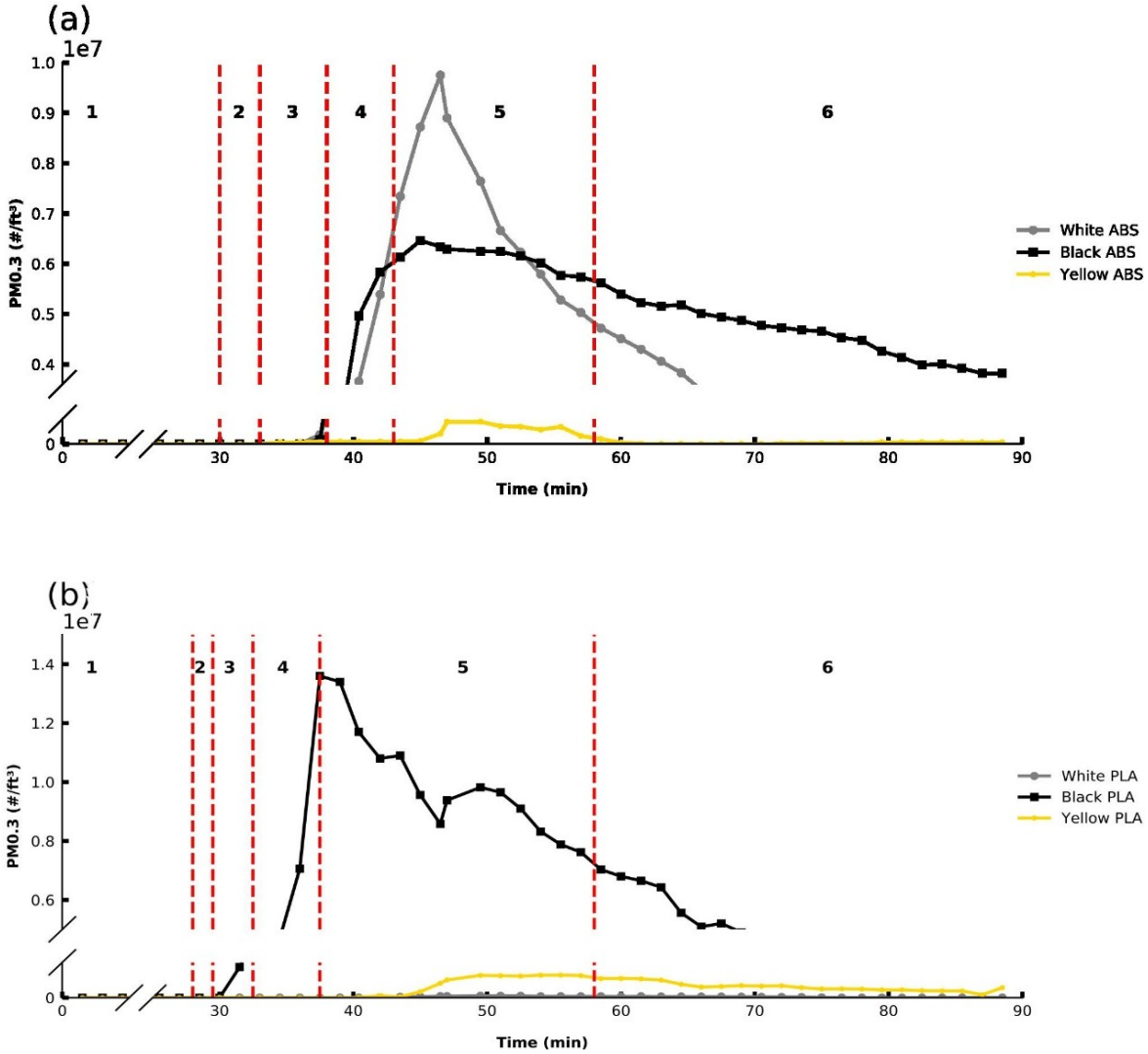

Figure 1-2-$PM_{0.3}$ emission of a cube in different colors for (a) ABSB5 (bedplate temperature: 80 °C, extruder temp: 245 °C, 0% fan, 20% infill) and (b) PLAB8 (bedplate temperature: 50 °C, extruder temp: 205 °C, 20% fan, 20% infill).·

The white filament exhibited more significant overall PM emissions than the ABS filaments, followed by black and yellow. The OT_{PM} and the PM_{MAX} emission varied considerably for the

different colors. OT_{PM} was the same for black and white (37.5 min), followed by yellow (43 min). OT_{PM} is related to the thermal stability of the filament and indicates that the yellow ABS filament is the most thermally stable. The PM_{MAX} emission is related to the pigment chemistry used and its susceptibility to produce PM and was observed to be highest for white, followed by black, and lowest for yellow when printing with ABS filaments.

Similar variability in PM emissions was observed for PLA filaments, where the black filament had the earliest OT_{PM} (34.5 min) and the highest PM_{MAX}. It should be noted that the PM_{MAX} for this filament was higher than for any ABS filament, despite it being printed at a lower temperature. The yellow and the white PLA filaments emitted lower $PM_{0.3}$ concentrations in comparison. The OT_{PM} was much later than other filaments for the yellow filament, not until Region 5 (40 min). The time point for the PM_{MAX} emission also occurs later. It has a significantly lower PM_{MAX} emission than the black filament. Finally, the white filament, printed under the same conditions, exhibited no OT_{PM} during the print. No increase from baseline $PM_{0.3}$ levels was noted for the print duration compared to all other filamentstested.

Overall, it is clear that there is wide variability in the impact of filament color and type on PM emissions, ranging from filaments that have a significant impact to those that do not appear to contribute significantly to PM levels in the home setting. These differences in PM emissions stem from different additives and pigments in the different colored materials. The observations are consistent with previous studies performed in closed chamber settings[402,408,409]. For example, Stefaniak et al.[232] reported that the number-based emission rates varied by up to nine when comparing the printing of black and white PLA filament materials. Although it is acknowledged that filament color significantly affects PM emissions, the mean particle size for both PLA and ABS has been reported to be equivalent[223,232,402,403].

2.3.2.2 Filament brand

The influence of the filament brand on $PM_{0.3}$ emissions was investigated for both ABS and PLA filaments, and black filaments were selected as both filament types showed significant $PM_{0.3}$ emissions for this color. Five ABS brands (ABSB1b, ABSB2b, ABSB3b, ABSB4b, ABSB5b) and six PLA brands (PLAB1b, PLAB2b, PLAB3b, PLAB6b, PLAB7b, PLAB8b), all black in color, were used to print the test cube and $PM_{0.3}$ monitored over time (Figure 2.3 a,b). The emissions data indicate that filament brand accounts for large differences in PM emission profiles during 3D printing.

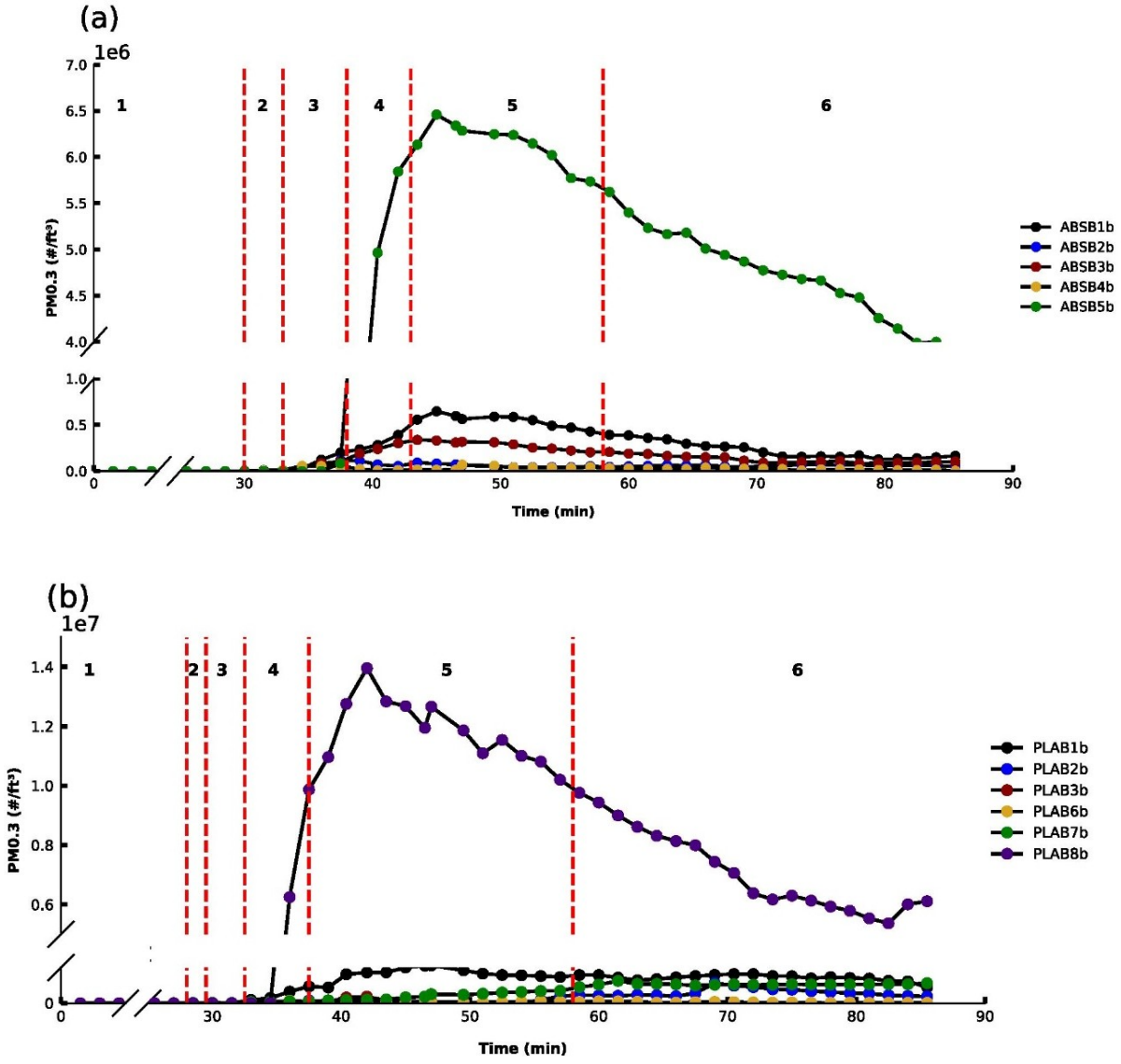

Figure 2-3- PM0.3 profiles for different brands for before, during, and after the printing of a cube for (a) ABSB1b, ABSB2b, ABSB3b, ABSB4b, ABSB5b (bedplate temp: 80 °C, extruder temp: 245 °C, 0% fan, 20% infill) and (b) PLAB1b, PLAB2b, PLAB3b, PLAB6b, PLAB7b, and PLAB8b)

For all ABS brands, similar emission profiles were observed whereby the OT_{PM} occurred in region 3, between 36 and 37.5 min, and PM_{MAX} occurred, as expected, early on in Region 5. However, there was variability in the $PM_{0.3}$ emissions profiles. PM_{MAX} for ABSB5b was approximately 10 times higher than for all other filaments. The PLA brand study also gave variable results, whereby the OT_{PM} occurred between 31.5 and 33 min. Most PLA filaments had low emissions over the entire print.

In contrast, one PLA brand (PLAB8b) had a PM_{MAX} approximately 10 times higher. These PM emission differences observed across brands can be explained because the type and loading of components within these filaments vary for different brands[410]. The additives' composition is not typically disclosed to consumers. More importantly, no awareness of the risks relating to the heating of the filaments and the corresponding emitted PM (and VOCs) is considered or disclosed to the home user.

2.3.3 Impact of user-controlled print settings on PM emissions

2.3.3.1 Fan speed

Printer fan speed on PM emissions was investigated as a parameter that the home user controls during printing. The fan is primarily used to cool the extruded filament as it prints. Recommendations around the use of the fan depend on the filament being printed and the structure of the piece being printed. Generally, the use of the fan is not recommended for ABS printing as ABS curing is sensitive to rapid losses in temperature, and utilizing a fan can lead to

delamination of the printed layers and structural integrity may be compromised. Therefore, the effect of fan speed was only investigated for PLA. The results shown in Figure 4 demonstrate a direct relationship between OT_{PM} (right axis, scatter plot) and PM_{MAX} (left axis, box plot) and fan speed setting during printing. Fan speed will influence the temperature cooling profile of extruded filament material, which will influence the direct emission rate of PM from the extruded material and may also affect the rates of SVOC emissions and thus particle formation rates. OT_{PM} was observed to increase with increasing fan speeds. Higher fan speeds potentially resulted in a cooling effect on the filament, shifting the OT_{PM} to later time points. PM_{MAX} emission decreased significantly with increasing fan speed, showing that fan speed can significantly impact a home user's PM exposure to PM during printing as a controllable print setting. Overall, increasing the fan speed in PLA printing significantly delayed OT_{PM} and lowered PM_{MAX} emissions.

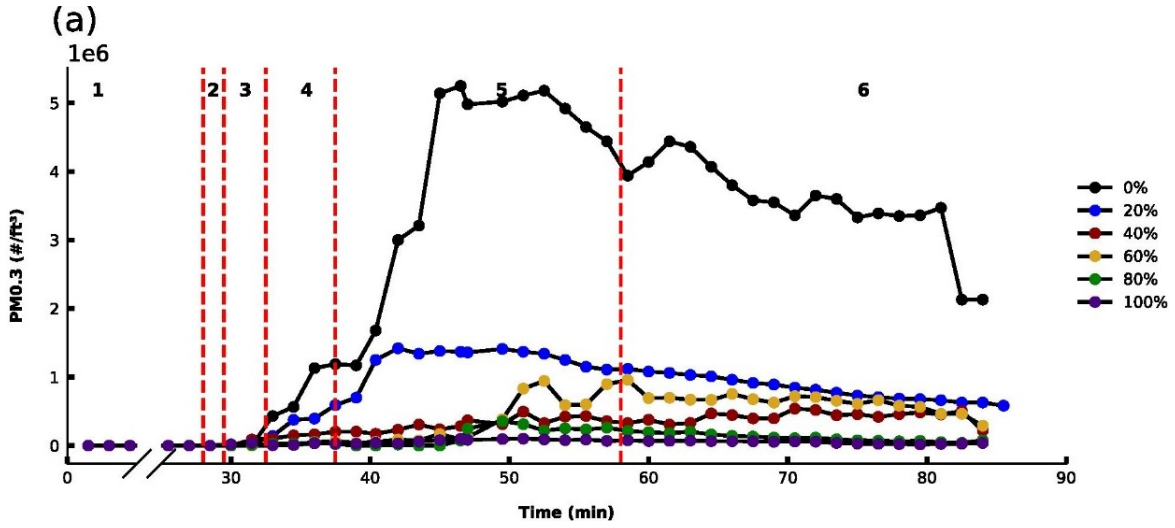

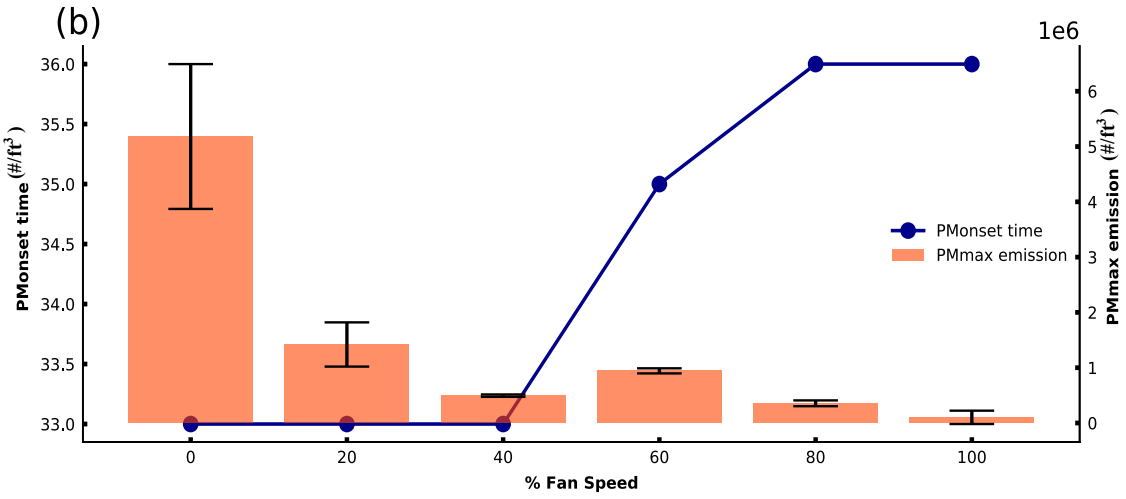

Figure 2-4- PM0.3 profiles for different Fan densities over time for: (a)before, during, and after the printing of the test cube using PLAB8b (bedplate temp: 50 °C, extruder temp: 205 °C, 20% infill), (b) OTPM (left axis, scatterplot), and PMMAX emissions (right axis, scatter plot)

2.3.3.2 Infill density

The effect of infill density on PM emissions was also studied. The infill density parameter plays an important role in the strength, structure, and buoyancy of a printed piece. It is widely used to reduce printing weight and time. The effect of changing infill density on overall PM emissions from the printing process is shown in Figure 2.5a. The results demonstrate that as the infill density was increased, overall PM emissions decreased. It should be noted that the bulk print time (Region 5) varied as a function of infill density, ranging from 28 to 36 min. This region is marked with blue dotted lines in Figure 5a.

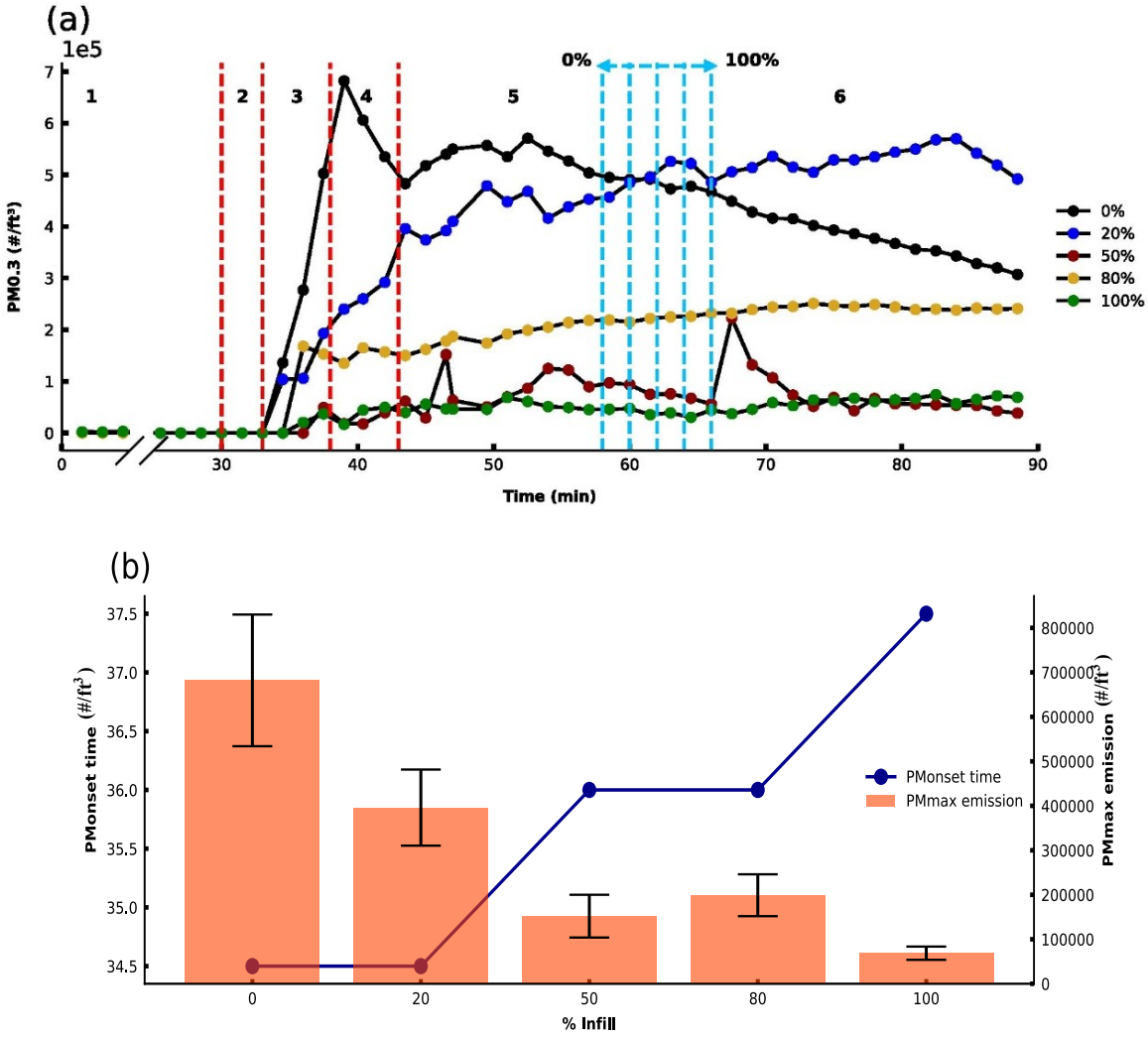

*Figure 2-5- PM0.3 profiles for different infill densities over time (a) before, during, and after the printing of the test cube using ABSB5b filament with printing end time marked within blue dotted lines (bedplate temp: 80 ℃, extruder temp: 245 ℃, 0% fan), (b) $PM_{0.3}$ OT_{PM} (left axis, box 1**(b)** $PM_{0.3}$ OT_{PM} (left axis, box plot), and PM_{MAX} emissions (right axis, scatter plot)*

2.3.3.3 Extruder temperature

Finally, extrusion temperature was investigated for its effect on PM emissions for both ABS and PLA filaments. Temperatures were investigated for each filament type within the recommended range of temperatures for the filament. As presented in Figure 2.6 a,b, the higher the extrusion temperature, the greater the overall PM emissions for both filament types.

For all temperatures investigated when printing ABS, similar emission profiles were observed. The OT_{PM} occurred in region 3 (between 34.5 and 36 min). When printing at higher temperatures, PM_{MAX} significantly increased and occurred later. The PLA studies exhibit similar results. The OT_{PM} is also seen in region 3 between 31.5 and 33 min. The highest PM_{MAX} values are observed when printing with higher extruder temperatures.

Previous studies have also observed this positive correlation between extruder temperature and PM emission profiles for different filaments[232,235,407], reporting that elevated temperatures lead to higher vapor pressures of the organic compound components, promoting particle formation.

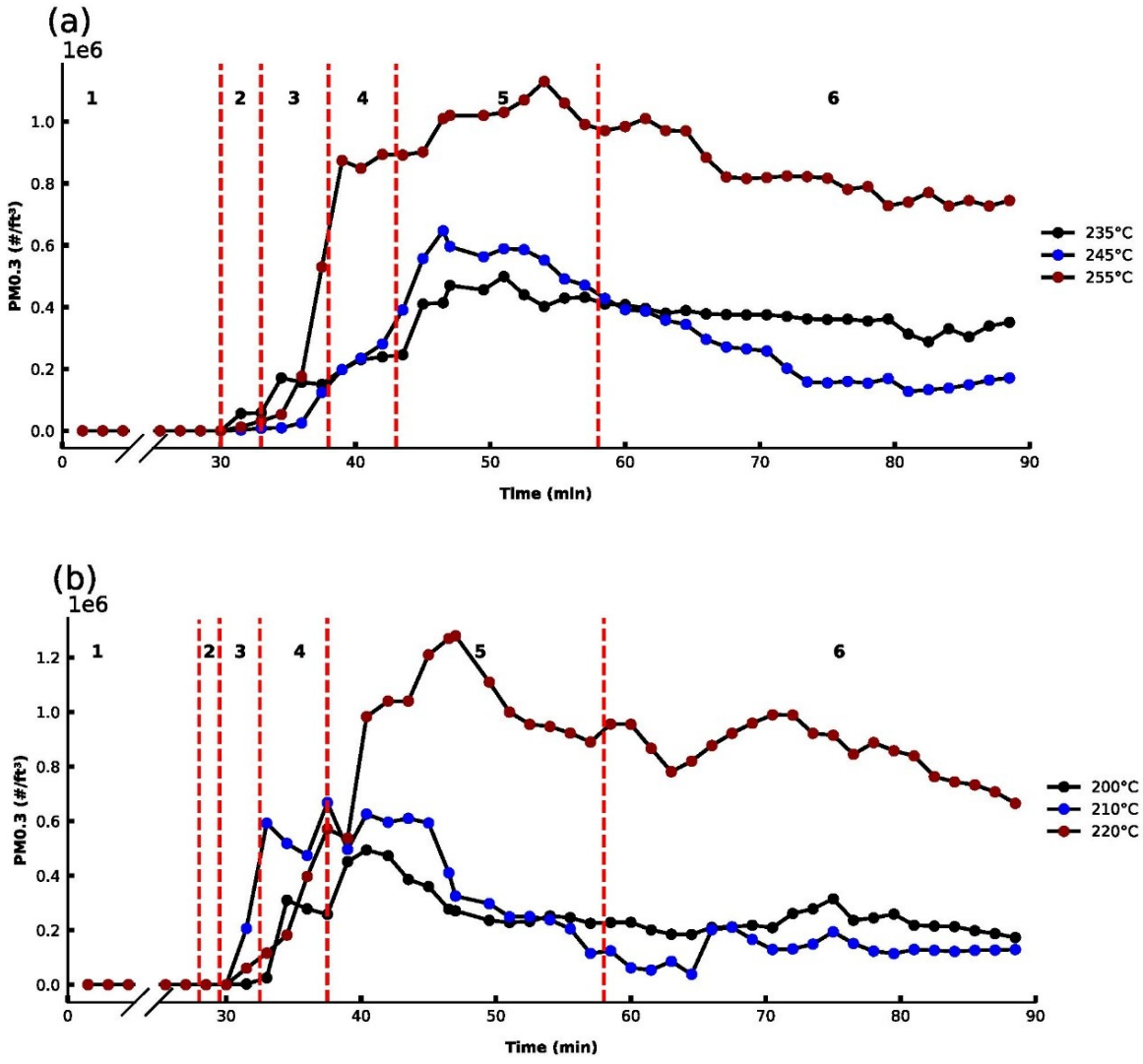

Figure 2-6- PM0.3 profiles for different extruder temperatures before, during, and after printing of a cube for (a) ABSB1b (bed plate temp: 80 °C, 0% fan, 20% infill) and (b) PLAB1b (bed plate temp: 50 °C, 20% fan, 20% infill).

2.4 Assessing the usefulness of low-cost IAQ sensors for PM emission monitoring during home 3D printing

Over the past decade, rapid advancements in sensor technology have led to commercially available low-cost sensors for air quality monitoring. The increased deployment of such sensors presents a new opportunity to improve air quality awareness and enable real-time personalized exposure monitoring[411,412]. These possibilities can only be fully realized if sensor precision is high enough to make the measurements meaningful[413]. To that effect, a commercial low-cost IAQ sensor (Cair sensor, NuWave, Dublin, Ireland) was investigated for its ability to track PM emissions from a home-based 3D printing activity. To investigate sensor response, the Cair sensor was deployed alongside the OPS sensor, and $PM_{2.5}$ channels were monitored during the 3D printing using both approaches. Note: the $PM_{2.5}$ channel was used to compare the Cair and OPS sensors, as the Cair sensor was not capable of $PM_{0.3}$ monitoring. It was shown previously that the profiles for different PM sizes (measured using the multiple OPS channels) were similar; however, it should be noted that the decay profiles following the PM_{MAX} were observed to be more rapid for larger PM sizes, specifically PM $_{2.5}$ (Figure S2).

PM2.5 data were collected using both sensors during numerous test cube prints (Figure 7) (print settings as per studies conducted in Section 3.2.1) to compare the OPS and Cair sensor responses. While the PM data shown here are collected for a range of print conditions, it is assumed there is no print condition influence (e.g., filament color, pigment, etc.) on sensor behavior; rather, the sensor responses are presented in this way to highlight their precision over a broad range of print conditions. Overall, the sensors showed consistent PM profiles for

each print. The OT_{PM} was very similar in all cases for both sensors, indicating that the low-cost IAQ Cair sensor could indicate to the user when PM is significantly increasing above baseline levels in a room. For example, the PM emission profile for the Cair sensor generally increased to a PM_{MAX} as expected. However, the time point when this occurs d for can differ by approximately 10 min relative to the OPS sensor. However, PM_{MAX} is approximately similar in magnitude for both sensors in most emissions profiles. The decay profile behaviors after PMmax different sensors for specific prints.

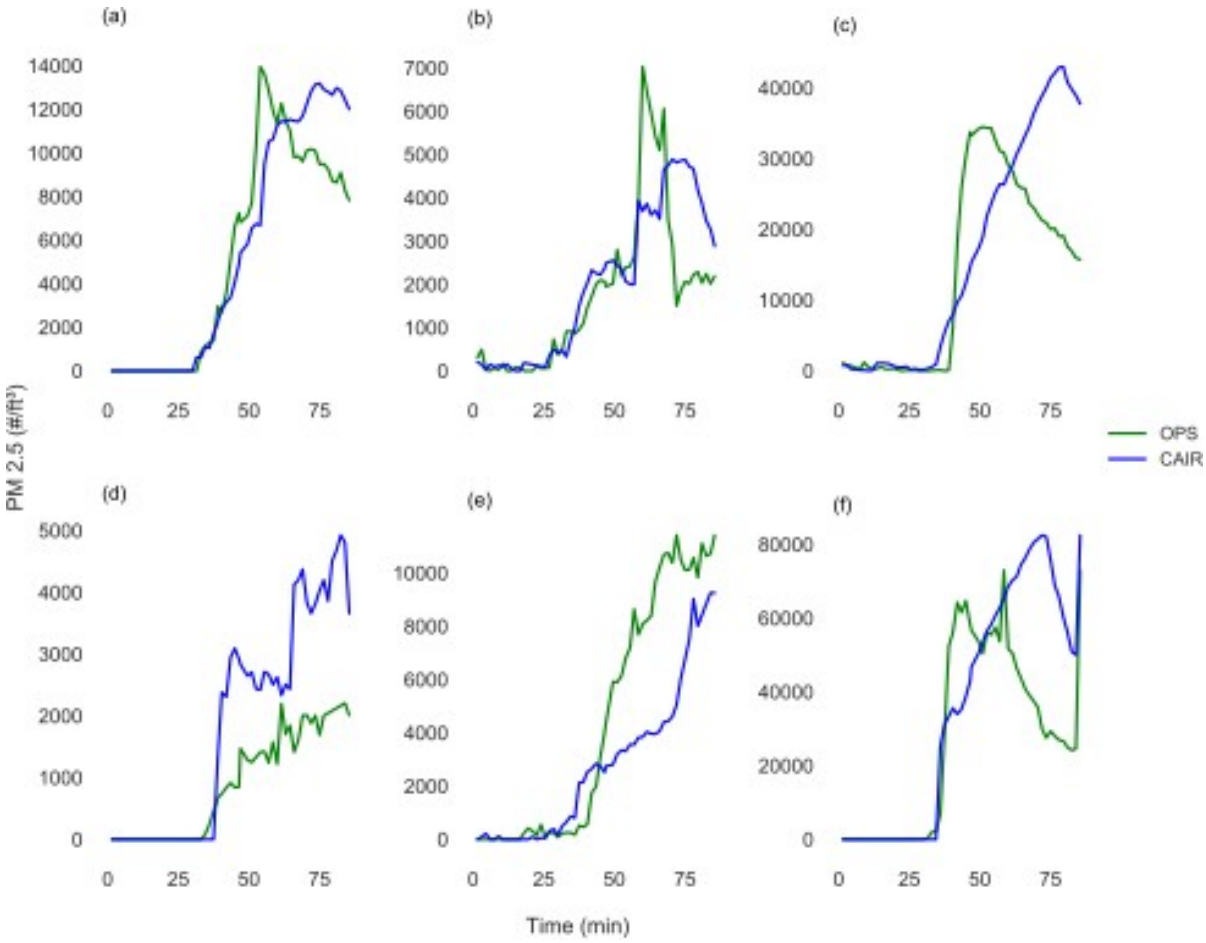

Figure 2-7- Comparison of PM2.5 emission profiles taken with the OPS and Cair sensors during the printing of the test cube using (a) ABSB5w, (b) ABSB5y, (c) ABSB5b, (d) PLAB8w, (e) PLAB8y, and (f) PLAB8b. Print conditions as stated in Figure 2.

Despite the differences between the Cair and OPS sensors, identifying the time there is a substantial increase in PM emissions (OT_{PM}) shows the value of using such a sensor for home PM emission monitoring during 3D printing. This would allow a user to ensure adequate ventilation once the OT_{PM} is reached (if they have not done so already) and allow the user to ultimately make informed choices about the filaments with which they print.

2.5 Conclusions

In this study, PM emission profiles from 3D printing activities undertaken in a domestic setting were investigated to assess the potential for 3D printing in the home to impact IAQ. 3D printing was carried out in an open format under various conditions, and the PM emission was monitored. Most studies on PM emissions from 3D printers have been designed in closed chamber settings, which are significantly different from that used by the typical home user. Therefore, the results of this study could be applied to investigate personal exposures to PM for 3D printer home users.

A range of print parameters within the home user's control was examined to determine how they impacted PM emission profiles. In addition to the overall profiles, quantitative measures of the PM emission profile were utilized (OT_{PM} and PM_{MAX}). Significant impacts on PM emissions were observed for many of the investigated parameters. For example, PM_{MAX} for one ABS brand was approximately 10 times higher than for all other filaments, and in case of colors, the white filament exhibited more significant overall PM emissions than the ABS filaments, followed by black and yellow. Therefore, according to our findings, The filament brand and color can dramatically influence the PM emission and influence personal exposure,

ultimately, user health. While the scope of this study was limited to sub-micron PM size ranges, further work will examine ultrafine PM and VOC emission profiles arising from 3D printing.

Using the approaches in this study, home users of 3D printers can be made aware of the potential impacts of print settings and filament types on PM emissions, helping the user make informed choices around the print parameters they choose. For example, to give users awareness of PM emissions during their printing activities, low-cost IAQ PM sensors have been demonstrated here as a viable way to monitor PM emissions during printing to alert the home user when increased ventilation into the space they are printing is needed. Findings from this study could serve as evidence to support the need for commercial suppliers of filaments to provide information on the PM emissions associated with their printing materials so that the potential for PM exposure can be considered by the user when making choices on filament use for their home-based printing activities.

Chapter 3:

Monitoring of volatile organic compounds emissions from 3D printing filaments

3.1 Introduction

It is known that the melting of polymer filaments during printing leads to the emission of both PMs and VOCs. The emission of PMs during printing has been discussed in several studies and the previous chapter. A comprehensive meta-analysis of the body of research around this area has also been tackled[407]. Previous studies have found that gas-phase emissions from 3D printers are complex and contain a mixture of VOCs, including odorants, irritants, and carcinogens. However, studies of qualitative and quantitative emissions of VOCs during 3D printing are relatively scarce. There have been several attempts to quantitatively characterize the emission of VOCs, predominantly in the form of TVOCs. However, several studies tackled the analysis and determination of emitted individual VOCs driven by the filament type[223,231,233,414]. In the following section, these studies, their methods, and their findings will be discussed.

In one of the largest studies on this topic, five commercially available desktop 3D printers from various manufacturers were studied [236]. Two printers were fully enclosed, one equipped with a high-efficiency particle air (HEPA) filter, and the others were designed to be used openly. Twenty different materials from ABS, PLA, nylon, and PVA from 8 different brands were sampled for 25 different print runs. All experiments printed the same object, a cube. Printers were placed in a standardized stainless steel environmental chamber. VOC samples were collected directly on a Tenax sorption tube with DNPH using a mass flow controller. Background samples were collected for 30 minutes during the pre-operation phase, with filament loaded in the chamber but without printing. The test sample was collected during the last hour of printing to capture the maximum chamber emission. After collection, the samples were thermally desorbed and further analyzed using GC-MS.

TVOC emission rate varied by filament, where ABS filaments generated 4.3 times higher TVOCs than PLA. TVOC emission rates of HIPS and ABS were similar. PVA emissions were comparable to PLA. A total of 216 individual VOCs were identified in the samples. ABS had the highest - 177 individual VOCs in recovered VOCs, followed by PLA with 57 VOCs. Caprolactam from nylon filament had an emission rate as high as 1749 μg/h, followed by styrene from ABS, with its emission rate being approximately 276 μg/h. The emission rate of lactide from PLA (111 μg/h) was less than half the emission rate of styrene from ABS. The overall profiles of recovered VOCs varied by the filament material. Common thermal degradation byproducts of filament monomers such as benzenes, toluene, xylenes, hydrocarbons, and aldehydes were also detected. Out of approx. 100 VOCs were recovered, and only 5 for PLA and 8 for ABS were consistently detected for each filament material. This inconsistency may be due to the wide range of chemical formulations for 3D printer filaments. Out of the most common individual VOCs emitted, 13 VOCs for ABS, 13 for PLA, and 11 for nylon have toxic, irritant, or odorant properties.

VOC ranges from 5 other desktop 3D printers were also studied using nine different filaments. All the measurements were conducted in a 3.6 m^3 stainless steel chamber[233]. The standardized sample from NIST was chosen as the printing object. Tenax sorbent tubes were used to sample chamber VOCs during the last 45 minutes of printing after the VOC concentrations reached a steady state. TD-GC-MS was used as the method of analysis.

The individual VOCs emitted in the largest quantities included caprolactam from nylon-based and imitation wood and brick filaments (ranging from ∼2 to ∼180 μg/min), styrene from acrylonitrile butadiene styrene (ABS), and high-impact polystyrene (HIPS) filaments (ranging from ∼10 to ∼110 μg/min), and lactide from polylactic acid (PLA) filaments (ranging from ∼4 to ∼5 μg/min). In this study, it was hypothesized that the filament material drove the majority

of differences in the types of VOCs emitted while printer make and model drove the majority of differences in the overall mass of VOCs emitted with the same filament.

In another study, real-time, quantitative monitoring of the composition of the VOCs during the heating of PLA filaments using the PTR-TOFMS method was used. The qualitative determination of the monitored compounds was confirmed using GC-TOFMS [231]. The filaments were from two grades called economy and premium, each in three colors: black, yellow, and neutral (white). SPME-GC-TOF-MS was used for the qualitative identification of VOCs. The most abundant volatiles emitted during 3D printing were lactide, acetaldehyde, acetic acid, and 2-butanone. The emission profile of the tested filaments was not very dissimilar. In both filament grades, the emission rate of lactide was approximately 20% lower in the white filament. One notable outlier was the emission of acetaldehyde in black economy filament, with its emission being nearly four times higher than that of other filaments.

Our study described in this chapter developed a novel method for characterizing VOC emissions from 3D printers and tested emissions for varying print conditions, including filament material, color and brand, and extrusion temperature. Systematically designed experiments were conducted using HS SMPE sampling. The qualitative determination of the monitored VOC was confirmed using the GC-MS method. Furthermore, the relationships between VOC and UFP emissions during printing have been discussed. A broad range of VOCs from 3D printing, including VOCs with potential health concerns, has been identified. With a better understanding of the emission levels from the tested printing conditions, our study could provide insight into evaluating potential health concerns and adds another piece to the difficult 3D printer emission characteristics puzzle.

3.2 Material and methods

3.2.1 3D printer and print chamber enclosure

The 3D printer employed in this work was a desktop home printer, Creality Ender-3 (www.l3D.ie), costing €215. This FDM ranked as the best budget 3D printer; the motorized printer has a single extruder nozzle, a heating bedplate (235 mm × 235 mm), an active cooling fan, and a hot-end fan. The cooling fan is located next to the extruder nozzle, operating consistently at a user-defined speed to cool the extruded filament during active printing. The hot-end fan is directed onto the motor to maintain its temperature. All printing was carried out in a self-designed print chamber. The chamber comprised two transparent plastic boxes

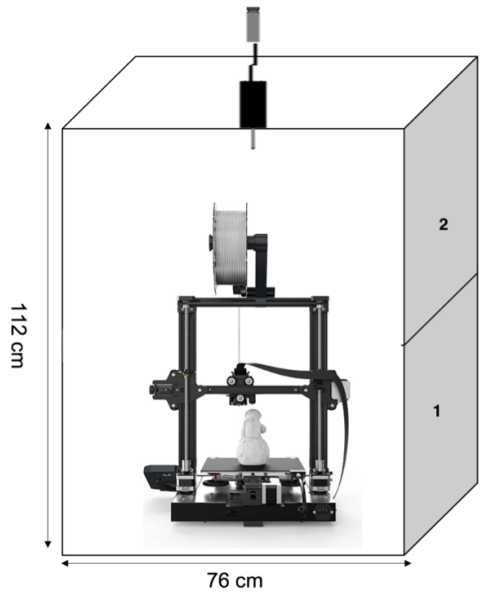

Figure 3-1- VOC experimental setup

(dimension: 780 × 560 × 430 cm to give a volume of 130 L). The Creality printer was placed in one of the boxes, and the other box was placed on top to create the enclosure of 260 L. the septum was fitted in a hole in the top box (Figure 3.1). The septum holding the SPME fiber was placed on the printer's top to asses the VOC emission.

3.2.2 Filament and printing object

A cube was 3D printed as the object for all VOC studies (20 mm × 20 mm × 20 mm) with print parameters set out in Table 3.1 using a gcode file, with a print duration between 27 and 36 min, depending on filament type and print settings. A range of printing temperatures was investigated for their impact on measured VOC emissions. In addition, certain settings were maintained constant throughout the study, as specified in Table 3.1.

Table 3-1- Print settings used to print objects for VOC emission study.

Print Settings	Value
Print speed (mm/s) *	50
Filament diameter (mm) *	1.75
Bed temperature (°C) *	80 (ABS) 50 (PLA)
Filament colour	white, yellow, black
Cooling fan speed (%)	0, 20, 40, 60, 80, 100
Infill density (%)	0, 20, 50, 80, 100
Extruder temperature (°C)	235-255 (ABS) 200-220(PLA)

ABS and PLA filaments were used for printing. Several different brands of black filament materials were purchased from [1–3]Two additional filament colors (white and yellow) for a single ABS and PLA brand were purchased. A summary of the filament materials investigated is presented in Table 3.2.

Table3-2. A detailed list of tested filaments

Filament	Brand	Color	Code
ABS	1	Black	ABSB1b
ABS	2	Black	ABSB2b
ABS	3	Black	ABSB3b
ABS	4	Black	ABSB4b
ABS	5	Black	ABSB5b
ABS	5	White	ABSB5w
ABS	5	Yellow	ABSB5y
PLA	1	Black	PLAB1b
PLA	2	Black	PLAB2b
PLA	3	Black	PLAB3b
PLA	4	Black	PLAB6b
PLA	5	Black	PLAB7b
PLA	6	Black	PLAB8b
PLA	6	White	PLAB8w
PLA	6	Yellow	PLAB8y

The temperature and humidity were constantly monitored within the chamber using a Cair sensor (NuWave, Ireland). This temperature increased from approx. 21°C ± 1 to 24 °C ± 1. After printing each test cube, the enclosure was opened and vented until the printer cooled down. The TVOC reported from the sensor returned to baseline before a subsequent test cube was printed.

3.2.3 Sampling procedure

VOC sampling was performed within the print chamber described above using an SPME fiber – divinylbenzencarboxyen/polydimethylsiloxane (DVB/CAR/PDMS), 50-30 μm (Supelco, Bellefonte, PA, USA), which was pre-conditioned for 20 min at 300 °C before use. Immediately after the printing of the object was complete, the SPME fiber was inserted into the print chamber through the septum positioned above the printer nozzle. It was left in place for 15 min unless otherwise specified. After sampling, the SPME fiber was retracted and removed from the chamber, and immediately analyzed via GC-MS. The print chamber was

opened up to allow the print head to cool down and remove VOC buildup. Once the enclosure was re-assembled, a background SPME sample was collected and analyzed to ensure the filament emissions were fully removed from the print chamber before the next print. The experimental setup is illustrated in Figure 3.1.

3.2.4 GC-MS analysis

Following sampling, SPME fibers were injected onto an Agilent 7890A series GC/MS (Agilent Technologies, Santa Clara, USA). Volatiles were separated using a mid-polarity capillary SLB-5ms column (30 m×0.25 mm×0.25 μm d f, Supelco, Bellefonte, PA, USA) with a film thickness of 1.8 μm. The carrier gas was helium at a 1 ml/min flow rate. VOCs were desorbed from the fiber in the GC injection port at 260 °C, and the injector was set in a splitless mode for 4 min. The oven temperature program was isothermal for the first 4 min at 35 °C, then raised to 120 °C at the rate of 5 °C /min, holding for 2 min, then raised again to 270 °C at a rate of 10 °C /min and held for 2 min, with the total running time approx 40 min. The transfer line to the MS was maintained at 250 °C. The mass spectra were obtained by EI at 70 eV and scanning over the mass range of 33-330 m/z.

3.2.5 Data analysis

GC-MS data were analyzed using Agilent MassHunter Acquisition Data Qualitative Analysis version 10.0 (Agilent Technologies). Features were identified by deconvolution, excluding ion 28 m/z with an area filter greater than 70,000 counts. Ions were extracted from 0.3 to 0.7 m/z, and the base peak shape was with a 25% sharpness threshold. The obtained spectra were searched using the NIST Mass Spectral Search Program for the NIST Tandem Mass Spectral

Library Version 2.3 (built May 2017). A minimum match score of 700 was set to accept initial identifications. The match score reflects how closely the sample spectrum and reference spectrum are compared and calculated using a built-in field[421]. Background samples were paired with the corresponding models for the analysis. All identified data for each of the pieces were then cross-matched with replicates. Compounds identified in at least 3 of the replicates were accepted along with their abundances as part of the refined data sets. They were considered for retention index (RI) matching. The usual approach to confirm compound identification is the measurement of retention indices of chemical compounds and comparison with available retention data collections. Compounds with retention indices ≤ 11 units of the RI values found in the NIST, the database was deemed as acceptable matches. A standard external mixture of saturated alkanes (C7– C30; Merck, Cork, Ireland) was injected into the GC-MS under the same temperature conditions as the samples and used for retention indices matching. This was done by rapidly dipping an exhausted SPME needle into the mixture and injecting it into the GC-MS. Note: fully functional SPME fibers were not used because hexane exposure can degrade fiber integrity.

3.2.5.1 Chemometric analysis

Data analysis was carried out using principal component analysis (PCA) and hierarchial clustering using the R (version 1.2.5033) packages: “FactoMineR” (version: 2.4), “factoextra” (version: 1.0.7), “heatmap” (version: 1.0.12), and “cluster” (version:2.1.0). Euclidean distance was used for the hierarchical clustering analysis to measure (dis)similarity. Other R packages used for the graphics in this study were: “ggplot2” and “ggfortify”. PCA, mentioned above, allows reducing the number of variables that characterize a set of data in a

a small number of components (principal components), which are linear combinations of the original variable, orthogonal among them, and ordered on the variance they subtract to the system. For example, the first two components describing most system variability may be represented as orthogonal axes, and samples may be projected in a bi-dimensional space. Data were further visualized using Tableau software (2021.2) to plot bar charts and clustered data.

An overall flowchart for the sampling, analysis, and data processing is presented in Figure 3.2.

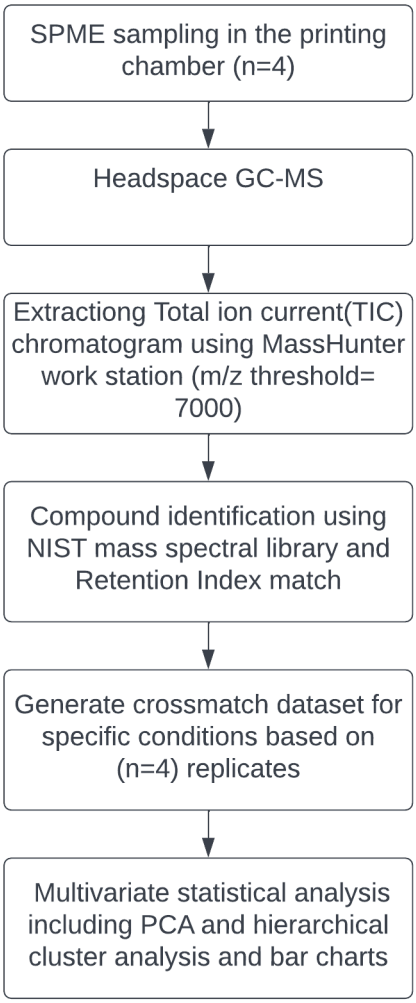

Figure 3-2- GC/MS data processing flow chart

3.3 Results & discussion

3.3.1 Method development

To assess the VOCs recovered from 3D printing using different filaments, a method was developed and optimized to sample VOCs from the print enclosure that served as the headspace (HS) for sampling. The technique used is described earlier in the Methods Section, where sampling of the HS was carried out directly after printing a cube object (20 mm × 20 mm × 20 mm). Following the print, a conditioned SPME fiber (triple phase to capture VOCs and SVOCs) was inserted into the HS via the septum placed above the printer. The method was optimized concerning extraction time to ensure the SPME fiber reached equilibrium with the HS and maximum extraction efficiency was reached under the conditions used. The sampling technique was also characterized by its reproducibility after replicating prints.

The number of chromatographic peaks detected in untargeted GC-MS is important to maximize. The greater the number of detected peaks, the greater the number of compounds trapped by the SPME fiber. The goal was to optimize SPME sampling time to obtain a high extraction efficiency within a reasonable time. Since SPME is an equilibrium extraction technique, the maximum amount of analyte that the fiber can extract is achieved at equilibrium time[415][422]. The amount of extracted analytes increases the distribution constant and equilibration time. Thus, a component with a high affinity for the fiber will reach equilibrium later than compounds with low affinity at the same concentration. When the system (that is, fiber, HS, and sample) comes to equilibrium, the amount of all analytes extracted should be approximately constant in all 3 phases and independent of the exposure time of fiber to the

model. As such, fibers were exposed to the chamber post-printing of the cube object for different periods (5, 10, 15, and 20 min). Each print run was carried out in triplicate. Figure 3.3 shows the representative effect of extraction time on recovered VOCs from one filament (PLAb1, see Table 3.2 for detail). It was observed that longer extraction times were required for an equilibrium where it can be seen that the less volatile, later eluting compounds were only detected after 15 min. At 15 min, the abundance of volatiles appeared to reach a steady-state, indicating equilibrium between the SPME fiber and the print enclosure. Thus, 15 min sampling time was chosen for all subsequent work.

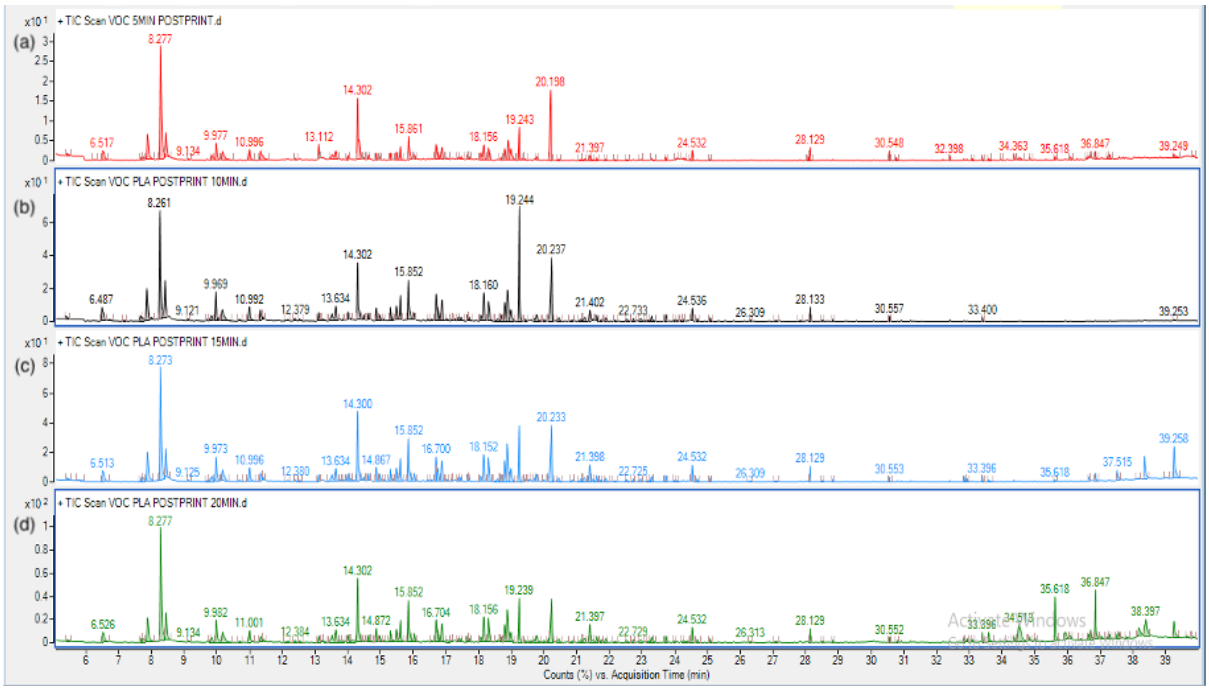

Figure 3-3- Total ion chromatograms (TIC) after sampling in the printer chamber HS post-printing of the test cube using filament PLAb1 for sampling times of (a) 5 (b) 10 (c) 15 and (d) 20 min.

Before deploying the method for detailed analysis of the VOC emissions, it was important to investigate sampling repeatability to ensure good confidence in the data. Repeatability represents variation in repeated measurements on the same sample[416]. To investigate this, a

replicate analysis (n=4) of the HS chamber post-printing with filament PLAb8 was carried out. The resulting chromatograms were analyzed (Figure 3.4) [417]. The data were normalized to the TIC and log-transformed to compare across data sets.

It can be seen that 3 out of 4 chromatograms are visually similar, with one of the replicates appearing significantly different (Figure 3.4)

where recovered VOC abundance in Figure 3.4, rep2 is significantly lower than in other replicates. For example, in the case of butanoic acid (RT being 14.7. 14,7, 14,73, and 14.72, respectively), the abundance was approximately three times lower in Rep 2 than in others. When considering all replicate data, the relative standard deviation (% RSD) for butanoic acid, o-xylene and TVOCs were 46%, 45%, and 36%, respectively. However, when Rep 2 was omitted from the dataset, %RSD values dropped to 12%, 10%, and 10%, respectively. Therefore, for all further analysis, when %RSD values were greater than 30%, the chromatograms were examined further to identify outliers and, if significantly different, were not included in refined datasets.

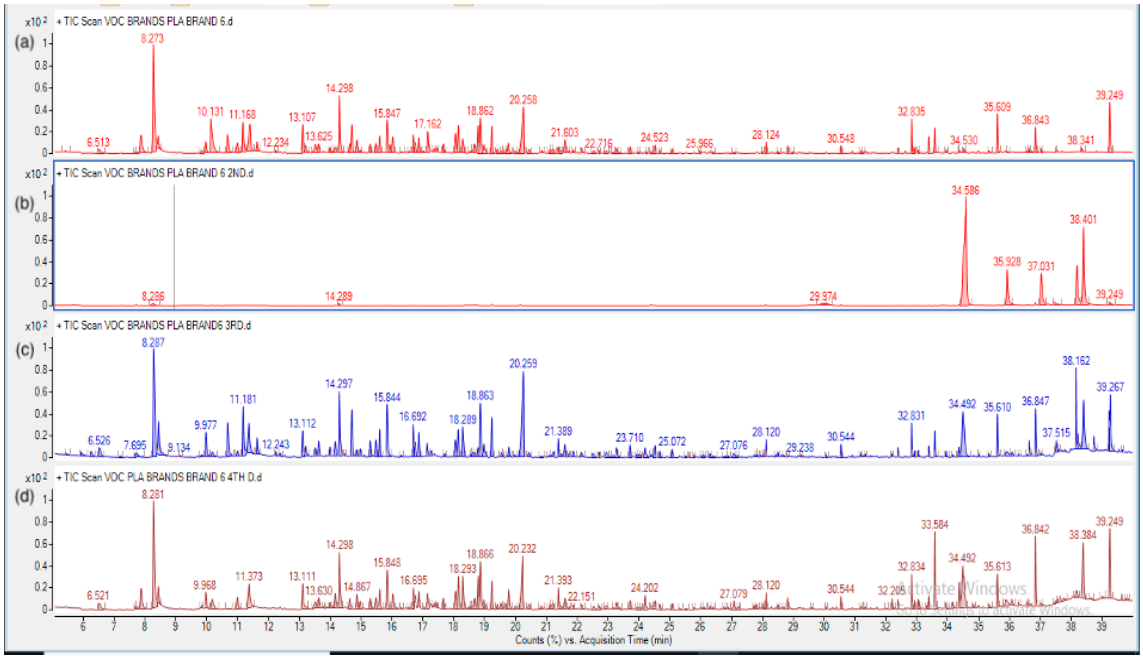

Figure 3-4- Total ion chromatograms (TIC) after sampling in the printer chamber HS post-printing of the test cube using filament PLAB8b for n=4 replicates: (a) Rep 1,(b) Rep 2,(c) Rep 3, (d) Rep 4. The sampling procedure and analysis are as described in 3.2.5 and analysis are as described in 3.2.5 and 3.2.6.

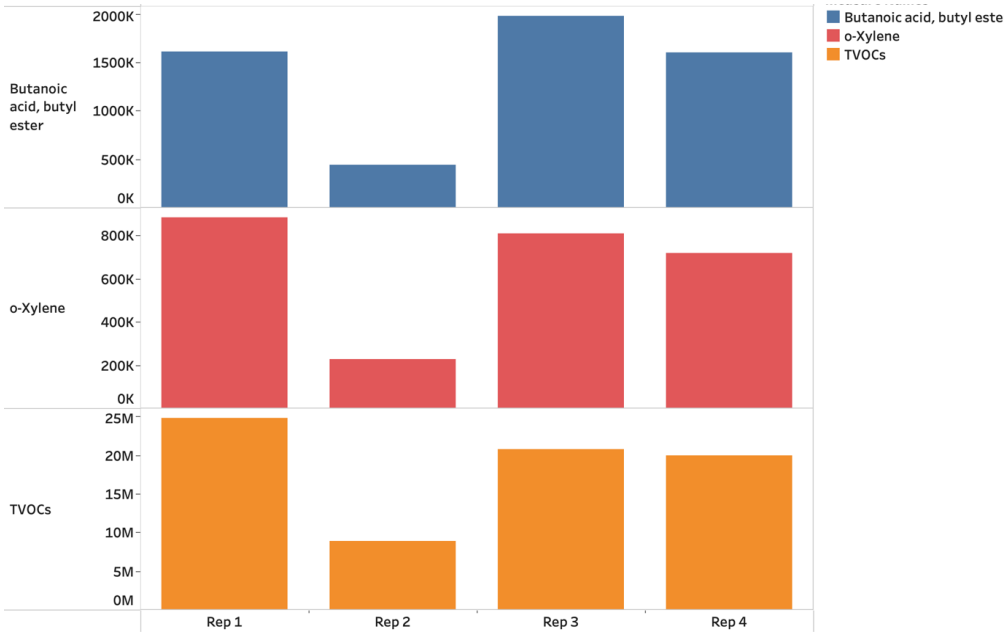

Figure 3-5- Recovered abundances of butanoic acid, O-xylene, and TVOCs for a set of replicate analyses (n=4) from Figure 3.4, represented in millions (M), and thousands (K).

The values in the y axis representants the abundance of each component. The abundance represents the area ,which is a reflection of the amount of a specific analyte that's present and it is based on the number of counts taken by the mass spectrometer detector at the point of retention.

3.3.2 Colour studies

Colour pigment and additives in the filaments are assumed to cause differences in emitted VOCs and their abundances. This impact was studied by printing the test cube in different colors for ABS (ABSB5b, ABSB5w, ABSB5y) and PLA (PLAB8b, PLAB8w, PLAB8y), where the emitted VOCs were recovered following the method described in sections 3.2.3 and 3.2.4. Figure 3.6 shows a PCA analysis used first to visualize the impact of filament type and color differences on VOC emissions. The plot shows some samples clustered more closely

together (PLAB8y, ABSB5w, ABSB5y) than others (ABSB5b, PLAB8w), indicating greater similarity in VOC emission profiles across replicates for some filaments compared to others. Comparing filament type and color, the different filaments were not classified as dissimilar, with many overlapping clusters observed.

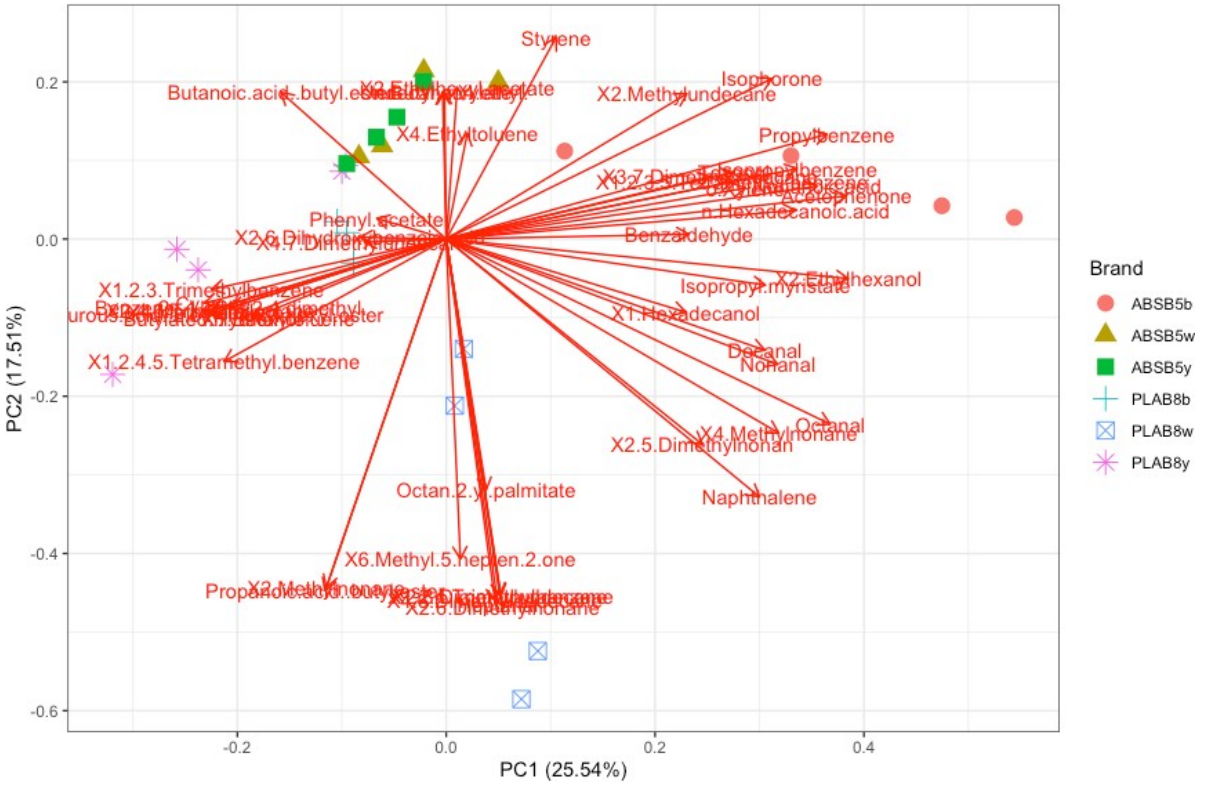

Figure 3-6- PCA scores plot for replicate datasets (n=4) for ABS and PLA filaments containing black, white, and yellow pigments. Principal component 1 (PC1) and principal component 2 (PC2) summarised 43% of the variance of the overall dataset, with 25.5% being summarized by PC1 and 17.5% being summarized by PC2.

Quantitative data was also depicted with hierarchical clustering analysis (HCA). Figure 3.7 shows the resulting dendrogram associated with the heatmap, where datasets were grouped based on their nearness or similarity. The heat map shows all recovered compounds from each of the filaments. However, ABSB5b was the most dissimilar of all filaments where significantly higher abundances of many compounds were recovered, including aldehydes such

as octanal and decanal and propanoic and octanoic acids BTEX, which has been grouped as a carcinogen by the IARC[56].

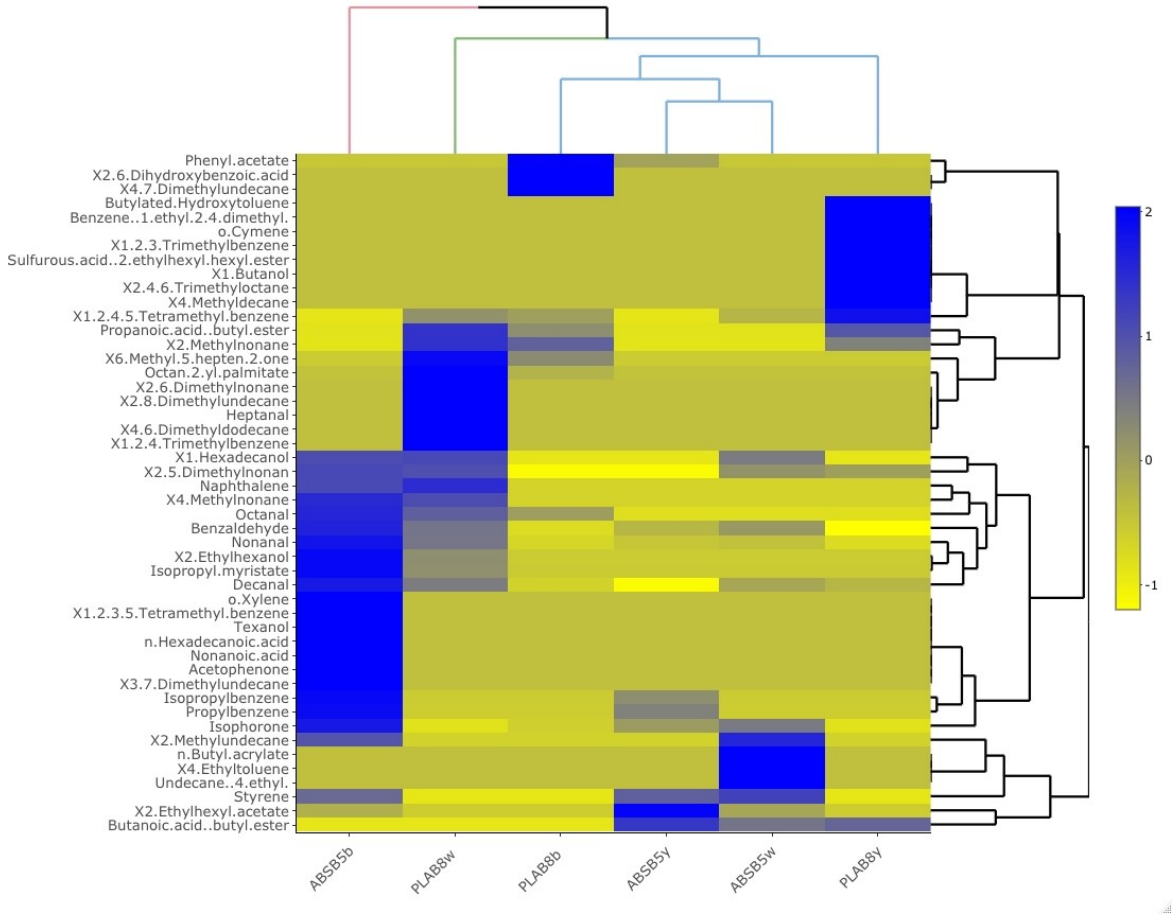

Figure 3-7- Heatmap showing the mean abundance of VOCs recovered (columns) from different ABS and PLA filaments (rows). Values were scaled and centred by their respective rows.

Recovered VOCs were also grouped and visualized based on the chemical class to further understand differences in filament VOC profiles. Acids, aldehydes, aromatic hydrocarbons, and branched alkanes were recovered from all filaments. Other recovered compounds belonging to either ether, ester, or ketone functional groups were classed as others. Interesting differences in composition in terms of chemical class across the different filament types and colors were noted. As expected, ABSB5b recovered the highest abundance of VOCs. The

TVOC was approximately double that of the ABSB5w and approximately five times that of the ABSB5y. All ABS filaments emitted styrene in high abundances, as ABS comprises monomer units of styrene and acrylonitrile, 1,3-butadiene. High amounts of aromatic hydrocarbons were also recovered from ABSB5w and ABSB5b.

In the case of PLA, TVOCs recovered were much lower than ABS in general. Of the three PLA colors, the highest number of VOCs were recovered from white, followed by yellow, and then black. High abundances of acids were retrieved for all PLA colors, likely due to the acidic nature of the polymer itself. Of all the PLA colors, alcohols were recovered in the highest abundances for white, indicating that this compound class may be related to pigment chemistry.

The reasons for different acidic VOC emission colors are not clear yet. One study hypothesized that the admixture of colorants serves to lower the melting temperature of the filament and that the emission of lactide, for example, is much lower in the case of white than black PLA at its melting point[231]. Nevertheless, given the fact that the composition of the filaments is a trade secret of the manufacturers, further research is needed to isolate and assess the effect of admixtures.

Comparing the PM emissions studied in Chapter 2 with the recovered VOC emission levels is interesting to identify any relative correlations between the measurements. Figure 2.2 showed that PMmax value order as ABSb5w>ABSb5b>ABSb5y. In the case of the TVOCs from ABS filaments, the order of abundance was ABSb5b>ABSb5b>ABSb5y. Although the order of black and white pigments changed, ABSb5y had significantly lower TVOCs emitted, consistent with its low PMmax. However, no correlation was noted for the PLA colors,

comparing the two filament types. The white filaments are twice as high as the black filament for $PM_{0.3}$[225].

Besides styrene, aromatic hydrocarbons were a major class of VOC recovered from ABS filaments. This class was further analyzed at the compound level (Figure 3.9). Significant differences for certain recovered compounds were observed across the ABS colors. In previous studies, it has been estimated that styrene accounts for more than 30% of the emission of the TVOCs, with its abundance being highest for black filaments and lowest in the case of yellow filaments with intermediate emission in the case of white filament[410,418].

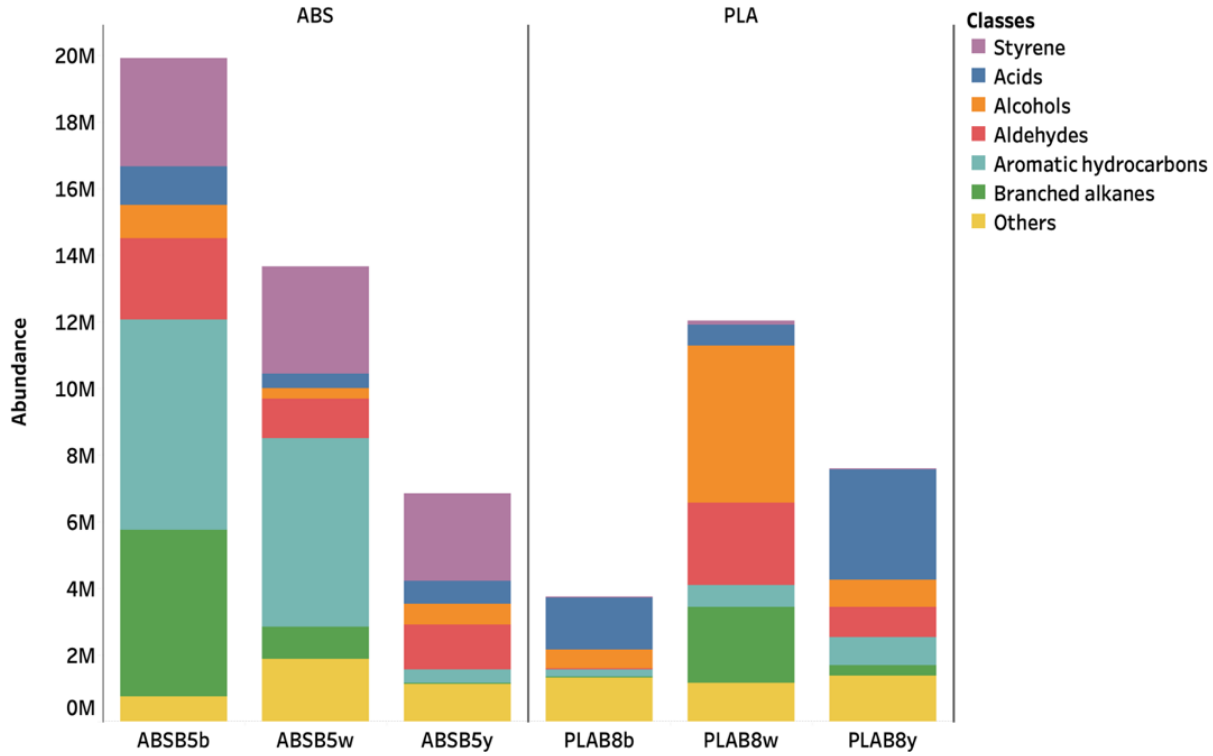

Figure 3-8- Stacked bar plot illustrating average abundances of the different compound classes recovered from black, white, and yellow ABS and PLA filaments (n=3), represented in millions (M).

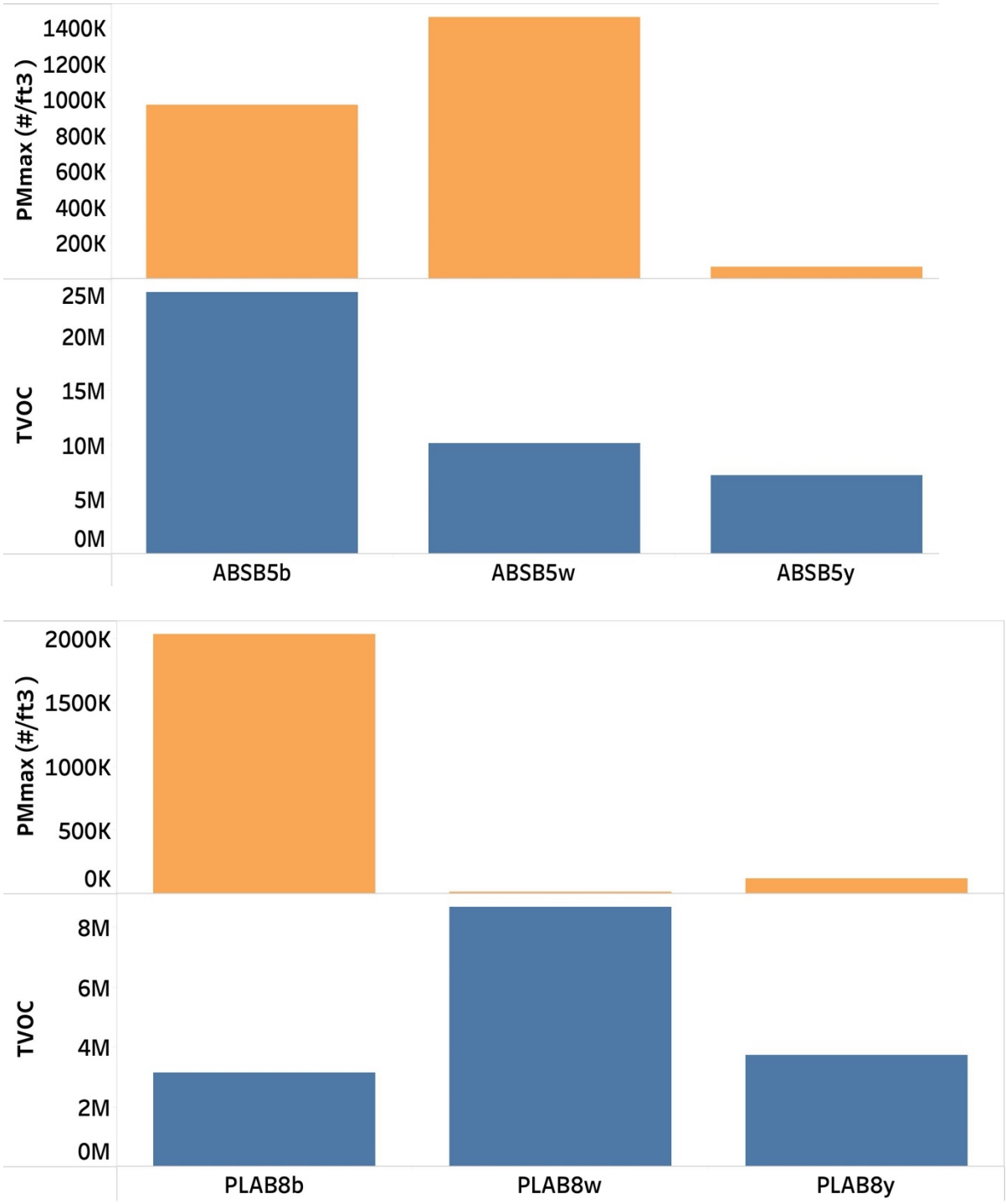

Figure 3-9-Comparison of TVOC and PMmax emission profiles for different colors (a) ABS filament and (b) PLA filament, represented in millions (M), and thousands (K).

The values in the y axis representants the abundance of each component. The abundance represents the area ,which is a reflection of the amount of a specific analyte that's present and it is based on the number of counts taken by the mass spectrometer detector at the point of retention.

BTEX was also detected in this work. Ethylbenzene, for example, was recovered from black (ABSB5b) and white (ABSB5w) filaments but not from yellow (ABSB5y), which may be attributed to styrene, as ethylbenzene is a precursor to styrene synthesis. While not being the main constituents of the VOC profile emitted during 3D printing of ABS, their presence has been confirmed in several other studies regardless of the color of the pigment[232,236,407]. Benzaldehyde was recovered for all colors but in the highest abundances for black (ABSB5b), which is in agreement with the previous findings[407].

Several other aromatic hydrocarbons were also recovered. It was noted that apart from ethyltolune and 1,2,4,5-Tetramethylbenzene, all other aromatic hydrocarbons were emitted in the highest abundance from the ABS black filament (ABSB5b). However, looking at filament color's impact on VOC emissions (Figure 3.8), ABSB5b emitted almost double the abundance of TVOCs compared to ABSB5w.

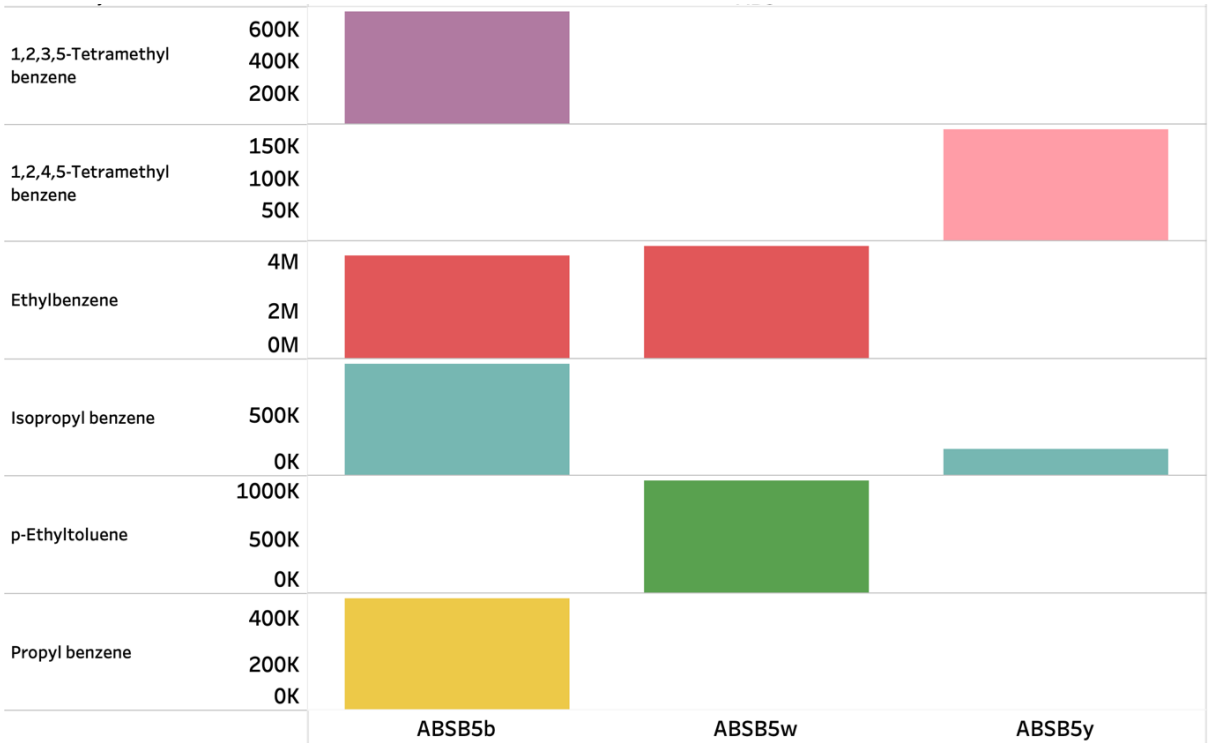

Figure 3-10- Abundance values for frequently recovered aromatic hydrocarbons from ABS filaments (n=3), represented in millions (M),

and thousands (K).

With PLA being an acid-based thermoplastic, the recovered compounds differed significantly from ABS. The acid profile (comprising five acids) was more deeply analyzed and represented in Figure 3.10. Propanoic acid was recovered from all filament colors, but its abundance was highest in yellow (PLAB8y). This compound has been detected in previous studies on the black, white and yellow filaments; however, the relative abundances were not given225. Both acetic acid and benzoic acid were only recovered from the black filament (PLAB8b). In contrast, butanoic acid was only detected from the yellow filament (PLAB8y).

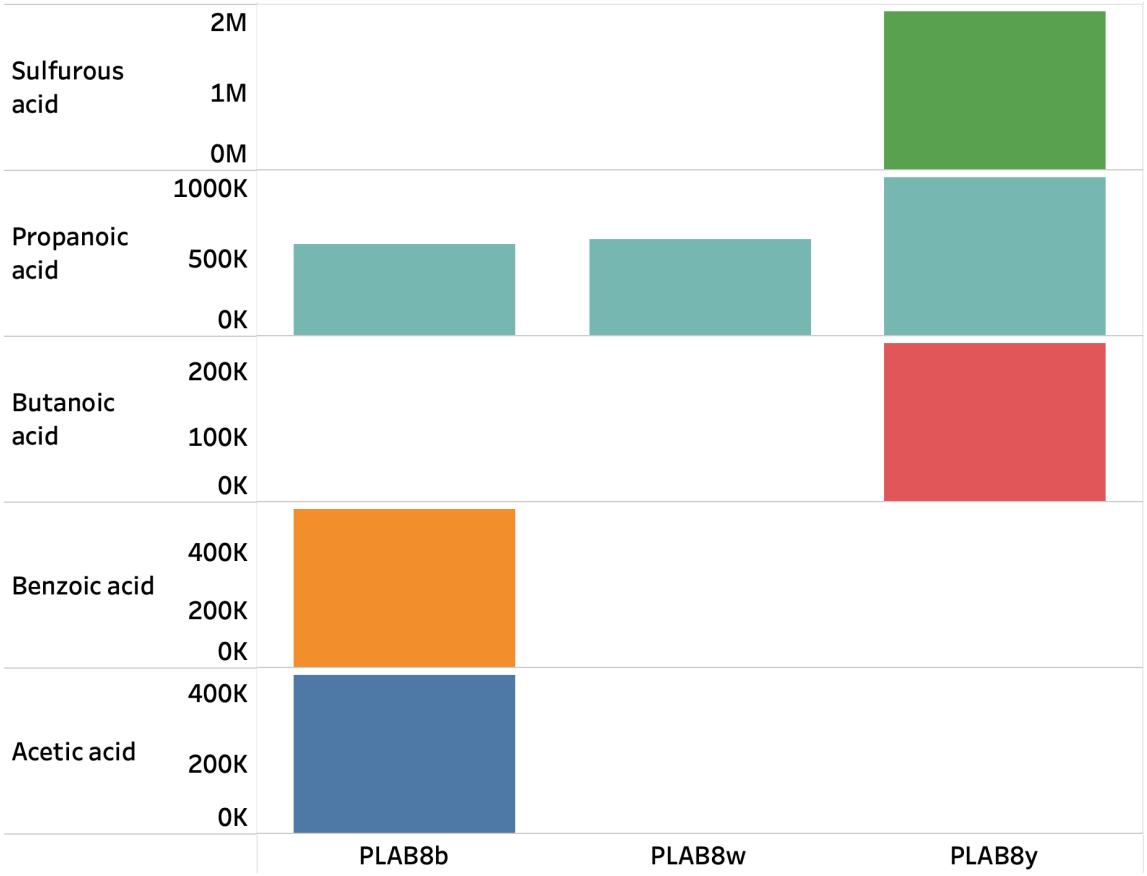

Figure 3-11- Abundance values for frequently recovered acids from PLA filaments (n=3), represented in millions (M), and thousands (K).

The values in the y axis representants the abundance of each component. The abundance represents the area ,which is a reflection of the amount of a specific analyte that's present and it is based on the number of counts taken by the mass spectrometer detector at the point of retention.

3.3.3 Brand studies

The influence of the filament brand on PM0.3 emissions was investigated in Chapter 2 for both ABS and PLA filaments, where black colored filaments were used for all brands. For ABS, the order of decreasing PMmax values in filaments was found to be as follows: ABSB5b>ABSB1b>ABSB3b>ABSB2b=ABSB4b. For PLA, PLAB8b> PLAB1b>PLAB7b= PLAB6b=PLAB2b=PLAB3b). In this study, the same brands were used to print the test cube, and the emitted VOCs were recovered following the method described in sections 3.2.3 and 3.2.4. The emission data indicate that filament brand accounts for large differences in emission profiles during 3D printing. Figure 3.11 shows the PCA to visualize the effect of ABS filament type (ABS or PLA) and brand on VOC emissions. It can be seen that some brands of ABS (ABSB2b, ABSB4b) clustered closely together in terms of their replicates, indicating greater similarity in VOC emission profiles across replicates, and others (ABSB1b, ABSB3b, ABSB5)b were more variable in terms of their emissions, potentially indicating filament heterogeneities or the presence of impurities. In the case of PLA, the replicates were more clustered, and the different brands were much more similar, with only one replicate from PLAB8b being an outlier.

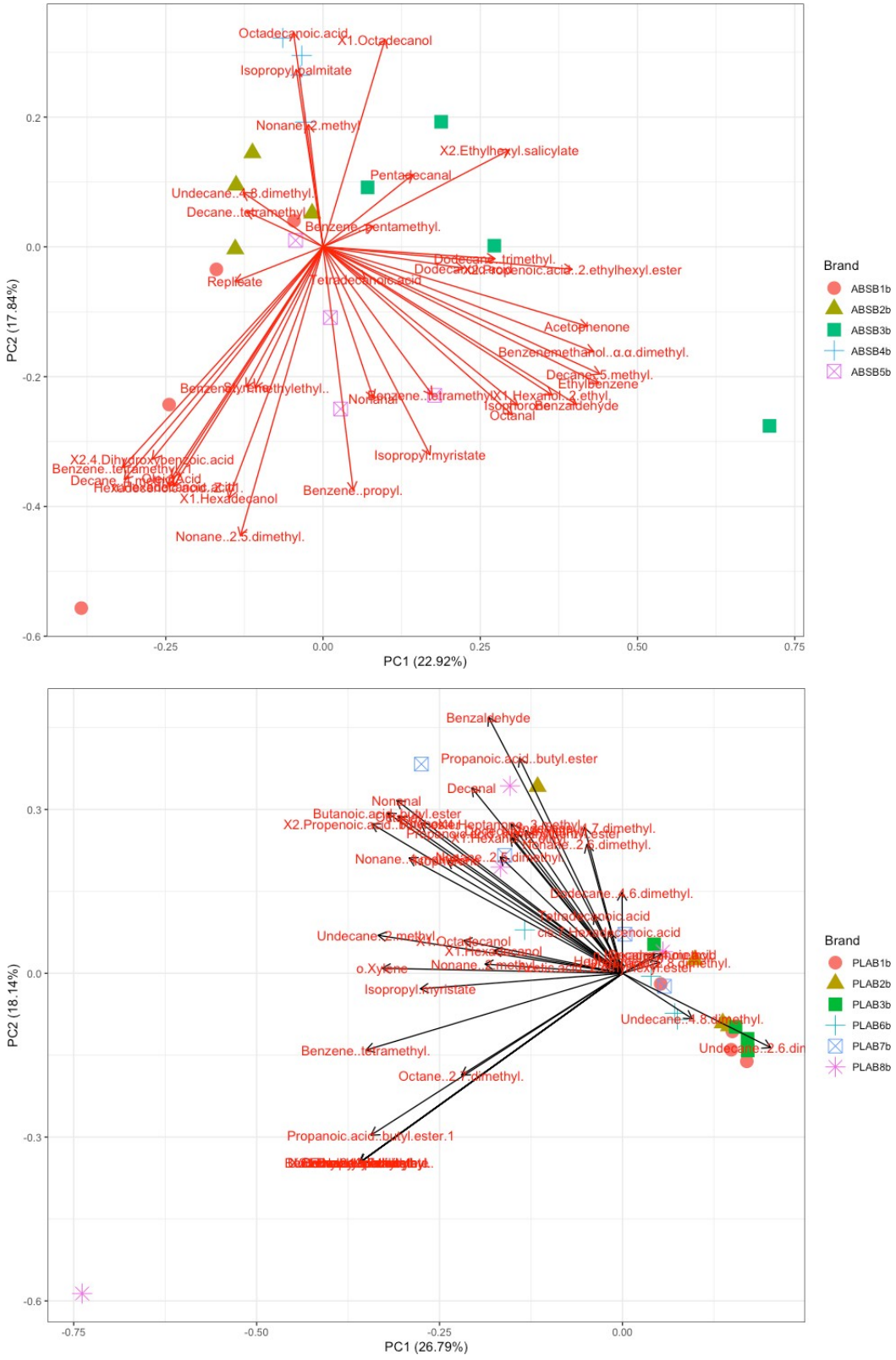

Figure 3-12- PCA scores plot for replicate datasets (n=4) for (a) 5 different brands of ABS filaments. PC 1 and PC2 summarized 41.7% of the variance of the overall dataset, with 22.9% being summarised by PC1 and 17.84% being summarised by PC2. (b) 6 different brands of PLA filaments. . PC 1 and PC2 summarised 45% of the variance of the overall dataset, with 26.8% being summarised by PC1 and 18.1% being summarised by PC2.

In addition, compound-level data was depicted using hierarchical cluster analysis (HCA) Fig.

3.13 displays a dendrogram of the heatmap indicating the grouping of datasets based on their similarity. The heat map shows all recovered compounds from each of the studied brands. Among ABS brands, ABSB3b was the most dissimilar of all filaments, as it is clustered separately from the rest of the brands. High abundances of carcinogenic compounds, including ethylbenzene, benzaldehyde, and acetophenone, were recovered from this brand. PLAB8b exhibits a high abundance of 14 unique compounds, including O-xylene and naphthalene, which are not recovered in other brands of PLA. Thus, this brand is likewise clustered separately from the others.

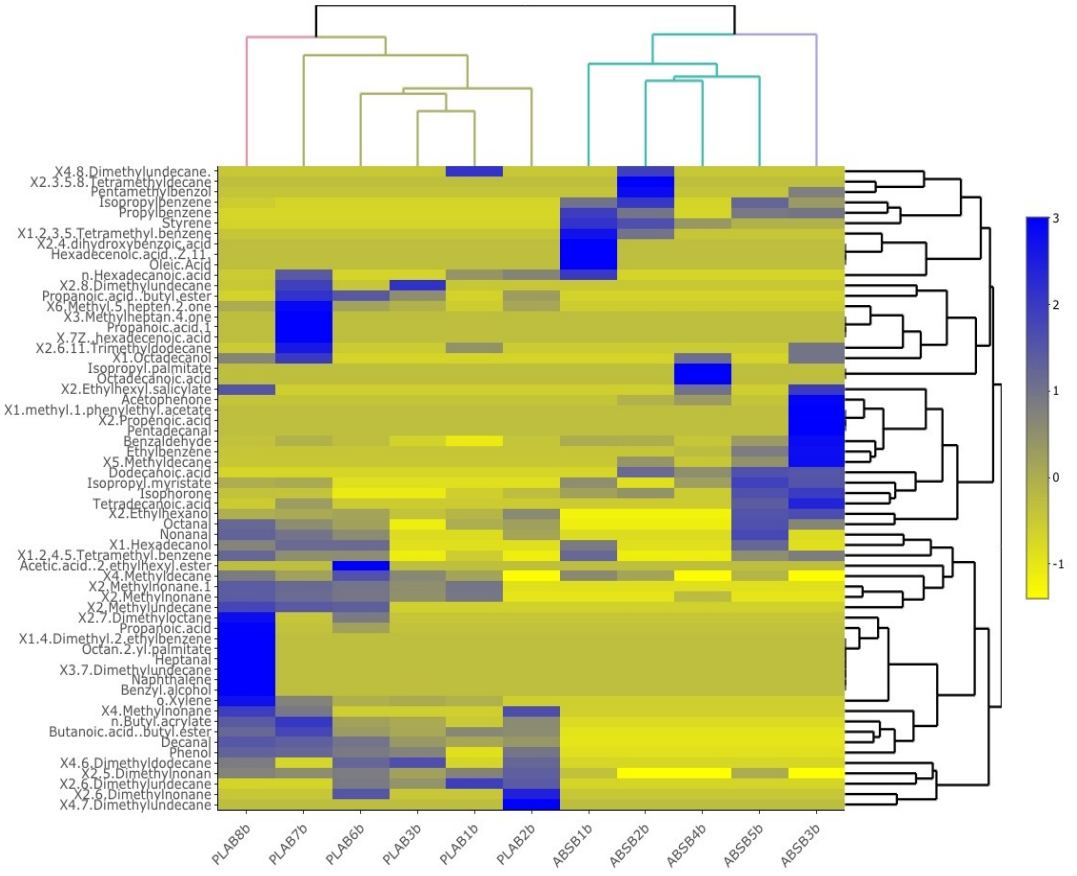

Figure 3-13- Heatmap showing the mean abundance of VOCs recovered (columns) from different ABS and PLA brands (rows). Values were scaled and centered by their respective rows.

.

Recovered VOCs were also grouped and visualized based on their TVOCs and emitted VOC chemical classes, as shown in Figure 3.14, to understand the effect of brands on compound

class profiles. Acids, alcohols, aldehydes, aromatic hydrocarbons, and branched alkanes were recovered from all brands, regardless of their type. TVOCs also varied significantly by filament brand, whereby TVOCs generated by ABSB3b was almost 2.5 times higher than those from ABSB5b and ABSB1b, with styrene emissions making up almost 50% of the composition. All ABS brands emitted styrene in high abundance, as expected. A high abundance of acetophenone, classified within others, was also recovered. This compound, whose presence has been acknowledged in other studies[235,419,420], is another suspected breakdown product, likely derived from styrene.

In the case of PLA, TVOCs recovered were much lower than ABS in general. Of all PLA brands, the highest TVOCs were recovered from PLAB8b and PLAB7b. High abundances of alcohols and acids were recovered across all brands, likely due to the acidic nature of the PLA polymer itself. Relatively high amounts of branched alkanes were also recovered from PLAB6b. The difference in TVOC emissions for different brands was also reported in other studies. One study claimed that the difference in TVOC emission rates was as high as 49% for ABS and 14% for PLA. The brand has a large effect on the monomer emission rate for each filament type. In the case of ABS brands tested here, the styrene emission rate varies by 45%, and the lactide emission rate varies by 35% in the case of PLA[236]. These differences in VOC

emissions from the different filaments of the same type likely arise from their different chemical compositions. Different brands will likely contain different additives compositions such as plasticizers, fillers, dyes, flame retardants, and UV stabilizers or antioxidants. The presence of additives may affect the VOC emission directly (thermal decomposition of additives) or indirectly (by affecting the thermal stability of the main polymeric component)[410].

PM emissions, it was noted, do not strictly follow the same trend as TVOC emission abundances. ABSB5 was found to have a significantly higher PM_{MAX} value - over ten times

higher than ABSB1, the second-highest PM emitter[225]. This difference in the emission trend profile may be because PM formation is associated with vapors with low saturation vapor pressure (SVOCs)[236]. In terms of VOC emissions, ABSB5b was found to have the highest abundance. In the case of PLA, when considering PM emissions, PLAB8 had the highest PMMAX, approximately ten times higher than all other brands. Interestingly, this brand also had the highest TVOC emissions along with PLAB7b. However, PLAB7b emitted relatively lower amounts of PM.

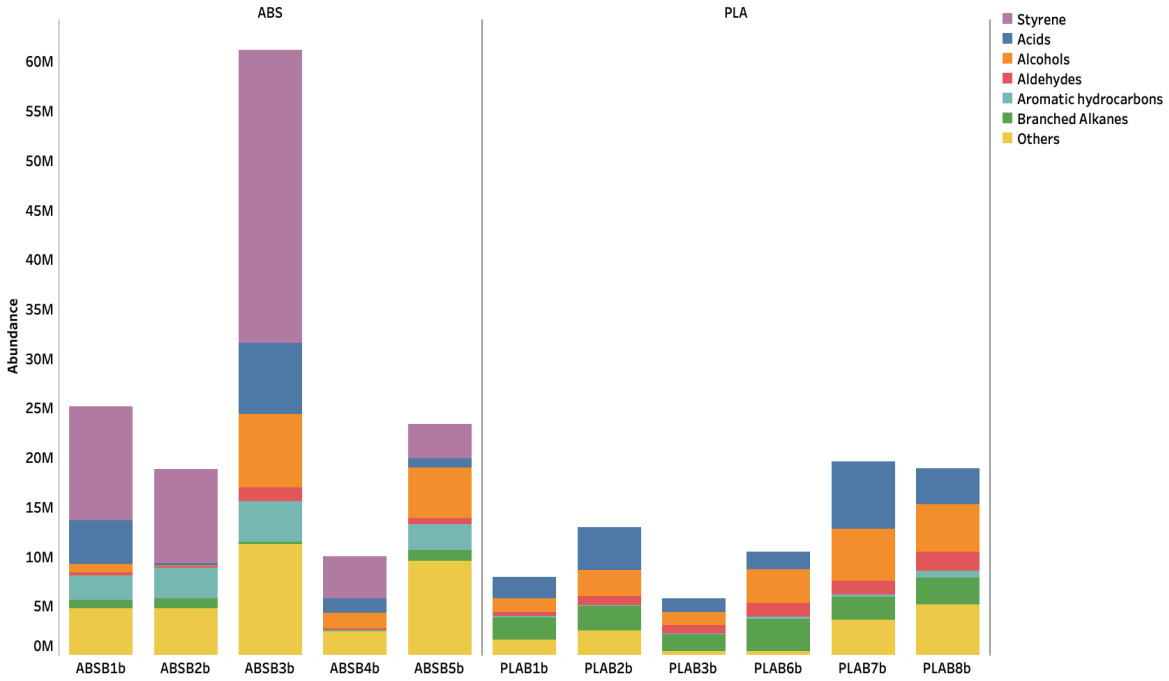

Figure 3-14- Stacked bar plot illustrating average abundances of the different compound classes recovered from different brands of ABS and PLA, represented in millions (M).

The values in the y axis representants the abundance of each component. The abundance represents the area ,which is a reflection of the amount of a specific analyte that's present and it is based on the number of counts taken by the mass spectrometer detector at the point of retention.

Aromatic hydrocarbons were a major class of VOCs emitted from ABS filaments and are examined in more detail in Figure 3.16. Significant differences for certain recovered compounds were observed across the ABS brands. Ethylbenzene, a potential human carcinogen was recovered in high abundances in ABSB3 and ABSB5. Isopropylbenzene and propylene were recovered from all ABS brands except ABSB4. The presence of these compounds was also observed in previous findings[407].

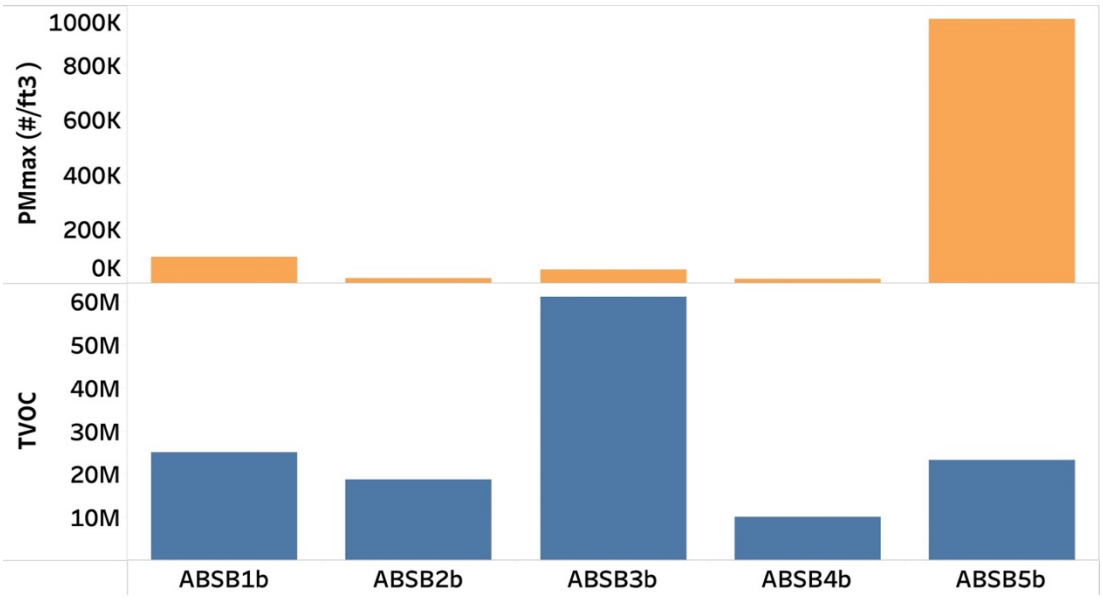

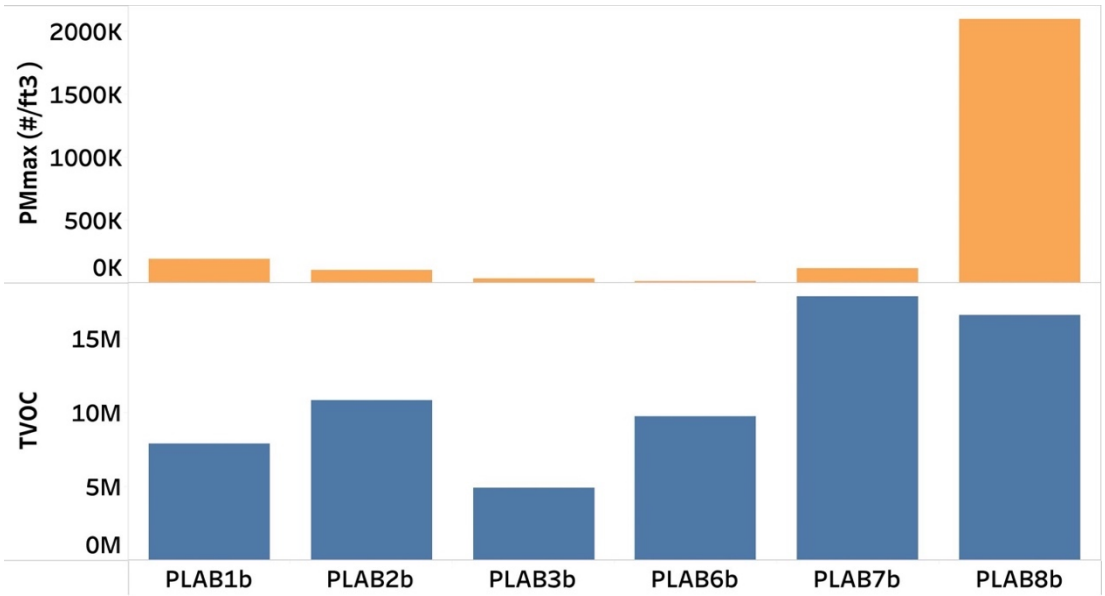

Figure 3-15- Comparison of TVOC and PMmax emission profiles for different brands (a) ABS filament (b) PLA filament, represented in millions (M).

The presence of isopropyl benzene, which has been highlighted in previous research, may be attributed to the decomposition of cumene—commonly added as a flame retardant[421,422].

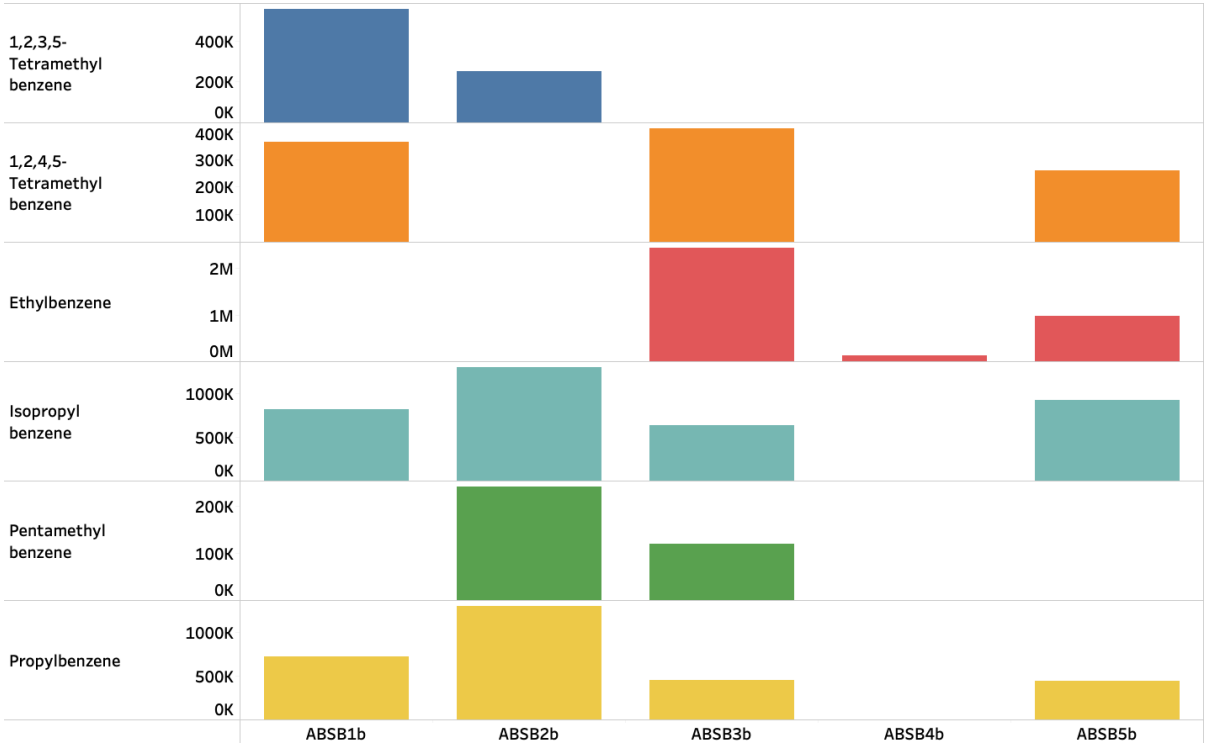

Figure 3-16- Abundance values for frequently recovered aromatic hydrocarbons from different brands of ABS filaments (n=3),

represented in millions (M).

The acid profile of PLA emissions was further analyzed and represented in Figure 3.17. 8 acids were identified as recovered from different brands of PLA. Propanoic acid and butanoic acid have been detected for all brands; the abundance is highest for PLAB7b and PLAB8b. Acetic acid and benzoic acid were only recovered from PLAB6b and PLAB7b, respectively.

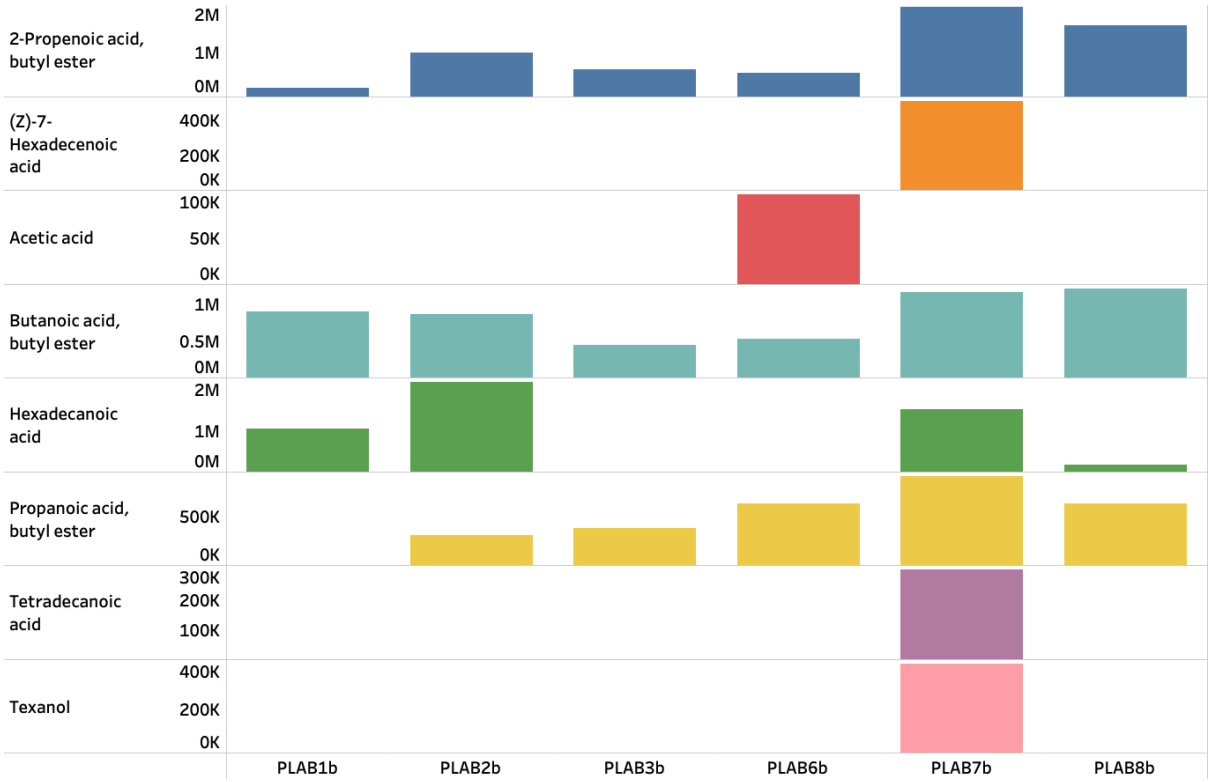

Figure 3-17- Abundance values for frequently recovered acids from different brands of PLA filaments (n=3), represented in millions (M), and thousands (K).

The values in the y axis representants the abundance of each component. The abundance represents the area ,which is a reflection of the amount of a specific analyte that's present and it is based on the number of counts taken by the mass spectrometer detector at the point of retention.

3.3.4 Temperature studies

Finally, extrusion temperature was investigated for its effect on VOC emissions for both ABS and PLA filaments. Temperature variations were investigated for each filament type within the recommended range of temperatures for the filament. Figure 3.18 represents recovered and class-based grouped VOCs. It was found that the higher the extrusion temperature, the greater the TVOC emissions for all filaments. Acids, alcohols, aldehydes, aromatic hydrocarbons, and branched alkanes increased in abundance with temperature for all filaments.

TVOC emission rates when setting nozzle temperature to 235 °C and 245 °C were comparable. However, increasing the nozzle temperature to 255 °C increases. The TVOC abundance recovered to almost 2.5 times higher, with compounds classified as others, specifically isophorone and o-xylene, showing the highest abundance level and making up almost 50% of the composition. As expected, the emission rate of styrene also increased with higher extrusion temperatures. In the case of PLA, TVOCs abundances recovered also increased with temperature. The compound class most impacted by temperature was alcohol. As seen for ABS filaments, the level of isophorone and o-xylene elevated with higher extrusion temperatures. These observed trends have also been noted in other published studies. One study indicated that the increase in nozzle temperature from 230 °C to 255 °C when using ABS filament increases the TVOC and styrene abundances by 25% and 27%, respectively[236]. An increase in TVOC abundance has been reported in another study using different nozzle temperatures (245°C and 270 °C) when printing with two different ABS brands[421].

Previous studies have observed a positive correlation between VOC and PM emissions with the increase in the extruder temperature, reporting that this elevation in temperature has a much greater effect on PM emission (128% increase in Pnum) than it does for VOC emission[236][230].

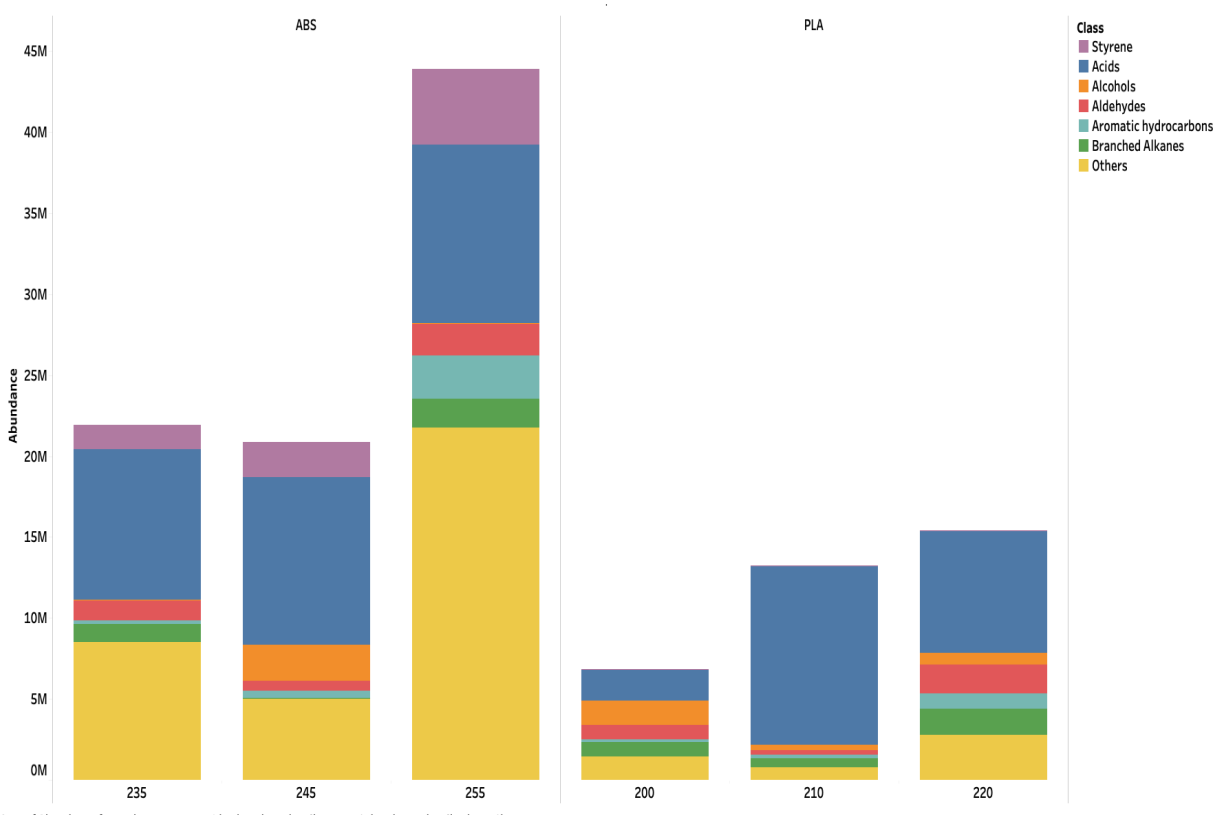

Figure 3-18- Stacked bar plot illustrating average abundances of the different compound classes recovered from different extruder temperatures when printing ABS and PLA, represented in millions (M).

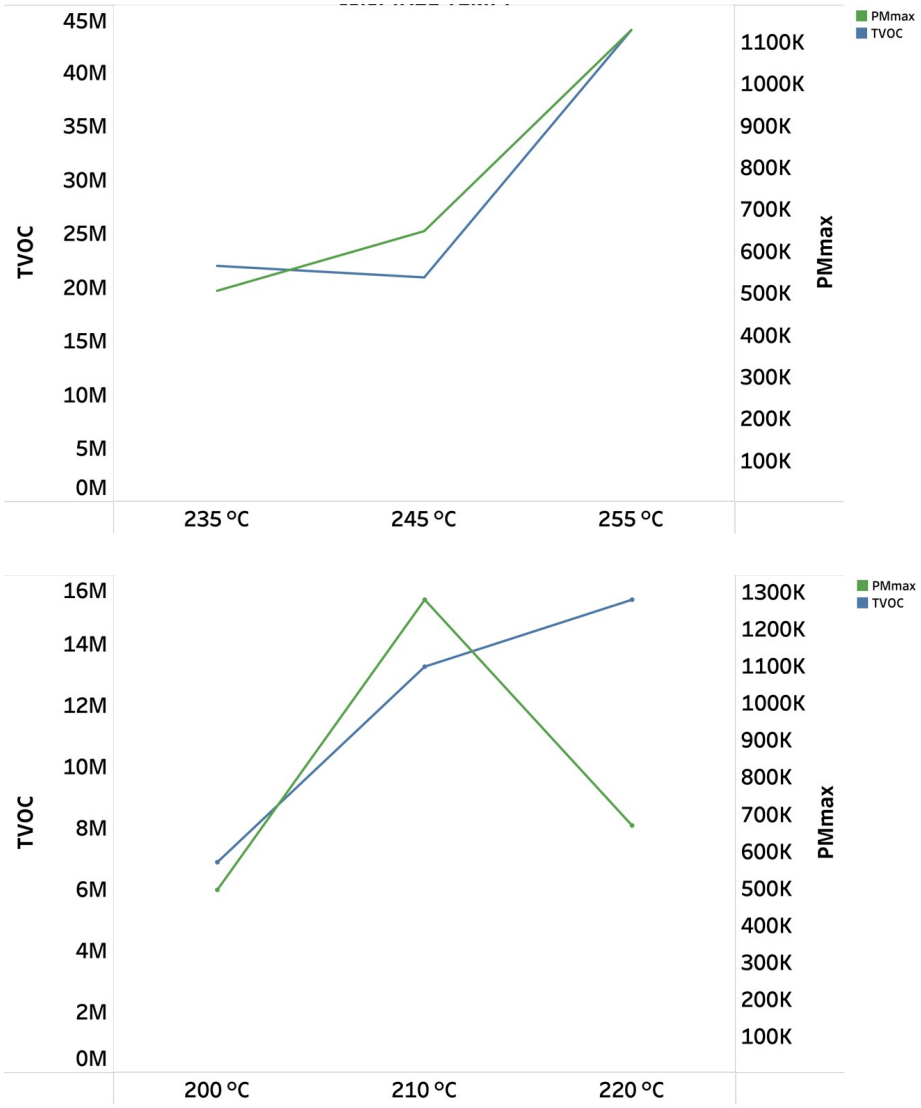

Figure 3-19- Comparison of TVOC and PMmax emission profiles for different nozzle temperatures(a) ABS filament (b) PLA filament, represented in millions (M), and thousands (K).

The values in the y axis representants the abundance of each component. The abundance represents the area ,which is a reflection of the amount of a specific analyte that's present and it is based on the number of counts taken by the mass spectrometer detector at the point of retention.

Aromatic hydrocarbons compounds emitted by ABS filaments were further analyzed in Figure 3.20. Seven compounds from this class were recovered, all in the highest abundance when

printing with the highest temperature of 255 °C. The presence of naphthalene, which is classified as a Group C, a possible human carcinogen by the EPA, was only recovered when printing at this high temperature.

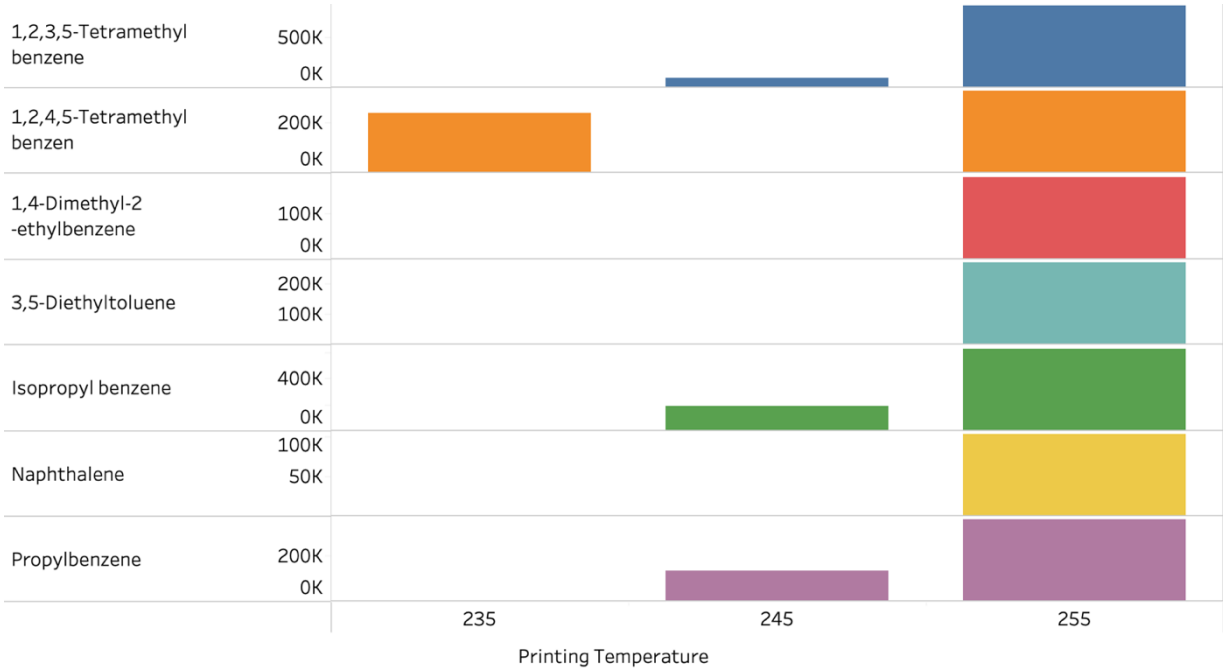

Figure 3-20- Abundance values for frequently recovered aromatic hydrocarbons from different extruder temperatures of ABS filaments (n=3), represented in millions (M), and thousands (K).

The PLA acid profile for different extruder temperatures was also analyzed (Figure 3.21). Tetra decanoic acid and octadecanoic acid were recovered for different extruder temperatures with relatively different abundances. Propanoic and benzoic acid were detected in abundance when increasing the extruder temperature to 220 °C.

Overall, this study shows that the higher the temperature used for extrusion, the greater the abundance of VOCs and the greater the diversity of VOCs, e.g., naphthalene was only recovered when printing ABS at the highest temperate was within the recommended range.

Thus, in a domestic environment, the user is made aware of the implications of using higher temperatures in terms of both the VOC emissions and the impact on PM emissions.

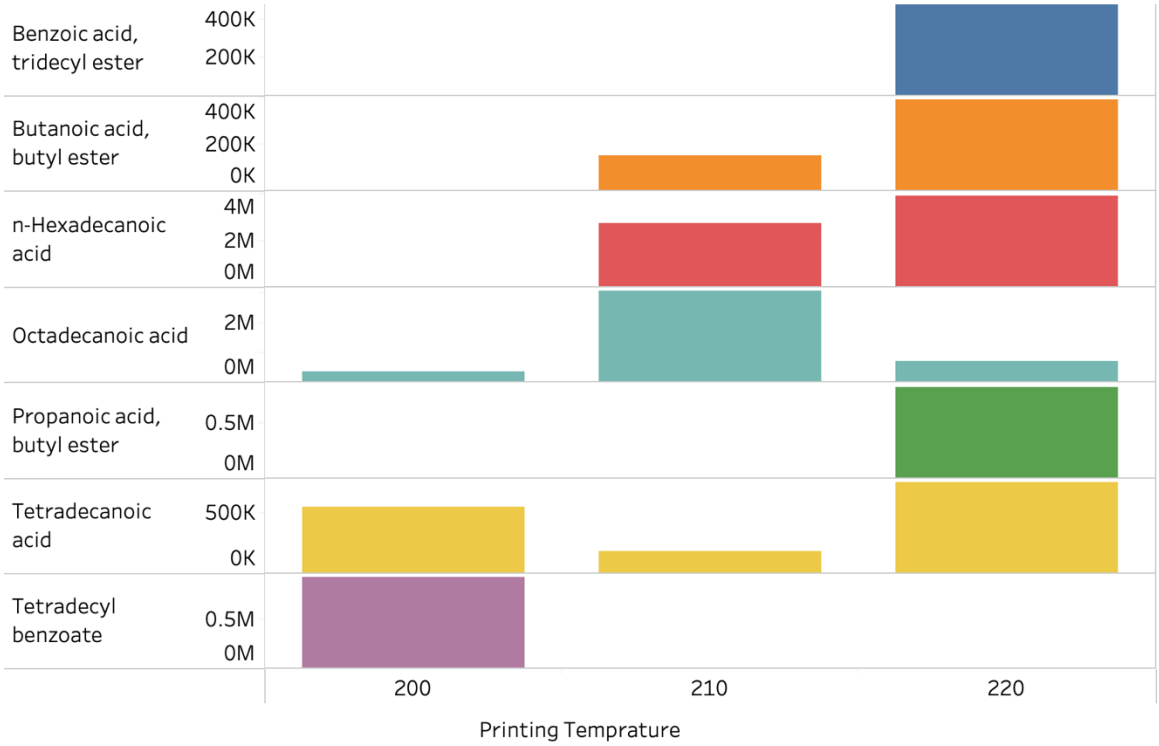

Figure 3-21- Abundance values for frequently recovered acids from different extruder temperatures of PLA filaments (n=3), represented in

millions (M), and thousands (K).

The values in the y axis representants the abundance of each component. The abundance represents the area ,which is a reflection of the amount of a specific analyte that's present and it is based on the number of counts taken by the mass spectrometer detector at the point of retention.

3.4 Conclusions

This chapter investigated the VOC profiles of 3D printer emissions using a closed printing chamber setup and SPME sampling. An untargeted GC-MS analysis was carried out. Overall, the data shows that significantly higher TVOC abundances were recovered from ABS than PLA, regardless of the color, brand, or extruder temperature. ABS's most frequently identified

VOCs included styrene, ethylbenzene, benzaldehyde, and acrylonitrile, all categorized as carcinogenic by the EPA and IARC. The most frequently identified VOCs from PLA included acetaldehyde, lactide, and caprolactam.

The abundances of these compounds and classes of compounds vary depending on polymer type, producer/manufacturer, and filament color. Certain filament VOC profiles were more reproducible across numerous prints, indicating that certain filaments may have had significant heterogeneity. All differences can be associated with the chemical composition of the filament, particularly related to the various additives (fillers, dyes, flame retardants, plasticizers) contained within. The correlation of the VOC emissions with the PM emissions was also examined, and some correlation was seen. However, it was not consistent.

Undoubtedly, additive manufacturing, particularly 3D printers, is a promising technology offering many new opportunities and enabling the home printing market as a consumer device. However, because most home 3D printers are currently sold as standalone devices without exhaust ventilation or filtration accessories, results from the work presented here suggest that more information on the impact of the filament being used on the emissions during printing should be provided to the consumer at the very least. Ultimately regulation is required to ensure commercial filaments are demonstrated to have minimal emissions and provide filtration systems/enclosures with these undoubtedly, additive manufacturing, particularly 3D printers,

is a promising technology offering many new opportunities and enabling the home printing market as a consumer device. However, because most home 3D printers are currently sold as standalone devices without exhaust ventilation or filtration accessories, the result from the work presented here suggests that more information on the impact of the filament being used on the emission during printing should be provided to the consumer at the very least. Ultimately regulation is required to ensure commercial filaments have minimal emissions and provide filtration systems/enclosures with these printers.

Chapter 4:

Future perspectives

Indoor Air Quality (IAQ) has significantly influenced peoples' health, comfort, productivity, and general well-being. People spend up to 90% of their time indoors, continuously interacting with their indoor environment. The ongoing COVID-19 pandemic has also highlighted the need for a better understanding of the effect of different sources on IAQ. Most indoor pollution comes from toxic substances emitted by building materials (asbestos, for example) and consumer products or from human activity like cooking, cleaning, smoking, burning candles, and using printers and photocopying machines. Other than that, new sources of indoor air pollutants are emerging due to advancements in technology and the shift in the living paradigm due to COVID-19, one of which is 3D printers in the home, office, and school settings.

3D printers function by melting plastic filaments. Heating plastic causes minor decomposition in the filament. Even though it does not impact print quality, it is enough to produce particulate matter in the ultrafine range (PM0.3), indicating that 3D printers using ABS and PLA may inhale these particles for 3D printer operators. The initial particle emission spike observed toward the end of warming up but before printing starts is due to elevated temperature, dripping of semi-liquid filament, and filament residue in the nozzle.

However, the gaseous emission from 3D printers is far more complex. It contains a mixture of VOCs, which may include odorants, irritants, and carcinogens. ABS generally releases more TVOC than PLA, regardless of color or brand, 30% of which is styrene, a group 1 carcinogenic. Other VOCs that have been commonly detected include ethylbenzene (ABS), O-xylene (ABS and PLA), benzaldehyde (ABS), and benzoic acid (PLA). Filament properties and 3D printer operating parameters, including extruder temperature, significantly affect the VOC emissions.

While 3D printing makes numerous products more readily available and at cheaper costs, as we have seen with the manufacturing of Covid-19 face shields, respirators, and other personal protective equipment, it is important to consider the potential risks associated with 3D printing. Moreover, as 3D printing technologies become more widespread, regulators, manufacturers, and users may need to focus their attention on better managing those risks. As 3D printers are sources of high ultrafine particles and hazardous gases, their emissions should be mitigated and regulated. However, consumers cannot identify which printer or filament is safer to operate due to the lack of information and standardization in the current market. A standard on 3D printer emissions is beneficial to regulate emissions and notify users of potential emissions and hazard levels during 3D printing.

A standardized method to test and assess 3D printer emissions could accurately measure ERs and evaluate the associated risks. The test data from various 3D printers could be compared, guiding consumers to choose manufacturers to produce lower-emitting 3D printers and filament formulations. 3D printer brand, filament brand, filament color, and nozzle temperature all influence VOC emissions. Some 3D printing conditions affect VOC and UFP emissions differently. Therefore, both must be considered when selecting a filament that minimizes potential adverse health effects.

References

1. World Health Organization. Regional Office for Europe The Right to Healthy Indoor Air : Report on a WHO Meeting, Bilthoven, The Netherlands 15-17 May 2000. **2000**.
2. Ortiz, A.; Guerreiro, C.; de Leeuw, F.; Horálek, J. *Air Quality in Europe - 2017 Report*; 2017;
3. Frontczak, M.; Wargocki, P. Literature Survey on How Different Factors Influence Human Comfort in Indoor Environments. *Build. Environ.* **2011**, *46*, 922–937, doi:10.1016/j.buildenv.2010.10.021.
4. Schweizer, C.; Edwards, R.D.; Bayer-Oglesby, L.; Gauderman, W.J.; Ilacqua, V.; Juhani Jantunen, M.; Lai, H.K.; Nieuwenhuijsen, M.; Künzli, N. Indoor Time–Microenvironment–Activity Patterns in Seven Regions of Europe. *J. Expo. Sci. Environ. Epidemiol.* **2007**, *17*, 170–181.
5. *Who Guidelines for Indoor Air Quality: Selected Pollutants*; World Health Organization, Ed.; WHO: Copenhagen, 2010; ISBN 978-92-890-0213-4.
6. Mannan, M.; Al-Ghamdi, S.G. Indoor Air Quality in Buildings: A Comprehensive Review on the Factors Influencing Air Pollution in Residential and Commercial Structure. *Int. J. Environ. Res. Public. Health* **2021**, *18*, 3276.
7. Wallace, L.; Gordon, S. Exposure to Volatile Organic Compounds. In *Exposure Analysis*; Wallace, L., Steinemann, A., Ott, W., Eds.; CRC Press, 2006; pp. 147–179 ISBN 978-1-56670-663-6.
8. Weschler, C.J. Ozone in Indoor Environments: Concentration and Chemistry. *Indoor Air* **2000**, *10*, 269–288.
9. Logue, J.; McKone, T.; Sherman, M.; Singer, B. Hazard Assessment of Chemical Air Contaminants Measured in Residences. *Indoor Air* **2011**, *21*, 92–109.
10. Arata, C.; Misztal, P.K.; Tian, Y.; Lunderberg, D.M.; Kristensen, K.; Novoselac, A.; Vance,

M.E.; Farmer, D.K.; Nazaroff, W.W.; Goldstein, A.H. Volatile Organic Compound Emissions during HOMEChem. *Indoor Air* **2021**, *31*, 2099–2117.

11. EC–European Commission Indoor Air Pollution: New EU Research Reveals Higher Risks than Previously Thought. *Jt. Res. Cent.* **2003**.
12. Paciência, I.; Rufo, J.C. Urban-Level Environmental Factors Related to Pediatric Asthma. *Porto Biomed. J.* **2020**, *5*.
13. Tham, K.W. Indoor Air Quality and Its Effects on Humans—A Review of Challenges and Developments in the Last 30 Years. *Energy Build.* **2016**, *130*, 637–650.
14. Domínguez-Amarillo, S.; Fernández-Agüera, J.; Cesteros-García, S.; González-Lezcano, R.A. Bad Air Can Also Kill: Residential Indoor Air Quality and Pollutant Exposure Risk during the COVID-19 Crisis. *Int. J. Environ. Res. Public. Health* **2020**, *17*, 7183.
15. Guo, M.; Xu, P.; Xiao, T.; He, R.; Dai, M.; Miller, S.L. Review and Comparison of HVAC Operation Guidelines in Different Countries during the COVID-19 Pandemic. *Build. Environ.* **2021**, *187*, 107368.
16. Yu, C.F.; Crump, D. Small Chamber Tests for Measurement of VOC Emissions from Flooring Adhesives. *Indoor Built Environ.* **2003**, *12*, 299–310.
17. Tran, V.; Park, D.-S.; Lee, Y.-C. Indoor Air Pollution, Related Human Diseases, and Recent Trends in the Control and Improvement of Indoor Air Quality. *Int. J. Environ. Res. Public. Health* **2020**, *17*, 2927, doi:10.3390/ijerph17082927.
18. Fang, L.; Clausen, G.; Fanger, P.O. Impact of Temperature and Humidity on the Perception of Indoor Air Quality. *Indoor Air* **1998**, *8*, 80–90.
19. Chithra, V.; Shiva, N.S. A Review of Scientific Evidence on Indoor Air of School Building: Pollutants, Sources, Health Effects and Management. *Asian J. Atmospheric Environ.* **2018**, *12*, 87–108.
20. Derbez, M.; Berthineau, B.; Cochet, V.; Lethrosne, M.; Pignon, C.; Riberon, J.; Kirchner, S.

Indoor Air Quality and Comfort in Seven Newly Built, Energy-Efficient Houses in France. *Build. Environ.* **2014**, *72*, 173–187.

21. Yamaguchi, T.; Nakajima, D.; Ezoe, Y.; Fujimaki, H.; Shimada, Y.; Kozawa, K.; Arashidani, K.; Goto, S. Measurement of Volatile Organic Compounds (VOCs) in New Residential Buildings and VOCs Behavior over Time. *J. UOEH* **2006**, *28*, 13–27.
22. Keeler, G.J.; Dvonch, T.; Yip, F.Y.; Parker, E.A.; Isreal, B.A.; Marsik, F.J.; Morishita, M.; Barres, J.A.; Robins, T.G.; Brakefield-Caldwell, W. Assessment of Personal and Community-Level Exposures to Particulate Matter among Children with Asthma in Detroit, Michigan, as Part of Community Action Against Asthma (CAAA). *Environ. Health Perspect.* **2002**, *110*, 173–181.
23. Abdel-Salam, M.M. Seasonal Variation in Indoor Concentrations of Air Pollutants in Residential Buildings. *J. Air Waste Manag. Assoc.* **2021**, *71*, 761–777.
24. Orola, B.A. Seasonal Variations in Indoor Air Quality Parameters and Occupants Self-Reported Physical Health within a Warm Humid Climatic Environment. *Sustain. Build.* **2020**, *5*, 2.
25. Massey, D.; Kulshrestha, A.; Masih, J.; Taneja, A. Seasonal Trends of PM10, PM5. 0, PM2. 5 & PM1. 0 in Indoor and Outdoor Environments of Residential Homes Located in North-Central India. *Build. Environ.* **2012**, *47*, 223–231.
26. Saini, J.; Dutta, M.; Marques, G. Indoor Air Quality Monitoring Systems and COVID-19. In *Emerging Technologies During the Era of COVID-19 Pandemic*; Springer, 2021; pp. 133–147.
27. Cocârţă, D.M.; Prodana, M.; Demetrescu, I.; Lungu, P.E.M.; Didilescu, A.C. Indoor Air Pollution with Fine Particles and Implications for Workers' Health in Dental Offices: A Brief Review. *Sustainability* **2021**, *13*, 599.
28. Coombs, K.C.; Chew, G.L.; Schaffer, C.; Ryan, P.H.; Brokamp, C.; Grinshpun, S.A.;

Adamkiewicz, G.; Chillrud, S.; Hedman, C.; Colton, M. Indoor Air Quality in Green-Renovated vs. Non-Green Low-Income Homes of Children Living in a Temperate Region of US (Ohio). *Sci. Total Environ.* **2016**, *554*, 178–185.

29. Földváry, V.; Bekö, G.; Langer, S.; Arrhenius, K.; Petráš, D. Effect of Energy Renovation on Indoor Air Quality in Multifamily Residential Buildings in Slovakia. *Build. Environ.* **2017**, *122*, 363–372.
30. Frey, S.E.; Destaillats, H.; Cohn, S.; Ahrentzen, S.; Fraser, M.P. The Effects of an Energy Efficiency Retrofit on Indoor Air Quality. *Indoor Air* **2015**, *25*, 210–219.
31. Gonzalez-Martin, J.; Kraakman, N.J.R.; Perez, C.; Lebrero, R.; Munoz, R. A State–of–the-Art Review on Indoor Air Pollution and Strategies for Indoor Air Pollution Control. *Chemosphere* **2021**, *262*, 128376.
32. Settimo, G.; Avino, P. The Dichotomy between Indoor Air Quality and Energy Efficiency in Light of the Onset of the Covid-19 Pandemic. *Atmosphere* **2021**, *12*, 791.
33. Meyer, W. Impact of Constructional Energy-saving Measures on Radon Levels Indoors. *Indoor Air* **2019**, *29*, 680–685.
34. Hinds, W.C.; Zhu, Y. *Aerosol Technology: Properties, Behavior, and Measurement of Airborne Particles*; John Wiley & Sons, 2022; ISBN 1-119-49404-4.
35. Krzyzanowski, M.; Cohen, A. Update of WHO Air Quality Guidelines. *Air Qual. Atmosphere Health* **2008**, *1*, 7–13.
36. Zhao, X.; Zhang, X.; Xu, X.; Xu, J.; Meng, W.; Pu, W. Seasonal and Diurnal Variations of Ambient PM2. 5 Concentration in Urban and Rural Environments in Beijing. *Atmos. Environ.* **2009**, *43*, 2893–2900.
37. Medina, S.; Plasencia, A.; Ballester, F.; Mücke, H.; Schwartz, J. Apheis: Public Health Impact of PM10 in 19 European Cities. *J. Epidemiol. Community Health* **2004**, *58*, 831–836.
38. Neuberger, M.; Schimek, M.G.; Horak Jr, F.; Moshammer, H.; Kundi, M.; Frischer, T.;

Gomiscek, B.; Puxbaum, H.; Hauck, H. Acute Effects of Particulate Matter on Respiratory Diseases, Symptoms and Functions:: Epidemiological Results of the Austrian Project on Health Effects of Particulate Matter (AUPHEP). *Atmos. Environ.* **2004**, *38*, 3971–3981.

39. Maté, T.; Guaita, R.; Pichiule, M.; Linares, C.; Díaz, J. Short-Term Effect of Fine Particulate Matter (PM2. 5) on Daily Mortality Due to Diseases of the Circulatory System in Madrid (Spain). *Sci. Total Environ.* **2010**, *408*, 5750–5757.
40. Pearce, D.; Crowards, T. Particulate Matter and Human Health in the United Kingdom. *Energy Policy* **1996**, *24*, 609–619.
41. Glasius, M.; Ketzel, M.; Wåhlin, P.; Jensen, B.; Mønster, J.; Berkowicz, R.; Palmgren, F. Impact of Wood Combustion on Particle Levels in a Residential Area in Denmark. *Atmos. Environ.* **2006**, *40*, 7115–7124.
42. Jung, C.-R.; Nishihama, Y.; Nakayama, S.F.; Tamura, K.; Isobe, T.; Michikawa, T.; Iwai-Shimada, M.; Kobayashi, Y.; Sekiyama, M.; Taniguchi, Y. Indoor Air Quality of 5,000 Households and Its Determinants. Part B: Volatile Organic Compounds and Inorganic Gaseous Pollutants in the Japan Environment and Children's Study. *Environ. Res.* **2021**, *197*, 111135.
43. Li, Z.; Wen, Q.; Zhang, R. Sources, Health Effects and Control Strategies of Indoor Fine Particulate Matter (PM2. 5): A Review. *Sci. Total Environ.* **2017**, *586*, 610–622.
44. Milhem, S.A.; Verriele, M.; Nicolas, M.; Thevenet, F. Indoor Use of Essential Oil-Based Cleaning Products: Emission Rate and Indoor Air Quality Impact Assessment Based on a Realistic Application Methodology. *Atmos. Environ.* **2021**, *246*, 118060.
45. World Health Organization Indoor Air Quality: Organic Pollutants: Report on a WHO Meeting. In *EURO Reports and Studies (WHO-EURO)*; World Health Organization. Regional Office for Europe, 1989 ISBN 92-890-1277-3.
46. Weisel, C.P.; Alimokhtari, S.; Sanders, P.F. Indoor Air VOC Concentrations in Suburban and

Rural New Jersey. *Environ. Sci. Technol.* **2008**, *42*, 8231–8238.

47. Huang, Y.; Ho, S.S.H.; Ho, K.F.; Lee, S.C.; Yu, J.Z.; Louie, P.K. Characteristics and Health Impacts of VOCs and Carbonyls Associated with Residential Cooking Activities in Hong Kong. *J. Hazard. Mater.* **2011**, *186*, 344–351.
48. Brickus, L.S.; Cardoso, J.N.; de Aquino Neto, F.R. Distributions of Indoor and Outdoor Air Pollutants in Rio de Janeiro, Brazil: Implications to Indoor Air Quality in Bayside Offices. *Environ. Sci. Technol.* **1998**, *32*, 3485–3490.
49. Kotzias, D. Indoor Air and Human Exposure Assessment–Needs and Approaches. *Exp. Toxicol. Pathol.* **2005**, *57*, 5–7.
50. Schneider, P.; Gebefügi, I.; Richter, K.; Wölke, G.; Schnelle, J.; Wichmann, H.-E.; Heinrich, J.; the INGA-Study, I.S.G. Indoor and Outdoor BTX Levels in German Cities. *Sci. Total Environ.* **2001**, *267*, 41–51.
51. Adgate, J.L.; Church, T.R.; Ryan, A.D.; Ramachandran, G.; Fredrickson, A.L.; Stock, T.H.; Morandi, M.T.; Sexton, K. Outdoor, Indoor, and Personal Exposure to VOCs in Children. *Environ. Health Perspect.* **2004**, *112*, 1386–1392.
52. Hwang, G.; Yoon, C.; Choi, J. A Case-Control Study: Exposure Assessment of VOCs and Formaldehyde for Asthma in Children. *Aerosol Air Qual. Res.* **2011**, *11*, 908–914.
53. Wolkoff, P.; Nielsen, G.D. Organic Compounds in Indoor Air—Their Relevance for Perceived Indoor Air Quality? *Atmos. Environ.* **2001**, *35*, 4407–4417.
54. Du, Z.; Mo, J.; Zhang, Y.; Xu, Q. Benzene, Toluene and Xylenes in Newly Renovated Homes and Associated Health Risk in Guangzhou, China. *Build. Environ.* **2014**, *72*, 75–81.
55. Jones, A.P. Indoor Air Quality and Health. *Atmos. Environ.* **1999**, *33*, 4535–4564.
56. Smoke, T.; Smoking, I. IARC Monographs on the Evaluation of Carcinogenic Risks to Humans. *IARC Lyon* **2004**, *1*, 1–1452.
57. Donald, J.M.; Hooper, K.; Hopenhayn-Rich, C. Reproductive and Developmental Toxicity of

Toluene: A Review. *Environ. Health Perspect.* **1991**, *94*, 237–244.

58. Taylor, J.; Fay, M.; Williams, R.L.; Wilbur, S.B.; McClure, P.R.; Zaccaria, K.; Johnson, H.D.; Citra, M.J. Toxicological Profile for Toluene. **2017**.
59. IARC Working Group on the Evaluation of Carcinogenic Risks to Humans; International Agency for Research on Cancer; World Health Organization *Some Industrial Chemicals*; World Health Organization, 2000; Vol. 77; ISBN 92-832-1277-0.
60. Hormigos-Jimenez, S.; Padilla-Marcos, M.Á.; Meiss, A.; Gonzalez-Lezcano, R.A.; Feijó-Muñoz, J. Ventilation Rate Determination Method for Residential Buildings According to TVOC Emissions from Building Materials. *Build. Environ.* **2017**, *123*, 555–563.
61. Panagiotaras, D.; Nikolopoulos, D.; Koulougliotis, D.; Petraki, E.; Zisos, I.; Yiannopoulos, A.; Bakalis, A.; Zisos, A. Indoor Air Quality Assessment: Review on the Topic of VOCs. **2013**.
62. KETTRUP, A.; RISSE, O. Total Volatile Organic Compounds (WOC) in Indoor Air Quality Investigations.
63. Jarvis, D.J.; Adamkiewicz, G.; Heroux, M.-E.; Rapp, R.; Kelly, F.J. Nitrogen Dioxide. In *WHO guidelines for indoor air quality: Selected pollutants*; World Health Organization, 2010.
64. Katsouyanni, K.; Touloumi, G.; Spix, C.; Schwartz, J.; Balducci, F.; Medina, S.; Rossi, G.; Wojtyniak, B.; Sunyer, J.; Bacharova, L. Short Term Effects of Ambient Sulphur Dioxide and Particulate Matter on Mortality in 12 European Cities: Results from Time Series Data from the APHEA Project. *Bmj* **1997**, *314*, 1658.
65. Agbo, K.E.; Walgraeve, C.; Eze, J.I.; Ugwoke, P.E.; Ukoha, P.O.; Van Langenhove, H. Household Indoor Concentration Levels of NO2, SO2 and O3 in Nsukka, Nigeria. *Atmos. Environ.* **2021**, *244*, 117978.
66. Siegel, J. Primary and Secondary Consequences of Indoor Air Cleaners. *Indoor Air* **2016**, *26*, 88–96.
67. Huang, Y.; Yang, Z.; Gao, Z. Contributions of Indoor and Outdoor Sources to Ozone in

Residential Buildings in Nanjing. *Int. J. Environ. Res. Public. Health* **2019**, *16*, 2587.

68. Fernández, L.C.; Alvarez, R.F.; González-Barcala, F.J.; Portal, J.A.R. Indoor Air Contaminants and Their Impact on Respiratory Pathologies. *Arch. Bronconeumol. Engl. Ed.* **2013**, *49*, 22–27.
69. Leung, D.Y. Outdoor-Indoor Air Pollution in Urban Environment: Challenges and Opportunity. *Front. Environ. Sci.* **2015**, *2*, 69.
70. Singh, D.; Kumar, A.; Kumar, K.; Singh, B.; Mina, U.; Singh, B.B.; Jain, V.K. Statistical Modeling of O3, NOx, CO, PM2. 5, VOCs and Noise Levels in Commercial Complex and Associated Health Risk Assessment in an Academic Institution. *Sci. Total Environ.* **2016**, *572*, 586–594.
71. He, G.; Pan, Y.; Tanaka, T. The Short-Term Impacts of COVID-19 Lockdown on Urban Air Pollution in China. *Nat. Sustain.* **2020**, *3*, 1005–1011.
72. Bao, R.; Zhang, A. Does Lockdown Reduce Air Pollution? Evidence from 44 Cities in Northern China. *Sci. Total Environ.* **2020**, *731*, 139052.
73. Siciliano, B.; Carvalho, G.; da Silva, C.M.; Arbilla, G. The Impact of COVID-19 Partial Lockdown on Primary Pollutant Concentrations in the Atmosphere of Rio de Janeiro and São Paulo Megacities (Brazil). *Bull. Environ. Contam. Toxicol.* **2020**, *105*, 2–8, doi:10.1007/s00128-020-02907-9.
74. Amoatey, P.; Omidvarborna, H.; Baawain, M.S.; Al-Mamun, A. Impact of Building Ventilation Systems and Habitual Indoor Incense Burning on SARS-CoV-2 Virus Transmissions in Middle Eastern Countries. *Sci. Total Environ.* **2020**, *733*, 139356.
75. Azuma, K.; Yanagi, U.; Kagi, N.; Kim, H.; Ogata, M.; Hayashi, M. Environmental Factors Involved in SARS-CoV-2 Transmission: Effect and Role of Indoor Environmental Quality in the Strategy for COVID-19 Infection Control. *Environ. Health Prev. Med.* **2020**, *25*, 1–16.
76. Adam, M.G.; Tran, P.T.; Balasubramanian, R. Air Quality Changes in Cities during the

COVID-19 Lockdown: A Critical Review. *Atmospheric Res.* **2021**, *264*, 105823.

77. Anderson, E.L.; Turnham, P.; Griffin, J.R.; Clarke, C.C. Consideration of the Aerosol Transmission for COVID-19 and Public Health. *Risk Anal.* **2020**, *40*, 902–907.
78. Fattorini, D.; Regoli, F. Role of the Chronic Air Pollution Levels in the Covid-19 Outbreak Risk in Italy. *Environ. Pollut.* **2020**, *264*, 114732.
79. Conticini, E.; Frediani, B.; Caro, D. Can Atmospheric Pollution Be Considered a Co-Factor in Extremely High Level of SARS-CoV-2 Lethality in Northern Italy? *Environ. Pollut.* **2020**, *261*, 114465.
80. Frontera, A.; Cianfanelli, L.; Vlachos, K.; Landoni, G.; Cremona, G. Severe Air Pollution Links to Higher Mortality in COVID-19 Patients: The "Double-Hit" Hypothesis. *J. Infect.* **2020**, *81*, 255–259.
81. Hulin, M.; Simoni, M.; Viegi, G.; Annesi-Maesano, I. Respiratory Health and Indoor Air Pollutants Based on Quantitative Exposure Assessments. *Eur. Respir. J.* **2012**, *40*, 1033–1045.
82. Kotzias, D.; Koistinen, K.; Kephalopoulos, S.; Schlitt, C.; Carrer, P.; Maroni, M.; Jantunen, M.; Cochet, C.; Kirchner, S.; Lindvall, T. Critical Appraisal of the Setting and Implementation of Indoor Exposure Limits in the EU. *INDEX Proj. Final Rep. EUR* **2005**, *21590*.
83. Koistinen, K.; Kotzias, D.; Kephalopoulos, S.; Schlitt, C.; Carrer, P.; Jantunen, M.; Kirchner, S.; McLaughlin, J.; Mølhave, L.; Fernandes, E. The INDEX Project: Executive Summary of a European Union Project on Indoor Air Pollutants. *Allergy* **2008**, *63*, 810–819.
84. Fernández-Agüera, J.; Domínguez-Amarillo, S.; Alonso, C.; Martín-Consuegra, F. Thermal Comfort and Indoor Air Quality in Low-Income Housing in Spain: The Influence of Airtightness and Occupant Behaviour. *Energy Build.* **2019**, *199*, 102–114.
85. Shrubsole, C.; Dimitroulopoulou, S.; Foxall, K.; Gadeberg, B.; Doutsi, A. IAQ Guidelines for Selected Volatile Organic Compounds (VOCs) in the UK. *Build. Environ.* **2019**, *165*, 106382.
86. Agence nationale de sécurité sanitaire de l'alimentation, de l'environnement et du travail

Valeurs Guides de Qualité d'Air Intérieur (VGAI). Available online: https://www.anses.fr/en/content/indoor-air-quality-guidelines-iaqgs.

87. Ahola, M.; Säteri, J.; Sariola, L. Revised Finnish Classification of Indoor Climate 2018.; EDP Sciences, 2019; Vol. 111, p. 02017.
88. Gezondheidsraad, H. Indoor Air Quality in Belgium. *HGR Brussel* **2017**.
89. GB/T 18883-2002 Indoor Air Quality Standard. **2002**.
90. Reitze Jr, A.W.; Carof, S.-L. The Legal Control of Indoor Air Pollution. *BC Envtl Aff Rev* **1997**, *25*, 247.
91. Abdeen, A.; O'Brien, W.; Gunay, B.; Newsham, G.; Knudsen, H. Investigation of Occupant-Related Energy Aspects of the National Building Code of Canada: Energy Use Impact and Potential Least-Cost Code-Compliant Upgrades. *Sci. Technol. Built Environ.* **2021**, *27*, 1393–1424.
92. Kondo, J. Ministry of the Environment: Government of Japan. **2015**.
93. Abdul-Wahab, S.A.; En, S.C.F.; Elkamel, A.; Ahmadi, L.; Yetilmezsoy, K. A Review of Standards and Guidelines Set by International Bodies for the Parameters of Indoor Air Quality. *Atmospheric Pollut. Res.* **2015**, *6*, 751–767.
94. Azuma, K. Guidelines and Regulations for Indoor Environmental Quality. In *Indoor Environmental Quality and Health Risk toward Healthier Environment for All*; Kishi, R., Norbäck, D., Araki, A., Eds.; Springer Singapore: Singapore, 2020; pp. 303–318 ISBN 978-981-329-182-9.
95. Lippmann, M. Environmental Toxicants: Human Exposures and Their Health Effects. **2000**.
96. Raub, J. Health Effects of Exposure to Ambient Carbon Monoxide. *Chemosphere-Glob. Change Sci.* **1999**, *1*, 331–351.
97. Jetter, J.J.; Guo, Z.; McBrian, J.A.; Flynn, M.R. Characterization of Emissions from Burning Incense. *Sci. Total Environ.* **2002**, *295*, 51–67.

98. ARASHIDANI, K.; YOSHIKAWA, M.; KAWAMOTO, T.; MATSUNO, K.; KAYAMA, F.; KODAMA, Y. Indoor Pollution from Heating. *Ind. Health* **1996**, *34*, 205–215.

99. Harrison, R.; Saborit, J.M.D.; Dor, F.; Henderson, R.; Penney, D.; Benignus, V.; Kephalopoulos, S.; Kotzias, D.; Kleinman, M.; Verrier, A. WHO Guidelines for Indoor Air Quality: Selected Pollutants. *World Health Organ. Geneva* **2010**.

100. Hodgson, A.T.; Levin, H. Volatile Organic Compounds in Indoor Air: A Review of Concentrations Measured in North America since 1990. **2003**.

101. Duarte-Davidson, R.; Courage, C.; Rushton, L.; Levy, L. Benzene in the Environment: An Assessment of the Potential Risks to the Health of the Population. *Occup. Environ. Med.* **2001**, *58*, 2–13.

102. National Center for Biotechnology Information PubChem Compound Summary for CID 241, Benzene Available online: https://pubchem.ncbi.nlm.nih.gov/compound/benzene.

103. Harrison, R.M.; Delgado-Saborit; Dor, F. *Benzene. in WHO Guidelines for Indoor Air Quality: Selected Pollutants Ed Pollutants*; World Health Organization, 2020;

104. Salthammer, T.; Mentese, S.; Marutzky, R. Formaldehyde in the Indoor Environment. *Chem. Rev.* **2010**, *110*, 2536–2572.

105. Wisthaler, A.; Apel, E.; Bossmeyer, J.; Hansel, A.; Junkermann, W.; Koppmann, R.; Meier, R.; Müller, K.; Solomon, S.; Steinbrecher, R. Intercomparison of Formaldehyde Measurements at the Atmosphere Simulation Chamber SAPHIR. *Atmospheric Chem. Phys.* **2008**, *8*, 2189–2200.

106. Salthammer, T.; Mentese, S. Comparison of Analytical Techniques for the Determination of Aldehydes in Test Chambers. *Chemosphere* **2008**, *73*, 1351–1356.

107. Fonger, G.C. Hazardous Substances Data Bank (HSDB) as a Source of Environmental Fate Information on Chemicals. *Toxicology* **1995**, *103*, 137–145.

108. Nazaroff, W.W.; Weschler, C.J. Cleaning Products and Air Fresheners: Exposure to

Primary and Secondary Air Pollutants. *Atmos. Environ.* **2004**, *38*, 2841–2865.

109. European Commission. Joint Research Centre. Institute for Health and Consumer Protection. *Harmonisation Framework for Health Based Evaluation of Indoor Emissions from Construction Products in the European Union Using the EU-LCI Concept.*; Publications Office: LU, 2013;

110. Rosemond, Z.A. *Toxicological Profile for Styrene*; Agency for Toxic Substances and Disease Registry, 2010;

111. Agency for Toxic Substances and Disease Registry(ATSDR) *Toxicological Profile for Toluene*; 2017;

112. Fay, M.; Risher, J.; Wilson, J.D. Toxicological Profile for Xylene. **2007**.

113. National Center for Biotechnology Information PubChem Compound Summary for CID 7809, p-Xylene.

114. Leaderer, B.P.; Naeher, L.; Jankun, T.; Balenger, K.; Holford, T.R.; Toth, C.; Sullivan, J.; Wolfson, J.M.; Koutrakis, P. Indoor, Outdoor, and Regional Summer and Winter Concentrations of PM10, PM2. 5, SO4 (2)-, H+, NH4+, NO3-, NH3, and Nitrous Acid in Homes with and without Kerosene Space Heaters. *Environ. Health Perspect.* **1999**, *107*, 223–231.

115. Zhang, H.; Srinivasan, R. A Systematic Review of Air Quality Sensors, Guidelines, and Measurement Studies for Indoor Air Quality Management. *Sustainability* **2020**, *12*, 9045.

116. Settimo, G.; Manigrasso, M.; Avino, P. Indoor Air Quality: A Focus on the European Legislation and State-of-the-Art Research in Italy. *Atmosphere* **2020**, *11*, 370.

117. Aroonruengsawat, A.; Auffhammer, M.; Sanstad, A.H. The Impact of State Level Building Codes on Residential Electricity Consumption. *Energy J.* **2012**, *33*.

118. Framework Guidelines for Energy Efficiency Standards in Buildings. **2020**.

119. Cao, X.; Dai, X.; Liu, J. Building Energy-Consumption Status Worldwide and the State-

of-the-Art Technologies for Zero-Energy Buildings during the Past Decade. *Energy Build.* **2016**, *128*, 198–213.

120. Poza-Casado, I.; Cardoso, V.E.; Almeida, R.M.; Meiss, A.; Ramos, N.M.; Padilla-Marcos, M.Á. Residential Buildings Airtightness Frameworks: A Review on the Main Databases and Setups in Europe and North America. *Build. Environ.* **2020**, *183*, 107221.

121. Kersten, S.; NRW, E. Energieeinsparverordnung (EnEV 2014/2016). **2014**.

122. Charlot-Valdieu, C.; Outrequin, P. *Ecoquartier-Mode d'emploi*; Editions Eyrolles, 2011; ISBN 2-212-85319-X.

123. International Conference of Building Officials and Southern Building Code Congress *International Code Council and Building Officials and Code Administrators International*; 2000;

124. Davies, M.; Ucci, M.; McCarthy, M.; Oreszczyn, T.; Ridley, I.; Mumovic, D.; Singh, J.; Pretlove, S. A Review of Evidence Linking Ventilation Rates in Dwellings and Respiratory Health–a Focus on House Dust Mites and Mould. *Int. J. Vent.* **2004**, *3*, 155–168.

125. Rode, C.; Abadie, M.; Qin, M.; Grunewald, J.; Kolarik, J.; Laverge, J. Key Findings of IEA EBC Annex 68-Indoor Air Quality Design and Control in Low Energy Residential Buildings.; IOP Publishing, 2019; Vol. 609, p. 032057.

126. Derbez, M.; Wyart, G.; Le Ponner, E.; Ramalho, O.; Ribéron, J.; Mandin, C. Indoor Air Quality in Energy-efficient Dwellings: Levels and Sources of Pollutants. *Indoor Air* **2018**, *28*, 318–338.

127. Krstić, H.; Koški, Ž.; Teni, M.; Čolaković, B. Measurements and Analysis of Air Tightness and Indoor Air Quality in Non-Residential Buildings. *Ann. Fac. Eng. Hunedoara* **2019**, *17*, 23–29.

128. Collignan, B.; Le Ponner, E.; Mandin, C. Relationships between Indoor Radon Concentrations, Thermal Retrofit and Dwelling Characteristics. *J. Environ. Radioact.* **2016**,

165, 124–130.

129. Fleischer, R.L.; Mogro-Campero, A.; Turner, L.G. Indoor Radon Levels: Effects of Energy-Efficiency in Homes. *Environ. Int.* **1982**, *8*, 105–109.

130. Jiránek, M.; Kačmaříková, V. Dealing with the Increased Radon Concentration in Thermally Retrofitted Buildings. *Radiat. Prot. Dosimetry* **2014**, *160*, 43–47.

131. Ringer, W. Monitoring Trends in Civil Engineering and Their Effect on Indoor Radon. *Radiat. Prot. Dosimetry* **2014**, *160*, 38–42.

132. Collins, M.; Dempsey, S. Residential Energy Efficiency Retrofits: Potential Unintended Consequences. *J. Environ. Plan. Manag.* **2019**, *62*, 2010–2025.

133. Symonds, P.; Rees, D.; Daraktchieva, Z.; McColl, N.; Bradley, J.; Hamilton, I.; Davies, M. Home Energy Efficiency and Radon: An Observational Study. *Indoor Air* **2019**, *29*, 854–864.

134. Bataille, E. Impact of Low Energy Buildings on Indoor Air Quality (IAQ). *Rehva J* **2011**, *48*, 5–8.

135. Poirier, B.; Guyot, G.; Geoffroy, H.; Woloszyn, M.; Ondarts, M.; Gonze, E. Pollutants Emission Scenarios for Residential Ventilation Performance Assessment. A Review. *J. Build. Eng.* **2021**, *42*, 102488.

136. Morawska, L.; Afshari, A.; Bae, G.; Buonanno, G.; Chao, C.Y.H.; Hänninen, O.; Hofmann, W.; Isaxon, C.; Jayaratne, E.R.; Pasanen, P. Indoor Aerosols: From Personal Exposure to Risk Assessment. *Indoor Air* **2013**, *23*, 462–487.

137. Rivas, I.; Fussell, J.C.; Kelly, F.J.; Querol, X. Indoor Sources of Air Pollutants. In *Issues in Environmental Science and Technology*; Harrison, R.M., Hester, R.E., Eds.; Royal Society of Chemistry: Cambridge, 2019; pp. 1–34 ISBN 978-1-78801-514-1.

138. Farmer, D.K.; Vance, M.E.; Abbatt, J.P.; Abeleira, A.; Alves, M.R.; Arata, C.; Boedicker, E.; Bourne, S.; Cardoso-Saldaña, F.; Corsi, R. Overview of HOMEChem: House Observations of Microbial and Environmental Chemistry. *Environ. Sci. Process. Impacts* **2019**, *21*, 1280–

1300.

139. European Parliament. Directorate General for Internal Policies of the Union. *Air Pollution and COVID-19 :Including Elements of Air Pollution in Rural Areas, Indoor Air Pollution, Vulnerability and Resilience Aspects of Our Society against Respiratory Disease, Social Inequality Stemming from Air Pollution.*; Publications Office: LU, 2020;

140. Liu, S.; Li, R.; Wild, R.; Warneke, C.; De Gouw, J.; Brown, S.; Miller, S.; Luongo, J.; Jimenez, J.; Ziemann, P. Contribution of Human-related Sources to Indoor Volatile Organic Compounds in a University Classroom. *Indoor Air* **2016**, *26*, 925–938.

141. Dunagan, S.C.; Dodson, R.E.; Rudel, R.A.; Brody, J.G. Toxics Use Reduction in the Home: Lessons Learned from Household Exposure Studies. *J. Clean. Prod.* **2011**, *19*, 438–444.

142. Marć, M.; Zabiegała, B.; Namieśnik, J. Testing and Sampling Devices for Monitoring Volatile and Semi-Volatile Organic Compounds in Indoor Air. *TrAC Trends Anal. Chem.* **2012**, *32*, 76–86.

143. Missia, D.A.; Demetriou, E.; Michael, N.; Tolis, E.I.; Bartzis, J.G. Indoor Exposure from Building Materials: A Field Study. *Atmos. Environ.* **2010**, *44*, 4388–4395, doi:10.1016/j.atmosenv.2010.07.049.

144. Xu, Y.; Zhang, Y. A General Model for Analyzing Single Surface VOC Emission Characteristics from Building Materials and Its Application. *Atmos. Environ.* **2004**, *38*, 113–119.

145. Gao, M.; Liu, W.; Wang, H.; Shao, X.; Shi, A.; An, X.; Li, G.; Nie, L. Emission Factors and Characteristics of Volatile Organic Compounds (VOCs) from Adhesive Application in Indoor Decoration in China. *Sci. Total Environ.* **2021**, *779*, 145169.

146. Breysse, P.N.; Diette, G.B.; Matsui, E.C.; Butz, A.M.; Hansel, N.N.; McCormack, M.C. Indoor Air Pollution and Asthma in Children. *Proc. Am. Thorac. Soc.* **2010**, *7*, 102–106.

147. Hansel, N.N.; Breysse, P.N.; McCormack, M.C.; Matsui, E.C.; Curtin-Brosnan, J.; Williams, D.L.; Moore, J.L.; Cuhran, J.L.; Diette, G.B. A Longitudinal Study of Indoor Nitrogen Dioxide Levels and Respiratory Symptoms in Inner-City Children with Asthma. *Environ. Health Perspect.* **2008**, *116*, 1428–1432.

148. Chafe, Z.; Brauer, M.; Héroux, M.-E.; Klimont, Z.; Lanki, T.; Salonen, R.O.; Smith, K.R. Residential Heating with Wood and Coal: Health Impacts and Policy Options in Europe and North America. **2015**.

149. Kerimray, A.; Rojas-Solórzano, L.; Torkmahalleh, M.A.; Hopke, P.K.; Gallachóir, B.P.Ó. Coal Use for Residential Heating: Patterns, Health Implications and Lessons Learned. *Energy Sustain. Dev.* **2017**, *40*, 19–30.

150. World Health Organization *WHO Guidelines for Indoor Air Quality: Household Fuel Combustion*; World Health Organization, 2014; ISBN 92-4-154887-8.

151. Frasca, D.; Marcoccia, M.; Tofful, L.; Simonetti, G.; Perrino, C.; Canepari, S. Influence of Advanced Wood-Fired Appliances for Residential Heating on Indoor Air Quality. *Chemosphere* **2018**, *211*, 62–71.

152. Fullerton, D.G.; Bruce, N.; Gordon, S.B. Indoor Air Pollution from Biomass Fuel Smoke Is a Major Health Concern in the Developing World. *Trans. R. Soc. Trop. Med. Hyg.* **2008**, *102*, 843–851.

153. Lévesque, B.; Allaire, S.; Gauvin, D.; Koutrakis, P.; Gingras, S.; Rhainds, M.; Prud'Homme, H.; Duchesne, J.-F. Wood-Burning Appliances and Indoor Air Quality. *Sci. Total Environ.* **2001**, *281*, 47–62.

154. Vaishnav, P.; Fatimah, A.M. The Environmental Consequences of Electrifying Space Heating. *Environ. Sci. Technol.* **2020**, *54*, 9814–9823.

155. Abdullahi, K.L.; Delgado-Saborit, J.M.; Harrison, R.M. Emissions and Indoor Concentrations of Particulate Matter and Its Specific Chemical Components from Cooking: A

Review. *Atmos. Environ.* **2013**, *71*, 260–294.

156. Kim, K.-H.; Pandey, S.K.; Kabir, E.; Susaya, J.; Brown, R.J. The Modern Paradox of Unregulated Cooking Activities and Indoor Air Quality. *J. Hazard. Mater.* **2011**, *195*, 1–10.

157. Lee, K.; Xue, J.; Geyh, A.S.; Ozkaynak, H.; Leaderer, B.P.; Weschler, C.J.; Spengler, J.D. Nitrous Acid, Nitrogen Dioxide, and Ozone Concentrations in Residential Environments. *Environ. Health Perspect.* **2002**, *110*, 145–150.

158. Duffy, E.; Cauven, E.; Morrin, A. Colorimetric Sensing of Volatile Organic Compounds Produced from Heated Cooking Oils. *ACS Omega* **2021**, *6*, 7394–7401.

159. Kabir, E.; Kim, K.-H. An Investigation on Hazardous and Odorous Pollutant Emission during Cooking Activities. *J. Hazard. Mater.* **2011**, *188*, 443–454.

160. Duffy, E.; Huttunen, K.; Lahnavik, R.; Smeaton, A.F.; Morrin, A. Visualising Household Air Pollution: Colorimetric Sensor Arrays for Monitoring Volatile Organic Compounds Indoors. *PloS One* **2021**, *16*, e0258281.

161. Jo, S.-H.; Kim, K.-H.; Shon, Z.-H.; Parker, D. Identification of Control Parameters for the Sulfur Gas Storability with Bag Sampling Methods. *Anal. Chim. Acta* **2012**, *738*, 51–58.

162. Kurmi, O.P.; Lam, K.B.H.; Ayres, J.G. Indoor Air Pollution and the Lung in Low-and Medium-Income Countries. **2012**.

163. Baxter, L.K.; Clougherty, J.E.; Laden, F.; Levy, J.I. Predictors of Concentrations of Nitrogen Dioxide, Fine Particulate Matter, and Particle Constituents inside of Lower Socioeconomic Status Urban Homes. *J. Expo. Sci. Environ. Epidemiol.* **2007**, *17*, 433–444.

164. Dennekamp, M.; Howarth, S.; Dick, C.; Cherrie, J.W.; Donaldson, K.; Seaton, A. Ultrafine Particles and Nitrogen Oxides Generated by Gas and Electric Cooking. *Occup. Environ. Med.* **2001**, *58*, 511–516.

165. Kornartit, C.; Sokhi, R.; Burton, M.; Ravindra, K. Activity Pattern and Personal Exposure to Nitrogen Dioxide in Indoor and Outdoor Microenvironments. *Environ. Int.* **2010**, *36*, 36–45.

166. Dėdelė, A.; Miškinytė, A. Seasonal Variation of Indoor and Outdoor Air Quality of Nitrogen Dioxide in Homes with Gas and Electric Stoves. *Environ. Sci. Pollut. Res.* **2016**, *23*, 17784–17792.

167. Lin, W.; Brunekreef, B.; Gehring, U. Meta-Analysis of the Effects of Indoor Nitrogen Dioxide and Gas Cooking on Asthma and Wheeze in Children. *Int. J. Epidemiol.* **2013**, *42*, 1724–1737.

168. Zhao, H.; Chan, W.R.; Cohn, S.; Delp, W.W.; Walker, I.S.; Singer, B.C. Indoor Air Quality in New and Renovated Low-income Apartments with Mechanical Ventilation and Natural Gas Cooking in California. *Indoor Air* **2021**, *31*, 717–729.

169. Earnest, C.M.; Corsi, R.L. Inhalation Exposure to Cleaning Products: Application of a Two-Zone Model. *J. Occup. Environ. Hyg.* **2013**, *10*, 328–335.

170. Viegas, S.; Prista, J. Formaldehyde in Indoor Air: A Public Health Problem. *Air Pollut. XVIII* **2010**, *136*, 297.

171. Zarogianni, A.-M.; Loupa, G.; Rapsomanikis, S. A Comparison of Fragrance Ingredients in Green and Nongreen Detergents. *Environ. Forensics* **2017**, *18*, 110–121.

172. Odabasi, M. Halogenated Volatile Organic Compounds from the Use of Chlorine-Bleach-Containing Household Products. *Environ. Sci. Technol.* **2008**, *42*, 1445–1451.

173. Nair, A.; Yadav, P.; Behl, A.; Sharma, R.K.; Kulshrestha, S.; Butola, B.S.; Sharma, N. Toxic Blister Agents: Chemistry, Mode of Their Action and Effective Treatment Strategies. *Chem. Biol. Interact.* **2021**, *350*, 109654.

174. Mattila, J.M.; Arata, C.; Wang, C.; Katz, E.F.; Abeleira, A.; Zhou, Y.; Zhou, S.; Goldstein, A.H.; Abbatt, J.P.; DeCarlo, P.F. Dark Chemistry during Bleach Cleaning Enhances Oxidation of Organics and Secondary Organic Aerosol Production Indoors. *Environ. Sci. Technol. Lett.* **2020**, *7*, 795–801.

175. Odabasi, M.; Elbir, T.; Dumanoglu, Y.; Sofuoglu, S.C. Halogenated Volatile Organic

Compounds in Chlorine-Bleach-Containing Household Products and Implications for Their Use. *Atmos. Environ.* **2014**, *92*, 376–383.

176. Dewey, H.M.; Jones, J.M.; Keating, M.R.; Budhathoki-Uprety, J. Increased Use of Disinfectants during the COVID-19 Pandemic and Its Potential Impacts on Health and Safety. *ACS Chem. Health Saf.* **2021**, *29*, 27–38.

177. Dimitroulopoulou, C.; Trantallidi, M.; Carrer, P.; Efthimiou, G.; Bartzis, et J. EPHECT II: Exposure Assessment to Household Consumer Products. *Sci. Total Environ.* **2015**, *536*, 890–902.

178. Steinemann, A. Volatile Emissions from Common Consumer Products. *Air Qual. Atmosphere Health* **2015**, *8*, 273–281.

179. Kim, J.-H.; Lee, D.; Lim, H.; Kim, T.; Suk, K.; Seo, J. Risk Assessment to Human Health: Consumer Exposure to Ingredients in Air Fresheners. *Regul. Toxicol. Pharmacol.* **2018**, *98*, 31–40.

180. Lee, M.; Kim, J.-H.; Lee, D.; Kim, J.; Lim, H.; Seo, J.; Park, Y.-K. Health Risk Assessment on Hazardous Ingredients in Household Deodorizing Products. *Int. J. Environ. Res. Public. Health* **2018**, *15*, 744.

181. The United States Food and Drug Administration (FDA) Recognized Consensus Standard Available online: https://www.accessdata.fda.gov/scripts/cdrh/cfdocs/cfStandards/results.cfm?start_search=1&productcode=&category=&type=&title=&organization=&referencenumber=&regulationnumber=&recognitionnumber=&effectivedatefrom=&effectivedateto=&sortcolumn=pdd.

182. Steinemann, A. Health and Societal Effects from Exposure to Fragranced Consumer Products. *Prev. Med. Rep.* **2017**, *5*, 45–47.

183. Wallace, L. Assessing Human Exposure to Volatile Organic Compounds. *Indoor Air Qual. Handb.* **2001**, 33–1.

184. Edwards, R.D.; Jurvelin, J.; Saarela, K.; Jantunen, M. VOC Concentrations Measured in Personal Samples and Residential Indoor, Outdoor and Workplace Microenvironments in EXPOLIS-Helsinki, Finland. *Atmos. Environ.* **2001**, *35*, 4531–4543.

185. Geiss, O.; Giannopoulos, G.; Tirendi, S.; Barrero-Moreno, J.; Larsen, B.R.; Kotzias, D. The AIRMEX Study-VOC Measurements in Public Buildings and Schools/Kindergartens in Eleven European Cities: Statistical Analysis of the Data. *Atmos. Environ.* **2011**, *45*, 3676–3684.

186. Nazaroff, W.W. Indoor Particle Dynamics. *Indoor Air* **2004**, *14*, 175–183.

187. Singer, B.C.; Coleman, B.K.; Destaillats, H.; Hodgson, A.T.; Lunden, M.M.; Weschler, C.J.; Nazaroff, W.W. Indoor Secondary Pollutants from Cleaning Product and Air Freshener Use in the Presence of Ozone. *Atmos. Environ.* **2006**, *40*, 6696–6710.

188. Rossignol, S.; Rio, C.; Ustache, A.; Fable, S.; Nicolle, J.; Même, A.; D'anna, B.; Nicolas, M.; Leoz, E.; Chiappini, L. The Use of a Housecleaning Product in an Indoor Environment Leading to Oxygenated Polar Compounds and SOA Formation: Gas and Particulate Phase Chemical Characterization. *Atmos. Environ.* **2013**, *75*, 196–205.

189. Mercier, F.; Glorennec, P.; Thomas, O.; Bot, B.L. Organic Contamination of Settled House Dust, a Review for Exposure Assessment Purposes. *Environ. Sci. Technol.* **2011**, *45*, 6716–6727.

190. Vojta, Š.; Bečanová, J.; Melymuk, L.; Komprdová, K.; Kohoutek, J.; Kukučka, P.; Klánová, J. Screening for Halogenated Flame Retardants in European Consumer Products, Building Materials and Wastes. *Chemosphere* **2017**, *168*, 457–466.

191. Rauert, C.; Lazarov, B.; Harrad, S.; Covaci, A.; Stranger, M. A Review of Chamber Experiments for Determining Specific Emission Rates and Investigating Migration Pathways of Flame Retardants. *Atmos. Environ.* **2014**, *82*, 44–55.

192. 186., U.S.E.Agency. *Toxics Release Inventory List of Toxic Chemicals within the Nicotine*

and Salts Category; 1999;

193. Harrison, R.M.; Colbeck, I.; Simmons, A. Comparative Evaluation of Indoor and Outdoor Air Quality-chemical Considerations. *Environ. Technol.* **1988**, *9*, 521–530.

194. Lakey, P.S.; Wisthaler, A.; Berkemeier, T.; Mikoviny, T.; Pöschl, U.; Shiraiwa, M. Chemical Kinetics of Multiphase Reactions between Ozone and Human Skin Lipids: Implications for Indoor Air Quality and Health Effects. *Indoor Air* **2017**, *27*, 816–828.

195. Wisthaler, A.; Weschler, C.J. Reactions of Ozone with Human Skin Lipids: Sources of Carbonyls, Dicarbonyls, and Hydroxycarbonyls in Indoor Air. *Proc. Natl. Acad. Sci.* **2010**, *107*, 6568–6575.

196. Sahay, R.; Iraq, R. Human Skin Cells: A Potential Source of Building Contaminants. **2018**, *(IS-2018-185)*.

197. Fenske, J.D.; Paulson, S.E. Human Breath Emissions of VOCs. *J. Air Waste Manag. Assoc.* **1999**, *49*, 594–598.

198. Phillips, M.; Greenberg, J. Method for the Collection and Analysis of Volatile Compounds in the Breath. *J. Chromatogr. B. Biomed. Sci. App.* **1991**, *564*, 242–249.

199. Sun, X.; He, J.; Yang, X. Human Breath as a Source of VOCs in the Built Environment, Part I: A Method for Sampling and Detection Species. *Build. Environ.* **2017**, *125*, 565–573.

200. Kruza, M.; Carslaw, N. How Do Breath and Skin Emissions Impact Indoor Air Chemistry? *Indoor Air* **2019**, *29*, 369–379.

201. Awada, M.; Becerik-Gerber, B.; Hoque, S.; O'Neill, Z.; Pedrielli, G.; Wen, J.; Wu, T. Ten Questions Concerning Occupant Health in Buildings during Normal Operations and Extreme Events Including the COVID-19 Pandemic. *Build. Environ.* **2021**, *188*, 107480.

202. Koksoy Vayisoglu, S.; Oncu, E. The Use of Cleaning Products and Its Relationship with the Increasing Health Risks during the COVID-19 Pandemic. *Int. J. Clin. Pract.* **2021**, *75*, e14534.

203. Nwanaji-Enwerem, J.C.; Allen, J.G.; Beamer, P.I. Another Invisible Enemy Indoors: COVID-19, Human Health, the Home, and United States Indoor Air Policy. *J. Expo. Sci. Environ. Epidemiol.* **2020**, *30*, 773–775.

204. Schripp, T.; Wensing, M. Emission of VOCs and SVOCs from Electronic Devices and Office Equipment. In *Organic Indoor Air Pollutants*; Salthammer, T., Uhde, E., Eds.; Wiley-VCH Verlag GmbH & Co. KGaA: Weinheim, Germany, 2009; pp. 405–430 ISBN 978-3-527-62888-9.

205. Bako-Biro, Z.; Wargocki, P.; Weschler, C.J.; Fanger, P.O. Effects of Pollution from Personal Computers on Perceived Air Quality, SBS Symptoms and Productivity in Offices. *Indoor Air* **2004**, *14*, 178–187.

206. Hoshino, K. Measurement of SVOCs Emitted from Building Materials and Electric Appliances Using Thermal Desorption Test Chamber Method.; 2003; Vol. 1, pp. 474–479.

207. Destaillats, H.; Maddalena, R.L.; Singer, B.C.; Hodgson, A.T.; McKone, T.E. Indoor Pollutants Emitted by Office Equipment: A Review of Reported Data and Information Needs. *Atmos. Environ.* **2008**, *42*, 1371–1388.

208. Lee, C.-W.; Dai, Y.-T.; Chien, C.-H.; Hsu, D.-J. Characteristics and Health Impacts of Volatile Organic Compounds in Photocopy Centers. *Environ. Res.* **2006**, *100*, 139–149.

209. Barrese, E.; Gioffrè, A.; Scarpelli, M.; Turbante, D.; Trovato, R.; Iavicoli, S. Indoor Pollution in Work Office: VOCs, Formaldehyde and Ozone by Printer. *Occup. Dis. Environ. Med.* **2014**, *2014*.

210. Kagi, N.; Fujii, S.; Horiba, Y.; Namiki, N.; Ohtani, Y.; Emi, H.; Tamura, H.; Kim, Y.S. Indoor Air Quality for Chemical and Ultrafine Particle Contaminants from Printers. *Build. Environ.* **2007**, *42*, 1949–1954.

211. He, C.; Morawska, L.; Taplin, L. Particle Emission Characteristics of Office Printers. *Environ. Sci. Technol.* **2007**, *41*, 6039–6045.

212. Brown, E. Quantifying Pollutant Emissions from Office Equipment: A Concern in Energy-Efficient Buildings. *Calif. Energy Comm. Public Interest Energy Res. PIER Collab. Rep.* **2011**.

213. He, S.; Han, J. Electrostatic Fine Particles Emitted from Laser Printers as Potential Vectors for Airborne Transmission of COVID-19. *Environ. Chem. Lett.* **2021**, *19*, 17–24.

214. Morawska, L.; He, C.; Johnson, G.; Jayaratne, R.; Salthammer, T.; Wang, H.; Uhde, E.; Bostrom, T.; Modini, R.; Ayoko, G. An Investigation into the Characteristics and Formation Mechanisms of Particles Originating from the Operation of Laser Printers. *Environ. Sci. Technol.* **2009**, *43*, 1015–1022.

215. Ramos, C.; Wolterbeek, H.; Almeida, S. Exposure to Indoor Air Pollutants during Physical Activity in Fitness Centers. *Build. Environ.* **2014**, *82*, 349–360.

216. Ramos, C.; Reis, J.; Almeida, T.; Alves, F.; Wolterbeek, H.; Almeida, S. Estimating the Inhaled Dose of Pollutants during Indoor Physical Activity. *Sci. Total Environ.* **2015**, *527*, 111–118.

217. Buonanno, G.; Fuoco, F.; Marini, S.; Stabile, L. Particle Resuspension in School Gyms during Physical Activities. *Aerosol Air Qual. Res.* **2012**, *12*, 803–813.

218. Žitnik, M.; Bučar, K.; Hiti, B.; Barba, Ž.; Rupnik, Z.; Založnik, A.; Žitnik, E.; Rodrìguez, L.; Mihevc, I.; Žibert, J. Exercise-induced Effects on a Gym Atmosphere. *Indoor Air* **2016**, *26*, 468–477.

219. Castro, A.; Calvo, A.I.; Alves, C.; Alonso-Blanco, E.; Coz, E.; Marques, L.; Nunes, T.; Fernández-Guisuraga, J.M.; Fraile, R. Indoor Aerosol Size Distributions in a Gymnasium. *Sci. Total Environ.* **2015**, *524*, 178–186.

220. Dominski, F.H.; Brandt, R. Do the Benefits of Exercise in Indoor and Outdoor Environments during the COVID-19 Pandemic Outweigh the Risks of Infection? *Sport Sci. Health* **2020**, *16*, 583–588.

221. Mumith, A.; Thomas, M.; Shah, Z.; Coathup, M.; Blunn, G. Additive Manufacturing: Current Concepts, Future Trends. *Bone Jt. J* **2018**, *100*, 455–460.

222. Zhou, Y.; Kong, X.; Chen, A.; Cao, S. Investigation of Ultrafine Particle Emissions of Desktop 3D Printers in the Clean Room. *Procedia Eng.* **2015**, *121*, 506–512.

223. Afshar-Mohajer, N.; Wu, C.-Y.; Ladun, T.; Rajon, D.A.; Huang, Y. Characterization of Particulate Matters and Total VOC Emissions from a Binder Jetting 3D Printer. *Build. Environ.* **2015**, *93*, 293–301.

224. Sittichompoo, S.; Kanagalingam, S.; Thomas-Seale, L.; Tsolakis, A.; Herreros, J. Characterization of Particle Emission from Thermoplastic Additive Manufacturing. *Atmos. Environ.* **2020**, *239*, 117765.

225. Khaki, S.; Duffy, E.; Smeaton, A.F.; Morrin, A. Monitoring of Particulate Matter Emissions from 3D Printing Activity in the Home Setting. *Sensors* **2021**, *21*, 3247.

226. Steinle, P. Characterization of Emissions from a Desktop 3D Printer and Indoor Air Measurements in Office Settings. *J. Occup. Environ. Hyg.* **2016**, *13*, 121–132.

227. Zhang, Q.; Pardo, M.; Rudich, Y.; Kaplan-Ashiri, I.; Wong, J.P.; Davis, A.Y.; Black, M.S.; Weber, R.J. Chemical Composition and Toxicity of Particles Emitted from a Consumer-Level 3D Printer Using Various Materials. *Environ. Sci. Technol.* **2019**, *53*, 12054–12061.

228. Min, K.; Li, Y.; Wang, D.; Chen, B.; Ma, M.; Hu, L.; Liu, Q.; Jiang, G. 3D Printing-Induced Fine Particle and Volatile Organic Compound Emission: An Emerging Health Risk. *Environ. Sci. Technol. Lett.* **2021**, *8*, 616–625.

229. Farcas, M.T.; Stefaniak, A.B.; Knepp, A.K.; Bowers, L.; Mandler, W.K.; Kashon, M.; Jackson, S.R.; Stueckle, T.A.; Sisler, J.D.; Friend, S.A. Acrylonitrile Butadiene Styrene (ABS) and Polycarbonate (PC) Filaments Three-Dimensional (3-D) Printer Emissions-Induced Cell Toxicity. *Toxicol. Lett.* **2019**, *317*, 1–12.

230. Potter, P.M.; Al-Abed, S.R.; Lay, D.; Lomnicki, S.M. VOC Emissions and Formation

Mechanisms from Carbon Nanotube Composites during 3D Printing. *Environ. Sci. Technol.* **2019**, *53*, 4364–4370.

231. Wojnowski, W.; Kalinowska, K.; Majchrzak, T.; Zabiegała, B. Real-Time Monitoring of the Emission of Volatile Organic Compounds from Polylactide 3D Printing Filaments. *Sci. Total Environ.* **2022**, *805*, 150181.

232. Stefaniak, A.B.; LeBouf, R.F.; Yi, J.; Ham, J.; Nurkewicz, T.; Schwegler-Berry, D.E.; Chen, B.T.; Wells, J.R.; Duling, M.G.; Lawrence, R.B. Characterization of Chemical Contaminants Generated by a Desktop Fused Deposition Modeling 3-Dimensional Printer. *J. Occup. Environ. Hyg.* **2017**, *14*, 540–550.

233. Azimi, P.; Zhao, D.; Pouzet, C.; Crain, N.E.; Stephens, B. Emissions of Ultrafine Particles and Volatile Organic Compounds from Commercially Available Desktop Three-Dimensional Printers with Multiple Filaments. *Environ. Sci. Technol.* **2016**, *50*, 1260–1268.

234. Salthammer, T. Emerging Indoor Pollutants. *Int. J. Hyg. Environ. Health* **2020**, *224*, 113423.

235. Gu, J.; Wensing, M.; Uhde, E.; Salthammer, T. Characterization of Particulate and Gaseous Pollutants Emitted during Operation of a Desktop 3D Printer. *Environ. Int.* **2019**, *123*, 476–485.

236. Davis, A.Y.; Zhang, Q.; Wong, J.P.; Weber, R.J.; Black, M.S. Characterization of Volatile Organic Compound Emissions from Consumer Level Material Extrusion 3D Printers. *Build. Environ.* **2019**, *160*, 106209.

237. Weber, R.J.; Zhang, Q.; Wong, J.P.; Davis, A.; Black, M. Fine Particulate and Chemical Emissions from Desktop 3D Printers.; Society for Imaging Science and Technology, 2016; Vol. 2016, pp. 121–123.

238. Sakhi, A.K.; Cequier, E.; Becher, R.; Bølling, A.K.; Borgen, A.R.; Schlabach, M.; Schmidbauer, N.; Becher, G.; Schwarze, P.; Thomsen, C. Concentrations of Selected

Chemicals in Indoor Air from Norwegian Homes and Schools. *Sci. Total Environ.* **2019**, *674*, 1–8.

239. Chiappini, L.; Dagnelie, R.; Sassine, M.; Fuvel, F.; Fable, S.; Tran-Thi, T.-H.; George, C. Multi-Tool Formaldehyde Measurement in Simulated and Real Atmospheres for Indoor Air Survey and Concentration Change Monitoring. *Air Qual. Atmosphere Health* **2011**, *4*, 211–220.

240. Cipolla, M.; Izzotti, A.; Ansaldi, F.; Durando, P.; Piccardo, M.T. Volatile Organic Compounds in Anatomical Pathology Wards: Comparative and Qualitative Assessment of Indoor Airborne Pollution. *Int. J. Environ. Res. Public. Health* **2017**, *14*, 609.

241. Crump, D. Source Control: A European Perspective. *Indoor Built Environ.* **2017**, *26*, 587–589.

242. World Health Organization. Regional Office for Europe *Methods for Sampling and Analysis of Chemical Pollutants in Indoor Air: Supplementary Publication to the Screening Tool for Assessment of Health Risks from Combined Exposure to Multiple Chemicals in Indoor Air in Public Settings for Children*; World Health Organization. Regional Office for Europe: Copenhagen, 2020; ISBN 978-92-890-5523-9.

243. Adon, M.; Galy-Lacaux, C.; Yoboué, V.; Delon, C.; Lacaux, J.; Castera, P.; Gardrat, E.; Pienaar, J.; Al Ourabi, H.; Laouali, D. Long Term Measurements of Sulfur Dioxide, Nitrogen Dioxide, Ammonia, Nitric Acid and Ozone in Africa Using Passive Samplers. *Atmospheric Chem. Phys.* **2010**, *10*, 7467–7487.

244. Carmichael, G.R.; Ferm, M.; Thongboonchoo, N.; Woo, J.-H.; Chan, L.; Murano, K.; Viet, P.H.; Mossberg, C.; Bala, R.; Boonjawat, J. Measurements of Sulfur Dioxide, Ozone and Ammonia Concentrations in Asia, Africa, and South America Using Passive Samplers. *Atmos. Environ.* **2003**, *37*, 1293–1308.

245. ISO, I. 16000-1: Indoor Air—Part 1: General Aspects of Sampling Strategy. *ISO Geneva*

Switz. **2004**.

246. ISO, I. 16000–6: 2011 Indoor Air—Part. 6: Determination of Volatile Organic Compounds in Indoor and Test Chamber Air by Active Sampling on Tenax TA Sorbent, Thermal Desorption and Gas Chromatography Using MS or MS-FID. *Therm. Desorption Gas Chromatogr. Using MS MS-FID* **2011**.

247. Pienaar, J.; Beukes, J.P.; Van Zyl, P.G.; Lehmann, C.; Aherne, J. Passive Diffusion Sampling Devices for Monitoring Ambient Air Concentrations. In *Comprehensive analytical chemistry*; Elsevier, 2015; Vol. 70, pp. 13–52 ISBN 0166-526X.

248. McAlary, T.; Groenevelt, H.; Disher, S.; Arnold, J.; Seethapathy, S.; Sacco, P.; Crump, D.; Schumacher, B.; Hayes, H.; Johnson, P. Passive Sampling for Volatile Organic Compounds in Indoor Air-Controlled Laboratory Comparison of Four Sampler Types. *Environ. Sci. Process. Impacts* **2015**, *17*, 896–905.

249. Odencrantz, J.E.; Thornley, S.C.; O'Neill, H. An Evaluation of the Performance of Multiple Passive Diffusion Devices for Indoor Air Sampling of VOCs. *Remediat. J. J. Environ. Cleanup Costs Technol. Tech.* **2009**, *19*, 63–72.

250. Krupa, S.; Legge, A. Passive Sampling of Ambient, Gaseous Air Pollutants: An Assessment from an Ecological Perspective. *Environ. Pollut.* **2000**, *107*, 31–45.

251. Bohlin, P.; Jones, K.C.; Strandberg, B. Occupational and Indoor Air Exposure to Persistent Organic Pollutants: A Review of Passive Sampling Techniques and Needs. *J. Environ. Monit.* **2007**, *9*, 501–509.

252. Woolfenden, E. Sorbent-Based Sampling Methods for Volatile and Semi-Volatile Organic Compounds in Air. Part 2. Sorbent Selection and Other Aspects of Optimizing Air Monitoring Methods. *J. Chromatogr. A* **2010**, *1217*, 2685–2694.

253. Grosse, D.; McKernan, J. Passive Samplers for the Investigations of Air Quality: Method Description, Implementation, and Comparison to Alternative Sampling Methods. *US Environ.*

Prot. Agency **2014**.

254. Newton, S.; Sellström, U.; Harrad, S.; Yu, G.; De Wit, C.A. Comparisons of Indoor Active and Passive Air Sampling Methods for Emerging and Legacy Halogenated Flame Retardants in Beijing, China Offices. *Emerg. Contam.* **2016**, *2*, 80–88.

255. Albaseer, S.S.; Rao, R.N.; Swamy, Y.; Mukkanti, K. An Overview of Sample Preparation and Extraction of Synthetic Pyrethroids from Water, Sediment and Soil. *J. Chromatogr. A* **2010**, *1217*, 5537–5554.

256. Bohlin, P.; Audy, O.; Škrdlíková, L.; Kukučka, P.; Vojta, Š.; Přibylová, P.; Prokeš, R.; Čupr, P.; Klánová, J. Evaluation and Guidelines for Using Polyurethane Foam (PUF) Passive Air Samplers in Double-Dome Chambers to Assess Semi-Volatile Organic Compounds (SVOCs) in Non-Industrial Indoor Environments. *Environ. Sci. Process. Impacts* **2014**, *16*, 2617–2626.

257. Woolfenden, E. Sorbent-Based Sampling Methods for Volatile and Semi-Volatile Organic Compounds in Air: Part 1: Sorbent-Based Air Monitoring Options. *J. Chromatogr. A* **2010**, *1217*, 2674–2684.

258. Thammakhet, C.; Muneesawang, V.; Thavarungkul, P.; Kanatharana, P. Cost Effective Passive Sampling Device for Volatile Organic Compounds Monitoring. *Atmos. Environ.* **2006**, *40*, 4589–4596.

259. Li, Q.; Wang, X.; Wang, X.; Lan, Y.; Hu, J. Tube-Type Passive Sampling of Cyclic Volatile Methyl Siloxanes (CVMSs) and Benzene Series Simultaneously in Indoor Air: Uptake Rate Determination and Field Application. *Environ. Sci. Process. Impacts* **2020**, *22*, 973–980.

260. Brown, R.H. Environmental Use of Diffusive Samplers: Evaluation of Reliable Diffusive Uptake Rates for Benzene, Toluene and Xylene. *J. Environ. Monit.* **1999**, *1*, 115–116.

261. Cocheo, V.; Boaretto, C.; Sacco, P. High Uptake Rate Radial Diffusive Sampler Suitable

for Both Solvent and Thermal Desorption. *Am. Ind. Hyg. Assoc. J.* **1996**, *57*, 897–904.

262. Namieśnik, J.; Zabiegała, B.; Kot-Wasik, A.; Partyka, M.; Wasik, A. Passive Sampling and/or Extraction Techniques in Environmental Analysis: A Review. *Anal. Bioanal. Chem.* **2005**, *381*, 279–301.

263. Jalili, V.; Barkhordari, A.; Ghiasvand, A. A Comprehensive Look at Solid-Phase Microextraction Technique: A Review of Reviews. *Microchem. J.* **2020**, *152*, 104319.

264. Souza-Silva, É.A.; Jiang, R.; Rodríguez-Lafuente, Á.; Gionfriddo, E.; Pawliszyn, J.B. A Critical Review of the State of the Art of Solid-Phase Microextraction of Complex Matrices I. Environmental Analysis. *Trends Anal. Chem.* **2015**, *71*, 224–235.

265. Boyacı, E.; Rodríguez-Lafuente, Á.; Gorynski, K.; Mirnaghi, F.; Souza-Silva, É.A.; Hein, D.; Pawliszyn, J. Sample Preparation with Solid Phase Microextraction and Exhaustive Extraction Approaches: Comparison for Challenging Cases. *Anal. Chim. Acta* **2015**, *873*, 14–30.

266. Demirhan, B.; Kara, H.E.Ş.; Demirhan, B.E. Overview of Green Sample Preparation Techniques in Food Analysis. In *Ideas and applications toward sample preparation for food and beverage analysis*; IntechOpen, 2017 ISBN 953-51-3686-0.

267. Souza-Silva, É.A.; Reyes-Garcés, N.; Gómez-Ríos, G.A.; Boyacı, E.; Bojko, B.; Pawliszyn, J. A Critical Review of the State of the Art of Solid-Phase Microextraction of Complex Matrices III. Bioanalytical and Clinical Applications. *TrAC Trends Anal. Chem.* **2015**, *71*, 249–264.

268. Kamgang Nzekoue, F.; Angeloni, S.; Caprioli, G.; Cortese, M.; Maggi, F.; Marconi, U.M.B.; Perali, A.; Ricciutelli, M.; Sagratini, G.; Vittori, S. Fiber–Sample Distance, an Important Parameter to Be Considered in Headspace Solid-Phase Microextraction Applications. *Anal. Chem.* **2020**, *92*, 7478–7484.

269. Jagirani, M.S.; Soylak, M. A Review: Recent Advances in Solid Phase Microextraction of

Toxic Pollutants Using Nanotechnology Scenario. *Microchem. J.* **2020**, *159*, 105436.

270. Hübschmann, H.-J. *Handbook of GC-MS: Fundamentals and Applications*; John Wiley & Sons, 2015; ISBN 3-527-33474-2.

271. Schmidt, K.; Podmore, I. Solid Phase Microextraction (SPME) Method Development in Analysis of Volatile Organic Compounds (VOCS) as Potential Biomarkers of Cancer. *J. Mol. Biomark. Diagn.* **2015**, *6*.

272. Liberto, E.; Bicchi, C.; Cagliero, C.; Cordero, C.; Rubiolo, P.; Sgorbini, B. Chapter 1. Headspace Sampling: An "Evergreen" Method in Constant Evolution to Characterize Food Flavors through Their Volatile Fraction. In *Food Chemistry, Function and Analysis*; Tranchida, P.Q., Ed.; Royal Society of Chemistry: Cambridge, 2019; pp. 1–37 ISBN 978-1-78801-127-3.

273. Merkle, S.; Kleeberg, K.K.; Fritsche, J. Recent Developments and Applications of Solid Phase Microextraction (SPME) in Food and Environmental Analysis—a Review. *Chromatography* **2015**, *2*, 293–381.

274. Llompart, M.; Celeiro, M.; García-Jares, C.; Dagnac, T. Environmental Applications of Solid-Phase Microextraction. *TrAC Trends Anal. Chem.* **2019**, *112*, 1–12.

275. Beldean-Galea, M.S.; Dicu, T.; Cucoş, A.; Burghele, B.-D.; Catalina, T.; Botoş, M.; Ţenter, A.; Szacsvai, K.; Lupulescu, A.; Pap, I. Evaluation of Indoor Air Pollutants in 100 Retrofit Residential Buildings from Romania during Cold Season. *J. Clean. Prod.* **2020**, *277*, 124098.

276. Langer, S.; Ramalho, O.; Le Ponner, E.; Derbez, M.; Kirchner, S.; Mandin, C. Perceived Indoor Air Quality and Its Relationship to Air Pollutants in French Dwellings. *Indoor Air* **2017**, *27*, 1168–1176.

277. Dodson, R.E.; Bessonneau, V.; Udesky, J.O.; Nishioka, M.; McCauley, M.; Rudel, R.A. Passive Indoor Air Sampling for Consumer Product Chemicals: A Field Evaluation Study. *J.*

Expo. Sci. Environ. Epidemiol. **2019**, *29*, 95–108.

278. Bourdin, D.; Desauziers, V. Development of SPME On-Fiber Derivatization for the Sampling of Formaldehyde and Other Carbonyl Compounds in Indoor Air. *Anal. Bioanal. Chem.* **2014**, *406*, 317–328.

279. Lucaire, V.; Schwartz, J.-J.; Delhomme, O.; Ocampo-Torres, R.; Millet, M. A Sensitive Method Using SPME Pre-Concentration for the Quantification of Aromatic Amines in Indoor Air. *Anal. Bioanal. Chem.* **2018**, *410*, 1955–1963.

280. S. Lakka, N.; Kuppan, C. Principles of Chromatography Method Development. In *Biochemical Analysis Tools - Methods for Bio-Molecules Studies*; Boldura, O.-M., Baltă, C., Sayed Awwad, N., Eds.; IntechOpen, 2020 ISBN 978-1-78984-856-4.

281. Moldoveanu, S.C.; David, V. Short Overviews of the Main Analytical Techniques Containing a Separation Step. In *Selection of the HPLC Method in Chemical Analysis*; Elsevier, 2017; pp. 55–85 ISBN 978-0-12-803684-6.

282. Moldoveanu, S.C.; David, V. Gradient Elution. In *Selection of the HPLC Method in Chemical Analysis*; Elsevier, 2017; pp. 451–462 ISBN 978-0-12-803684-6.

283. Swartz, M. HPLC Detectors: A Brief Review. *J. Liq. Chromatogr. Relat. Technol.* **2010**, *33*, 1130–1150.

284. Aizpurua-Olaizola, O.; Omar, J.; Navarro, P.; Olivares, M.; Etxebarria, N.; Usobiaga, A. Identification and Quantification of Cannabinoids in Cannabis Sativa L. Plants by High Performance Liquid Chromatography-Mass Spectrometry. *Anal. Bioanal. Chem.* **2014**, *406*, 7549–7560.

285. Nahar, L.; Onder, A.; Sarker, S.D. A Review on the Recent Advances in HPLC, UHPLC and UPLC Analyses of Naturally Occurring Cannabinoids (2010–2019). *Phytochem. Anal.* **2020**, *31*, 413–457.

286. Roba, C.; Roşu, C.; Neamţiu, I.; Gurzău, E. Rp-Hplc Analysis of Carbonyl Compounds in

Some Indoor Air Samples in a Faculty from Cluj-Napoca. *Environ. Eng. Manag. J.* **2013**, *12*, 219–225.

287. Kondeti, R.R.; Mulpuri, K.S.; Meruga, B. Advancements in Column Chromatography: A Review. *World J. Pharm. Sci.* **2014**, 1375–1383.

288. Bower, N.W. Principles of Instrumental Analysis. (Skoog, DA; Leary, JJ). **1992**.

289. Hinshaw, J.V. A Compendium of GC Terms and Techniques. *LC-GC* **1992**, 22–26.

290. Shellie, R.A. Gas Chromatography. In *Encyclopedia of Forensic Sciences*; Elsevier, 2013; pp. 579–585 ISBN 978-0-12-382166-9.

291. Tranchida, P.Q.; Mondello, L. Detectors and Basic Data Analysis. In *Separation Science and Technology*; Elsevier, 2020; Vol. 12, pp. 205–227 ISBN 1877-1718.

292. Hage, D.S. Chromatography. In *Principles and Applications of Clinical Mass Spectrometry*; Elsevier, 2018; pp. 1–32 ISBN 978-0-12-816063-3.

293. Uyanik, A. ANAESTHETIC MIXTURES: GAS CHROMATOGRAPHY. **2000**.

294. Cowper, C.J. GAS ANALYSIS: GAS CHROMATOGRAPHY. In *Encyclopedia of Separation Science*; Elsevier, 2000; pp. 2925–2932 ISBN 978-0-12-226770-3.

295. Kitson, F.G.; Larsen, B.S.; McEwen, C.N. *Gas Chromatography and Mass Spectrometry: A Practical Guide*; Academic Press, 1996; ISBN 0-08-053232-2.

296. Poole, C.F. GAS CHROMATOGRAPHY | Detectors. In *Encyclopedia of Analytical Science*; Elsevier, 2005; pp. 95–105 ISBN 978-0-12-369397-6.

297. Ojanperä, I.; Rasanen, I. Forensic Screening by Gas Chromatography. In *Handbook of analytical separations*; Elsevier, 2008; Vol. 6, pp. 403–424 ISBN 1567-7192.

298. Holm, T. Aspects of the Mechanism of the Flame Ionization Detector. *J. Chromatogr. A* **1999**, *842*, 221–227.

299. Rubakhin, S.S.; Sweedler, J.V. A Mass Spectrometry Primer for Mass Spectrometry Imaging. In *Mass Spectrometry Imaging*; Springer, 2010; pp. 21–49.

300. Niessen, W. Gas Chromatography-Mass Spectrometry. *Curr. Pract. Gas Chromatogr.-Mass Spectrom.* **2001**, 1.

301. Medeiros, P.M. Gas Chromatography–Mass Spectrometry (GC–MS). In *Encyclopedia of Geochemistry*; White, W.M., Ed.; Encyclopedia of Earth Sciences Series; Springer International Publishing: Cham, 2018; pp. 530–535 ISBN 978-3-319-39311-7.

302. Son, Y.-S.; Lim, B.-A.; Park, H.-J.; Kim, J.-C. Characteristics of Volatile Organic Compounds (VOCs) Emitted from Building Materials to Improve Indoor Air Quality: Focused on Natural VOCs. *Air Qual. Atmosphere Health* **2013**, *6*, 737–746.

303. Rovelli, S.; Cattaneo, A.; Fazio, A.; Spinazzè, A.; Borghi, F.; Campagnolo, D.; Dossi, C.; Cavallo, D.M. VOCs Measurements in Residential Buildings: Quantification via Thermal Desorption and Assessment of Indoor Concentrations in a Case-Study. *Atmosphere* **2019**, *10*, 57.

304. Masih, A.; Lall, A.S.; Taneja, A.; Singhvi, R. Exposure Profiles, Seasonal Variation and Health Risk Assessment of BTEX in Indoor Air of Homes at Different Microenvironments of a Terai Province of Northern India. *Chemosphere* **2017**, *176*, 8–17.

305. Baghani, A.N.; Rostami, R.; Arfaeinia, H.; Hazrati, S.; Fazlzadeh, M.; Delikhoon, M. BTEX in Indoor Air of Beauty Salons: Risk Assessment, Levels and Factors Influencing Their Concentrations. *Ecotoxicol. Environ. Saf.* **2018**, *159*, 102–108.

306. Zhang, D.-C.; Liu, J.-J.; Jia, L.-Z.; Wang, P.; Han, X. Speciation of VOCs in the Cooking Fumes from Five Edible Oils and Their Corresponding Health Risk Assessments. *Atmos. Environ.* **2019**, *211*, 6–17.

307. Yang, S.; Perret, V.; Hager Jörin, C.; Niculita-Hirzel, H.; Goyette Pernot, J.; Licina, D. Volatile Organic Compounds in 169 Energy-efficient Dwellings in Switzerland. *Indoor Air* **2020**, *30*, 481–491.

308. *The IUPAC Compendium of Chemical Terminology: The Gold Book*; Gold, V., Ed.; 4th

ed.; International Union of Pure and Applied Chemistry (IUPAC): Research Triangle Park, NC, 2019;

309. Sonnette, A.; Delhomme, O.; Alleman, L.Y.; Coddeville, P.; Millet, M. A Versatile Method for the Quantification of 100 SVOCs from Various Families: Application to Indoor Air, Dust and Bioaccessibility Evaluation. *Microchem. J.* **2021**, *169*, 106574.

310. Mattinen, M.; Tuominen, J.; Saarela, K. Analysis of TVOC and Certain Selected Compounds from Indoor Air Using GC/FID-RIM Technique. *Indoor Air* **1995**, *5*, 56–61.

311. Begerow, J.; Jermann, E.; Keles, T.; Dunemann, L. Performance of Two Different Types of Passive Samplers for the GC/ECD-FID Determination of Environmental VOC Levels in Air. *Fresenius J. Anal. Chem.* **1999**, *363*, 399–403.

312. Dąbrowski, Ł. Multidetector Systems in Gas Chromatography. *TrAC Trends Anal. Chem.* **2018**, *102*, 185–193.

313. Windt, M.; Meier, D.; Marsman, J.H.; Heeres, H.J.; de Koning, S. Micro-Pyrolysis of Technical Lignins in a New Modular Rig and Product Analysis by GC–MS/FID and GC× GC–TOFMS/FID. *J. Anal. Appl. Pyrolysis* **2009**, *85*, 38–46.

314. Harb, P.; Locoge, N.; Thevenet, et F. Emissions and Treatment of VOCs Emitted from Wood-Based Construction Materials: Impact on Indoor Air Quality. *Chem. Eng. J.* **2018**, *354*, 641–652.

315. Mayhew, C.A.; Herbig, J.; Beauchamp, J.D. Proton Transfer Reaction–Mass Spectrometry. In *Breathborne Biomarkers and the Human Volatilome*; Elsevier, 2020; pp. 155–170 ISBN 978-0-12-819967-1.

316. Berbegal, C.; Khomenko, I.; Russo, P.; Spano, G.; Fragasso, M.; Biasioli, F.; Capozzi, V. PTR-ToF-MS for the Online Monitoring of Alcoholic Fermentation in Wine: Assessment of VOCs Variability Associated with Different Combinations of Saccharomyces/Non-Saccharomyces as a Case-Study. *Fermentation* **2020**, *6*, 55.

317. Klein, F.; Platt, S.M.; Farren, N.J.; Detournay, A.; Bruns, E.A.; Bozzetti, C.; Daellenbach, K.R.; Kilic, D.; Kumar, N.K.; Pieber, S.M. Characterization of Gas-Phase Organics Using Proton Transfer Reaction Time-of-Flight Mass Spectrometry: Cooking Emissions. *Environ. Sci. Technol.* **2016**, *50*, 1243–1250.

318. Gębicki, J.; Dymerski, T. –Application of Chemical Sensors and Sensor Matrixes to Air Quality Evaluation. **2016**.

319. Szulczyński, B.; Gębicki, J. Currently Commercially Available Chemical Sensors Employed for Detection of Volatile Organic Compounds in Outdoor and Indoor Air. *Environments* **2017**, *4*, 21.

320. Pitarma, R.; Marques, G.; Caetano, F. Monitoring Indoor Air Quality to Improve Occupational Health. In *New advances in information systems and technologies*; Springer, 2016; pp. 13–21.

321. Fine, G.F.; Cavanagh, L.M.; Afonja, A.; Binions, R. Metal Oxide Semi-Conductor Gas Sensors in Environmental Monitoring. *sensors* **2010**, *10*, 5469–5502.

322. Janata, J. *Principles of Chemical Sensors*; Springer Science & Business Media, 2010; ISBN 0-387-69931-7.

323. Liu, X.; Cheng, S.; Liu, H.; Hu, S.; Zhang, D.; Ning, H. A Survey on Gas Sensing Technology. *Sensors* **2012**, *12*, 9635–9665, doi:10.3390/s120709635.

324. Dey, A. Semiconductor Metal Oxide Gas Sensors: A Review. *Mater. Sci. Eng. B* **2018**, *229*, 206–217.

325. Moon, Y.K.; Jeong, S.-Y.; Kang, Y.C.; Lee, J.-H. Metal Oxide Gas Sensors with Au Nanocluster Catalytic Overlayer: Toward Tuning Gas Selectivity and Response Using a Novel Bilayer Sensor Design. *ACS Appl. Mater. Interfaces* **2019**, *11*, 32169–32177.

326. Kwon, Y.J.; Kim, H.W.; Ko, W.C.; Choi, H.; Ko, Y.-H.; Jeong, Y.K. Laser-Engineered Oxygen Vacancies for Improving the NO 2 Sensing Performance of SnO 2 Nanowires. *J.*

Mater. Chem. A **2019**, *7*, 27205–27211.

327. Shankar, P.; Rayappan, J.B.B. Gas Sensing Mechanism of Metal Oxides: The Role of Ambient Atmosphere, Type of Semiconductor and Gases-A Review. *Sci Lett J* **2015**, *4*, 126.

328. Kanan, S.M.; El-Kadri, O.M.; Abu-Yousef, I.A.; Kanan, M.C. Semiconducting Metal Oxide Based Sensors for Selective Gas Pollutant Detection. *Sensors* **2009**, *9*, 8158–8196.

329. Filipovic, L.; Lahlalia, A. System-on-Chip SMO Gas Sensor Integration in Advanced CMOS Technology. *J. Electrochem. Soc.* **2018**, *165*, B862.

330. Ng, K.T.; Boussaid, F.; Bermak, A. A CMOS Single-Chip Gas Recognition Circuit for Metal Oxide Gas Sensor Arrays. *IEEE Trans. Circuits Syst. Regul. Pap.* **2011**, *58*, 1569–1580.

331. Joshi, N.; Hayasaka, T.; Liu, Y.; Liu, H.; Oliveira, O.N.; Lin, L. A Review on Chemiresistive Room Temperature Gas Sensors Based on Metal Oxide Nanostructures, Graphene and 2D Transition Metal Dichalcogenides. *Microchim. Acta* **2018**, *185*, 1–16.

332. Isaac, N.A.; Valenti, M.; Schmidt-Ott, A.; Biskos, G. Characterization of Tungsten Oxide Thin Films Produced by Spark Ablation for NO2 Gas Sensing. *ACS Appl. Mater. Interfaces* **2016**, *8*, 3933–3939.

333. Gallego, E.; Folch, J.; Teixidor, P.; Roca, F.J.; Perales, J.F. Outdoor Air Monitoring: Performance Evaluation of a Gas Sensor to Assess Episodic Nuisance/Odorous Events Using Active Multi-Sorbent Bed Tube Sampling Coupled to TD-GC/MS Analysis. *Sci. Total Environ.* **2019**, *694*, 133752.

334. Baur, T.; Amann, J.; Schultealbert, C.; Schütze, A. Field Study of Metal Oxide Semiconductor Gas Sensors in Temperature Cycled Operation for Selective VOC Monitoring in Indoor Air. *Atmosphere* **2021**, *12*, 647.

335. Chen, K.; Gao, W.; Emaminejad, S.; Kiriya, D.; Ota, H.; Nyein, H.Y.Y.; Takei, K.; Javey, A. Printed Carbon Nanotube Electronics and Sensor Systems. *Adv. Mater.* **2016**, *28*, 4397–4414.

336. Wilson, A.D.; Baietto, M. Advances in Electronic-Nose Technologies Developed for Biomedical Applications. *Sensors* **2011**, *11*, 1105–1176.

337. Wilson, A.D.; Baietto, M. Applications and Advances in Electronic-Nose Technologies. *Sensors* **2009**, *9*, 5099–5148.

338. Wilson, A.D. Review of Electronic-Nose Technologies and Algorithms to Detect Hazardous Chemicals in the Environment. *Procedia Technol.* **2012**, *1*, 453–463.

339. Stitzel, S.E.; Aernecke, M.J.; Walt, D.R. Artificial Noses. *Annu. Rev. Biomed. Eng.* **2011**, *13*, 1–25.

340. Capelli, L.; Sironi, S.; Rosso, R.D. Electronic Noses for Environmental Monitoring Applications. *Sensors* **2014**, *14*, 19979–20007.

341. Suchorab, Z.; Frąc, M.; Guz, Ł.; Oszust, K.; Łagód, G.; Gryta, A.; Bilińska-Wielgus, N.; Czerwiński, J. A Method for Early Detection and Identification of Fungal Contamination of Building Materials Using E-Nose. *PLoS One* **2019**, *14*, e0215179.

342. Taştan, M.; Gökozan, H. Real-Time Monitoring of Indoor Air Quality with Internet of Things-Based E-Nose. *Appl. Sci.* **2019**, *9*, 3435.

343. Caron, A.; Redon, N.; Thevenet, F.; Hanoune, B.; Coddeville, P. Performances and Limitations of Electronic Gas Sensors to Investigate an Indoor Air Quality Event. *Build. Environ.* **2016**, *107*, 19–28.

344. Li, Z.; Askim, J.R.; Suslick, K.S. The Optoelectronic Nose: Colorimetric and Fluorometric Sensor Arrays. *Chem. Rev.* **2018**, *119*, 231–292.

345. Janzen, M.C.; Ponder, J.B.; Bailey, D.P.; Ingison, C.K.; Suslick, K.S. Colorimetric Sensor Arrays for Volatile Organic Compounds. *Anal. Chem.* **2006**, *78*, 3591–3600.

346. Azzouz, A.; Vikrant, K.; Kim, K.-H.; Ballesteros, E.; Rhadfi, T.; Malik, A.K. Advances in Colorimetric and Optical Sensing for Gaseous Volatile Organic Compounds. *TrAC Trends Anal. Chem.* **2019**, *118*, 502–516.

347. Kingsborough, R.P.; Wrobel, A.T.; Kunz, R.R. Colourimetry for the Sensitive Detection of Vapour-Phase Chemicals: State of the Art and Future Trends. *TrAC Trends Anal. Chem.* **2021**, *143*, 116397.

348. Huang, X.; Lv, R.; Yao, L.; Guan, C.; Han, F.; Teye, E. Non-Destructive Evaluation of Total Volatile Basic Nitrogen (TVB-N) and K-Values in Fish Using Colorimetric Sensor Array. *Anal. Methods* **2015**, *7*, 1615–1621.

349. Suslick, K.S.; Rakow, N.A.; Sen, A. Colorimetric Sensor Arrays for Molecular Recognition. *Tetrahedron* **2004**, *60*, 11133–11138.

350. Xiaowei, H.; Xiaobo, Z.; Jiewen, Z.; Jiyong, S.; Zhihua, L.; Tingting, S. Monitoring the Biogenic Amines in Chinese Traditional Salted Pork in Jelly (Yao-meat) by Colorimetric Sensor Array Based on Nine Natural Pigments. *Int. J. Food Sci. Technol.* **2015**, *50*, 203–209.

351. Qin, X.; Wang, R.; Tsow, F.; Forzani, E.; Xian, X.; Tao, N. A Colorimetric Chemical Sensing Platform for Real-Time Monitoring of Indoor Formaldehyde. *IEEE Sens. J.* **2014**, *15*, 1545–1551.

352. Li, Z.; Li, H.; LaGasse, M.K.; Suslick, K.S. Rapid Quantification of Trimethylamine. *Anal. Chem.* **2016**, *88*, 5615–5620.

353. Kumar, P.; Martani, C.; Morawska, L.; Norford, L.; Choudhary, R.; Bell, M.; Leach, M. Indoor Air Quality and Energy Management through Real-Time Sensing in Commercial Buildings. *Energy Build.* **2016**, *111*, 145–153.

354. Mead, M.; Popoola, O.; Stewart, G.; Landshoff, P.; Calleja, M.; Hayes, M.; Baldovi, J.; McLeod, M.; Hodgson, T.; Dicks, J. The Use of Electrochemical Sensors for Monitoring Urban Air Quality in Low-Cost, High-Density Networks. *Atmos. Environ.* **2013**, *70*, 186–203.

355. Lowther, S.D.; Jones, K.C.; Wang, X.; Whyatt, J.D.; Wild, O.; Booker, D. Particulate Matter Measurement Indoors: A Review of Metrics, Sensors, Needs, and Applications. *Environ. Sci. Technol.* **2019**, *53*, 11644–11656.

356. Wagner, J.; Leith, D. Passive Aerosol Sampler. Part I: Principle of Operation. *Aerosol Sci. Technol.* **2001**, *34*, 186–192.

357. Noble, C.A.; Vanderpool, R.W.; Peters, T.M.; McElroy, F.F.; Gemmill, D.B.; Wiener, R.W. Federal Reference and Equivalent Methods for Measuring Fine Particulate Matter. *Aerosol Sci. Technol.* **2001**, *34*, 457–464.

358. Leith, D.; Sommerlatt, D.; Boundy, M.G. Passive Sampler for PM10–2.5 Aerosol. *J. Air Waste Manag. Assoc.* **2007**, *57*, 332–336.

359. Whitehead, T.; Leith, D. Passive Aerosol Sampler for Particle Concentrations and Size Distributions. *J. Environ. Monit.* **2008**, *10*, 331–335.

360. Giechaskiel, B.; Maricq, M.; Ntziachristos, L.; Dardiotis, C.; Wang, X.; Axmann, H.; Bergmann, A.; Schindler, W. Review of Motor Vehicle Particulate Emissions Sampling and Measurement: From Smoke and Filter Mass to Particle Number. *J. Aerosol Sci.* **2014**, *67*, 48–86.

361. Amaral, S.S.; de Carvalho Jr, J.A.; Costa, M.A.M.; Pinheiro, C. An Overview of Particulate Matter Measurement Instruments. *Atmosphere* **2015**, *6*, 1327–1345.

362. Wang, Z.; Calderón, L.; Patton, A.P.; Sorensen Allacci, M.; Senick, J.; Wener, R.; Andrews, C.J.; Mainelis, G. Comparison of Real-Time Instruments and Gravimetric Method When Measuring Particulate Matter in a Residential Building. *J. Air Waste Manag. Assoc.* **2016**, *66*, 1109–1120.

363. Patel, S.; Li, J.; Pandey, A.; Pervez, S.; Chakrabarty, R.K.; Biswas, P. Spatio-Temporal Measurement of Indoor Particulate Matter Concentrations Using a Wireless Network of Low-Cost Sensors in Households Using Solid Fuels. *Environ. Res.* **2017**, *152*, 59–65.

364. Jose Chirayil, C.; Abraham, J.; Kumar Mishra, R.; George, S.C.; Thomas, S. Instrumental Techniques for the Characterization of Nanoparticles. In *Thermal and Rheological Measurement Techniques for Nanomaterials Characterization*; Elsevier, 2017; pp. 1–36 ISBN

978-0-323-46139-9.

365. Schmoll, L.H.; Peters, T.M.; O'Shaughnessy, P.T. Use of a Condensation Particle Counter and an Optical Particle Counter to Assess the Number Concentration of Engineered Nanoparticles. *J. Occup. Environ. Hyg.* **2010**, *7*, 535–545.

366. Cheng, Y. Condensation Particle Counters. *Aerosol Meas. Princ. Tech. Appl.* **2011**, 381–392.

367. Sem, G.J. Design and Performance Characteristics of Three Continuous-Flow Condensation Particle Counters: A Summary. *Atmospheric Res.* **2002**, *62*, 267–294.

368. Mills, J.B.; Park, J.H.; Peters, T.M. Comparison of the DiSCmini Aerosol Monitor to a Handheld Condensation Particle Counter and a Scanning Mobility Particle Sizer for Submicrometer Sodium Chloride and Metal Aerosols. *J. Occup. Environ. Hyg.* **2013**, *10*, 250–258.

369. Wehner, B.; Siebert, H.; Hermann, M.; Ditas, F.; Wiedensohler, A. Characterisation of a New Fast CPC and Its Application for Atmospheric Particle Measurements. *Atmospheric Meas. Tech.* **2011**, *4*, 823–833.

370. Hermann, M.; Wehner, B.; Bischof, O.; Han, H.-S.; Krinke, T.; Liu, W.; Zerrath, A.; Wiedensohler, A. Particle Counting Efficiencies of New TSI Condensation Particle Counters. *J. Aerosol Sci.* **2007**, *38*, 674–682.

371. Aggarwal, S.G. Recent Developments in Aerosol Measurement Techniques and the Metrological Issues. *Mapan* **2010**, *25*, 165–189.

372. Intra, P.; Tippayawong, N. An Overview of Aerosol Particle Sensors for Size Distribution Measurement. **2007**.

373. Sosnowski, T.R.; Odziomek, M. Particle Size Dynamics: Toward a Better Understanding of Electronic Cigarette Aerosol Interactions with the Respiratory System. *Front. Physiol.* **2018**, *9*, 853.

374. Kesavan, J.S.; Bottiger, J.R.; Schepers, D.R.; McFarland, A.R. Comparison of Particle Number Counts Measured with an Ink Jet Aerosol Generator and an Aerodynamic Particle Sizer. *Aerosol Sci. Technol.* **2014**, *48*, 219–227.

375. O'Leary, C.; de Kluizenaar, Y.; Jacobs, P.; Borsboom, W.; Hall, I.; Jones, B. Investigating Measurements of Fine Particle (PM 2.5) Emissions from the Cooking of Meals and Mitigating Exposure Using a Cooker Hood. *Indoor Air* **2019**, *29*, 423–438.

376. Fermo, P.; Artíñano, B.; De Gennaro, G.; Pantaleo, A.M.; Parente, A.; Battaglia, F.; Colicino, E.; Di Tanna, G.; da Silva Junior, A.G.; Pereira, I.G. Improving Indoor Air Quality through an Air Purifier Able to Reduce Aerosol Particulate Matter (PM) and Volatile Organic Compounds (VOCs): Experimental Results. *Environ. Res.* **2021**, *197*, 111131.

377. Stabile, L.; De Luca, G.; Pacitto, A.; Morawska, L.; Avino, P.; Buonanno, G. Ultrafine Particle Emission from Floor Cleaning Products. *Indoor Air* **2021**, *31*, 63–73.

378. Wallace, L.; Jeong, S.; Rim, D. Dynamic Behavior of Indoor Ultrafine Particles (2.3-64 Nm) Due to Burning Candles in a Residence. *Indoor Air* **2019**, *29*, 1018–1027.

379. Vu, T.V.; Ondracek, J.; Zdímal, V.; Schwarz, J.; Delgado-Saborit, J.M.; Harrison, R.M. Physical Properties and Lung Deposition of Particles Emitted from Five Major Indoor Sources. *Air Qual. Atmosphere Health* **2017**, *10*, 1–14.

380. Kumar, P.; Morawska, L.; Martani, C.; Biskos, G.; Neophytou, M.; Di Sabatino, S.; Bell, M.; Norford, L.; Britter, R. The Rise of Low-Cost Sensing for Managing Air Pollution in Cities. *Environ. Int.* **2015**, *75*, 199–205.

381. Wang, Y.; Li, J.; Jing, H.; Zhang, Q.; Jiang, J.; Biswas, P. Laboratory Evaluation and Calibration of Three Low-Cost Particle Sensors for Particulate Matter Measurement. *Aerosol Sci. Technol.* **2015**, *49*, 1063–1077.

382. Gao, M.; Cao, J.; Seto, E. A Distributed Network of Low-Cost Continuous Reading Sensors to Measure Spatiotemporal Variations of PM2. 5 in Xi'an, China. *Environ. Pollut.*

2015, *199*, 56–65.

383. Morawska, L.; Thai, P.K.; Liu, X.; Asumadu-Sakyi, A.; Ayoko, G.; Bartonova, A.; Bedini, A.; Chai, F.; Christensen, B.; Dunbabin, M. Applications of Low-Cost Sensing Technologies for Air Quality Monitoring and Exposure Assessment: How Far Have They Gone? *Environ. Int.* **2018**, *116*, 286–299.

384. Snyder, E.G.; Watkins, T.H.; Solomon, P.A.; Thoma, E.D.; Williams, R.W.; Hagler, G.S.; Shelow, D.; Hindin, D.A.; Kilaru, V.J.; Preuss, P.W. The Changing Paradigm of Air Pollution Monitoring. *Environ. Sci. Technol.* **2013**, *47*, 11369–11377.

385. Koehler, K.A.; Peters, T.M. New Methods for Personal Exposure Monitoring for Airborne Particles. *Curr. Environ. Health Rep.* **2015**, *2*, 399–411.

386. Borgese, L.; Chiesa, M.; Assi, A.; Marchesi, C.; Mutahi, A.W.; Kasemi, F.; Federici, S.; Finco, A.; Gerosa, G.; Zappa, D. Assessment of Integrated Aerosol Sampling Techniques in Indoor, Confined and Outdoor Environments Characterized by Specific Emission Sources. *Appl. Sci.* **2021**, *11*, 4360.

387. Shen, H.; Hou, W.; Zhu, Y.; Zheng, S.; Ainiwaer, S.; Shen, G.; Chen, Y.; Cheng, H.; Hu, J.; Wan, Y. Temporal and Spatial Variation of PM2. 5 in Indoor Air Monitored by Low-Cost Sensors. *Sci. Total Environ.* **2021**, *770*, 145304.

388. Wang, Z.; Delp, W.W.; Singer, B.C. Performance of Low-Cost Indoor Air Quality Monitors for PM2. 5 and PM10 from Residential Sources. *Build. Environ.* **2020**, *171*, 106654.

389. Weichenthal, S. Selected Physiological Effects of Ultrafine Particles in Acute Cardiovascular Morbidity. *Environ. Res.* **2012**, *115*, 26–36.

390. Castell, N.; Dauge, F.R.; Schneider, P.; Vogt, M.; Lerner, U.; Fishbain, B.; Broday, D.; Bartonova, A. Can Commercial Low-Cost Sensor Platforms Contribute to Air Quality Monitoring and Exposure Estimates? *Environ. Int.* **2017**, *99*, 293–302.

391. Sayahi, T.; Butterfield, A.; Kelly, K. Long-Term Field Evaluation of the Plantower PMS

Low-Cost Particulate Matter Sensors. *Environ. Pollut.* **2019**, *245*, 932–940.

392. Cincinelli, A.; Martellini, T. Indoor Air Quality and Health. *Int. J. Environ. Res. Public. Health* **2017**, *14*, 1286.

393. Kim, K.-H.; Kabir, E.; Kabir, S. A Review on the Human Health Impact of Airborne Particulate Matter. *Environ. Int.* **2015**, *74*, 136–143.

394. Schins, R.P.; Lightbody, J.H.; Borm, P.J.; Shi, T.; Donaldson, K.; Stone, V. Inflammatory Effects of Coarse and Fine Particulate Matter in Relation to Chemical and Biological Constituents. *Toxicol. Appl. Pharmacol.* **2004**, *195*, 1–11.

395. Bravi, L.; Murmura, F.; Santos, G. Additive Manufacturing: Possible Problems with Indoor Air Quality. *Procedia Manuf.* **2019**, *41*, 952–959.

396. Rayna, T.; Striukova, L. From Rapid Prototyping to Home Fabrication: How 3D Printing Is Changing Business Model Innovation. *Technol. Forecast. Soc. Change* **2016**, *102*, 214–224.

397. Chýlek, R.; Kudela, L.; Pospíšil, J.; Šnajdárek, L. Fine Particle Emission during Fused Deposition Modelling and Thermogravimetric Analysis for Various Filaments. *J. Clean. Prod.* **2019**, *237*, 117790.

398. Cheng, Y.-L.; Zhang, L.-C.; Chen, F.; Tseng, Y.-H. Particle Emissions of Material-Extrusion-Type Desktop 3D Printing: The Effects of Infill. *Int. J. Precis. Eng. Manuf.-Green Technol.* **2018**, *5*, 487–497.

399. Ding, S.; Ng, B.F.; Shang, X.; Liu, H.; Lu, X.; Wan, M.P. The Characteristics and Formation Mechanisms of Emissions from Thermal Decomposition of 3D Printer Polymer Filaments. *Sci. Total Environ.* **2019**, *692*, 984–994.

400. Stabile, L.; Scungio, M.; Buonanno, G.; Arpino, F.; Ficco, G. Airborne Particle Emission of a Commercial 3D Printer: The Effect of Filament Material and Printing Temperature. *Indoor Air* **2017**, *27*, 398–408.

401. Deng, Y.; Cao, S.-J.; Chen, A.; Guo, Y. The Impact of Manufacturing Parameters on

Submicron Particle Emissions from a Desktop 3D Printer in the Perspective of Emission Reduction. *Build. Environ.* **2016**, *104*, 311–319.

402. Kwon, O.; Yoon, C.; Ham, S.; Park, J.; Lee, J.; Yoo, D.; Kim, Y. Characterization and Control of Nanoparticle Emission during 3D Printing. *Environ. Sci. Technol.* **2017**, *51*, 10357–10368.

403. Kim, Y.; Yoon, C.; Ham, S.; Park, J.; Kim, S.; Kwon, O.; Tsai, P.-J. Emissions of Nanoparticles and Gaseous Material from 3D Printer Operation. *Environ. Sci. Technol.* **2015**, *49*, 12044–12053.

404. Jeon, H.; Park, J.; Kim, S.; Park, K.; Yoon, C. Effect of Nozzle Temperature on the Emission Rate of Ultrafine Particles during 3D Printing. *Indoor Air* **2020**, *30*, 306–314.

405. Vance, M.E.; Pegues, V.; Van Montfrans, S.; Leng, W.; Marr, L.C. Aerosol Emissions from Fuse-Deposition Modeling 3D Printers in a Chamber and in Real Indoor Environments. *Environ. Sci. Technol.* **2017**, *51*, 9516–9523.

406. McDonnell, B.; Jimenez Guzman, X.; Dolack, M.; Simpson, T.W.; Cimbala, J.M. 3D Printing in the Wild: A Preliminary Investigation of Air Quality in College Maker Spaces.; University of Texas at Austin, 2016.

407. Byrley, P.; George, B.J.; Boyes, W.K.; Rogers, K. Particle Emissions from Fused Deposition Modeling 3D Printers: Evaluation and Meta-Analysis. *Sci. Total Environ.* **2019**, *655*, 395–407.

408. Mendes, L.; Kangas, A.; Kukko, K.; Mølgaard, B.; Säämänen, A.; Kanerva, T.; Flores Ituarte, I.; Huhtiniemi, M.; Stockmann-Juvala, H.; Partanen, J. Characterization of Emissions from a Desktop 3D Printer. *J. Ind. Ecol.* **2017**, *21*, S94–S106.

409. Afshar-Mohajer, N.; Wu, C.-Y.; Ladun, T.; Rajon, D.A.; Huang, Y. Characterization of Particulate Matters and Total VOC Emissions from a Binder Jetting 3D Printer. *Build. Environ.* **2015**, *93*, 293–301.

410. Wojtyła, S.; Klama, P.; Baran, T. Is 3D Printing Safe? Analysis of the Thermal Treatment of Thermoplastics: ABS, PLA, PET, and Nylon. *J. Occup. Environ. Hyg.* **2017**, *14*, D80–D85.

411. Chojer, H.; Branco, P.; Martins, F.; Alvim-Ferraz, M.; Sousa, S. Development of Low-Cost Indoor Air Quality Monitoring Devices: Recent Advancements. *Sci. Total Environ.* **2020**, *727*, 138385.

412. Tiele, A.; Esfahani, S.; Covington, J. Design and Development of a Low-Cost, Portable Monitoring Device for Indoor Environment Quality. *J. Sens.* **2018**, *2018*.

413. Williams, D.E. Low Cost Sensor Networks: How Do We Know the Data Are Reliable? *ACS Sens.* **2019**, *4*, 2558–2565.

414. Contos, D.; Holdren, M.; Smith, D.; Brooke, R.; Rhodes, V.; Rainey, M. Sampling and Analysis of Volatile Organic Compounds Evolved during Thermal Processing of Acrylonitrile Butadiene Styrene Composite Resins. *J. Air Waste Manag. Assoc.* **1995**, *45*, 686–694.

415. Rodrigues, F.; Caldeira, M.; Câmara, J. de S. Development of a Dynamic Headspace Solid-Phase Microextraction Procedure Coupled to GC–QMSD for Evaluation the Chemical Profile in Alcoholic Beverages. *Anal. Chim. Acta* **2008**, *609*, 82–104.

416. Tabb, D.L.; Vega-Montoto, L.; Rudnick, P.A.; Variyath, A.M.; Ham, A.-J.L.; Bunk, D.M.; Kilpatrick, L.E.; Billheimer, D.D.; Blackman, R.K.; Cardasis, H.L. Repeatability and Reproducibility in Proteomic Identifications by Liquid Chromatography− Tandem Mass Spectrometry. *J. Proteome Res.* **2010**, *9*, 761–776.

417. Allwood, J.W.; Erban, A.; de Koning, S.; Dunn, W.B.; Luedemann, A.; Lommen, A.; Kay, L.; Löscher, R.; Kopka, J.; Goodacre, R. Inter-Laboratory Reproducibility of Fast Gas Chromatography–Electron Impact–Time of Flight Mass Spectrometry (GC–EI–TOF/MS) Based Plant Metabolomics. *Metabolomics* **2009**, *5*, 479–496.

418. Wojnowski, W.; Kalinowska, K.; Gębicki, J.; Zabiegała, B. Monitoring the BTEX Volatiles during 3D Printing with Acrylonitrile Butadiene Styrene (ABS) Using Electronic

Nose and Proton Transfer Reaction Mass Spectrometry. *Sensors* **2020**, *20*, 5531.

419. Byrley, P.; Wallace, M.A.G.; Boyes, W.K.; Rogers, K. Particle and Volatile Organic Compound Emissions from a 3D Printer Filament Extruder. *Sci. Total Environ.* **2020**, *736*, 139604.

420. Floyd, E.L.; Wang, J.; Regens, J.L. Fume Emissions from a Low-Cost 3-D Printer with Various Filaments. *J. Occup. Environ. Hyg.* **2017**, *14*, 523–533.

421. Wojtyła, S.; Klama, P.; Śpiewak, K.; Baran, T. 3D Printer as a Potential Source of Indoor Air Pollution. *Int. J. Environ. Sci. Technol.* **2020**, *17*, 207–218.

422. Kaspersma, J.; Doumen, C.; Munro, S.; Prins, A.-M. Fire Retardant Mechanism of Aliphatic Bromine Compounds in Polystyrene and Polypropylene. *Polym. Degrad. Stab.* **2002**, *77*, 325–331.

Supplementary Information

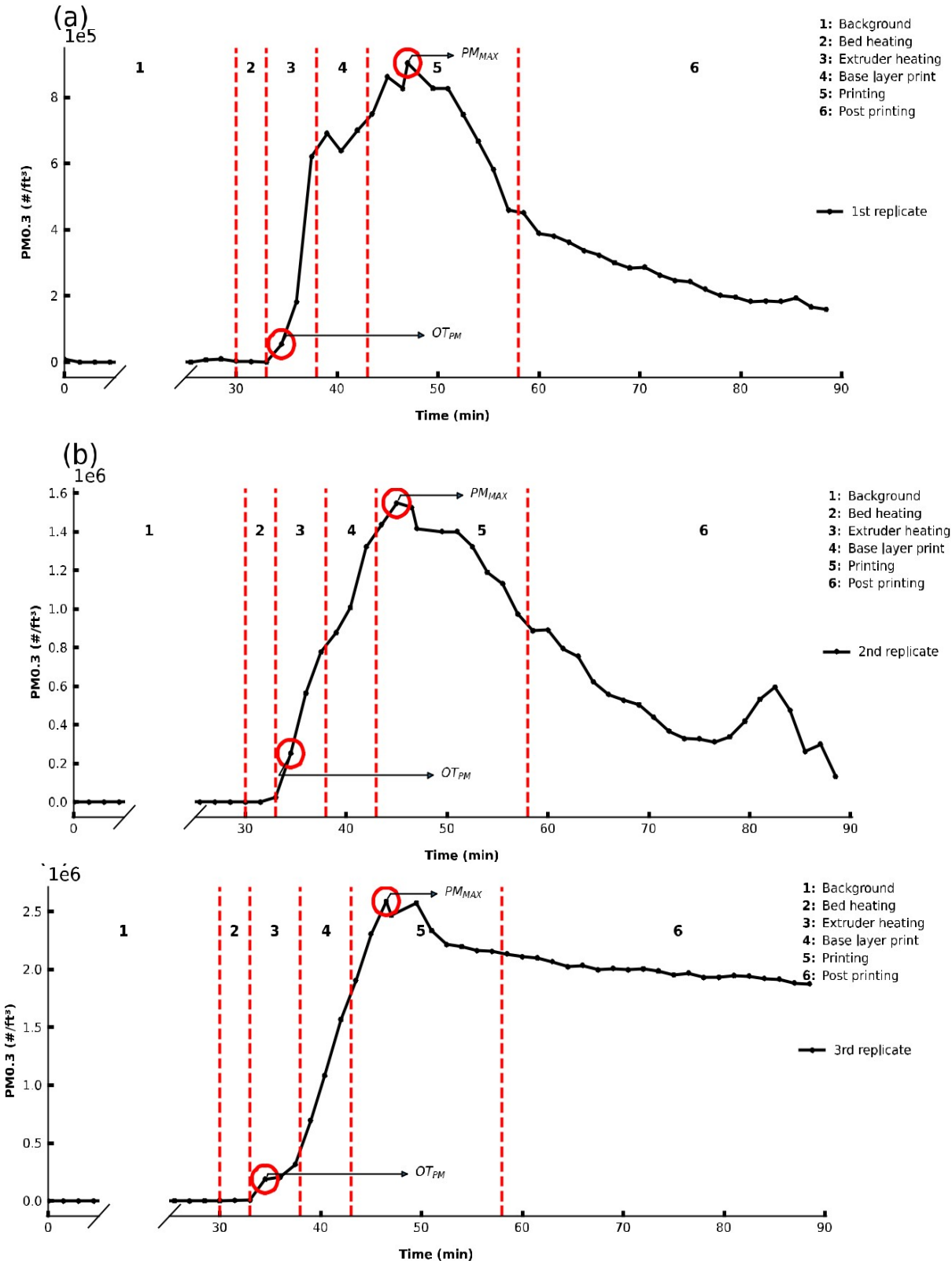

.

Figure S1. $PM_{0.3}$ emission profile for time before, during and after printing of a cube object for ABSB1b (bed plate temperature: 80 °C; extruder temp: 245 °C, 0% fan, 20% infill) for 3 replicates)

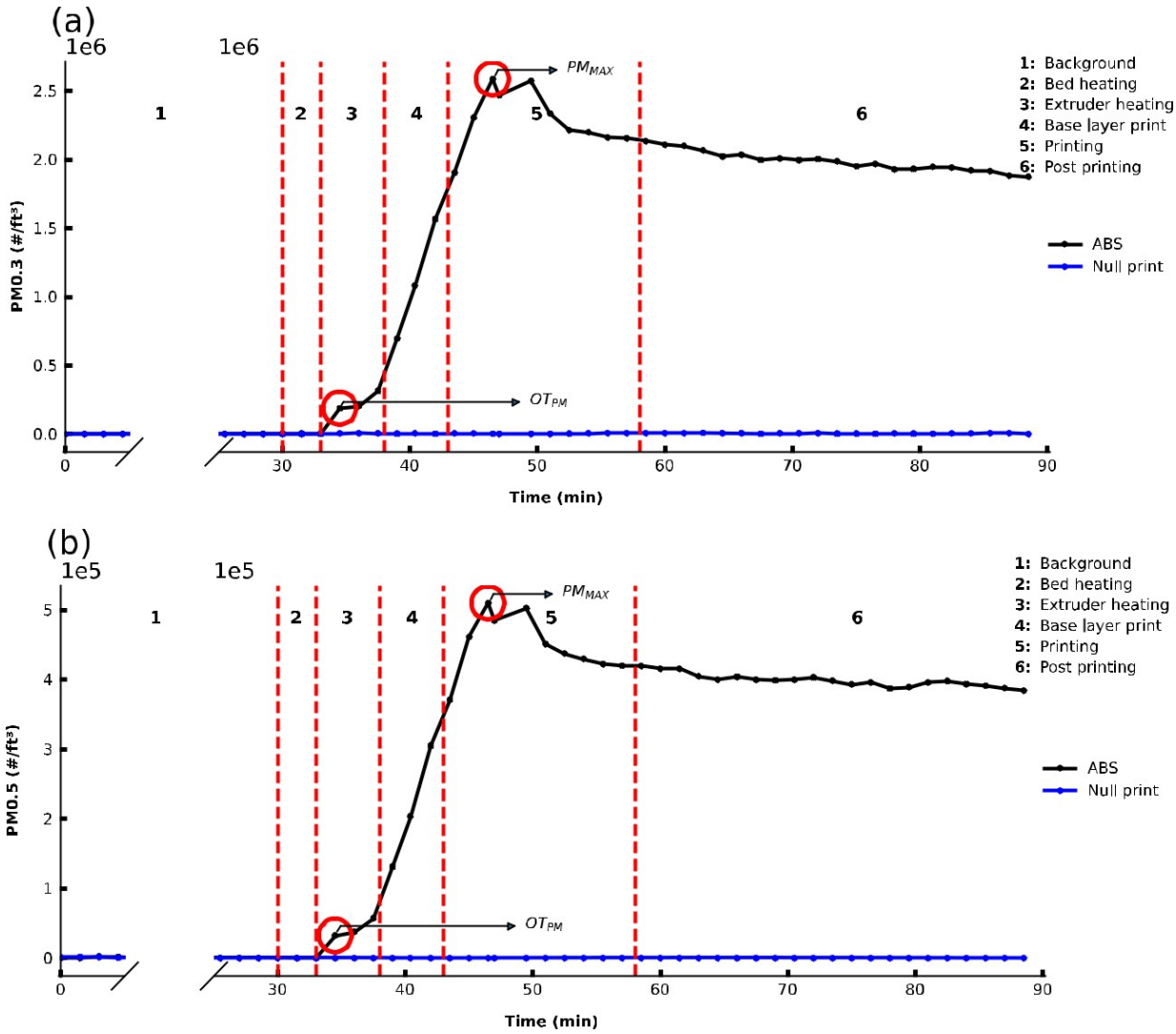

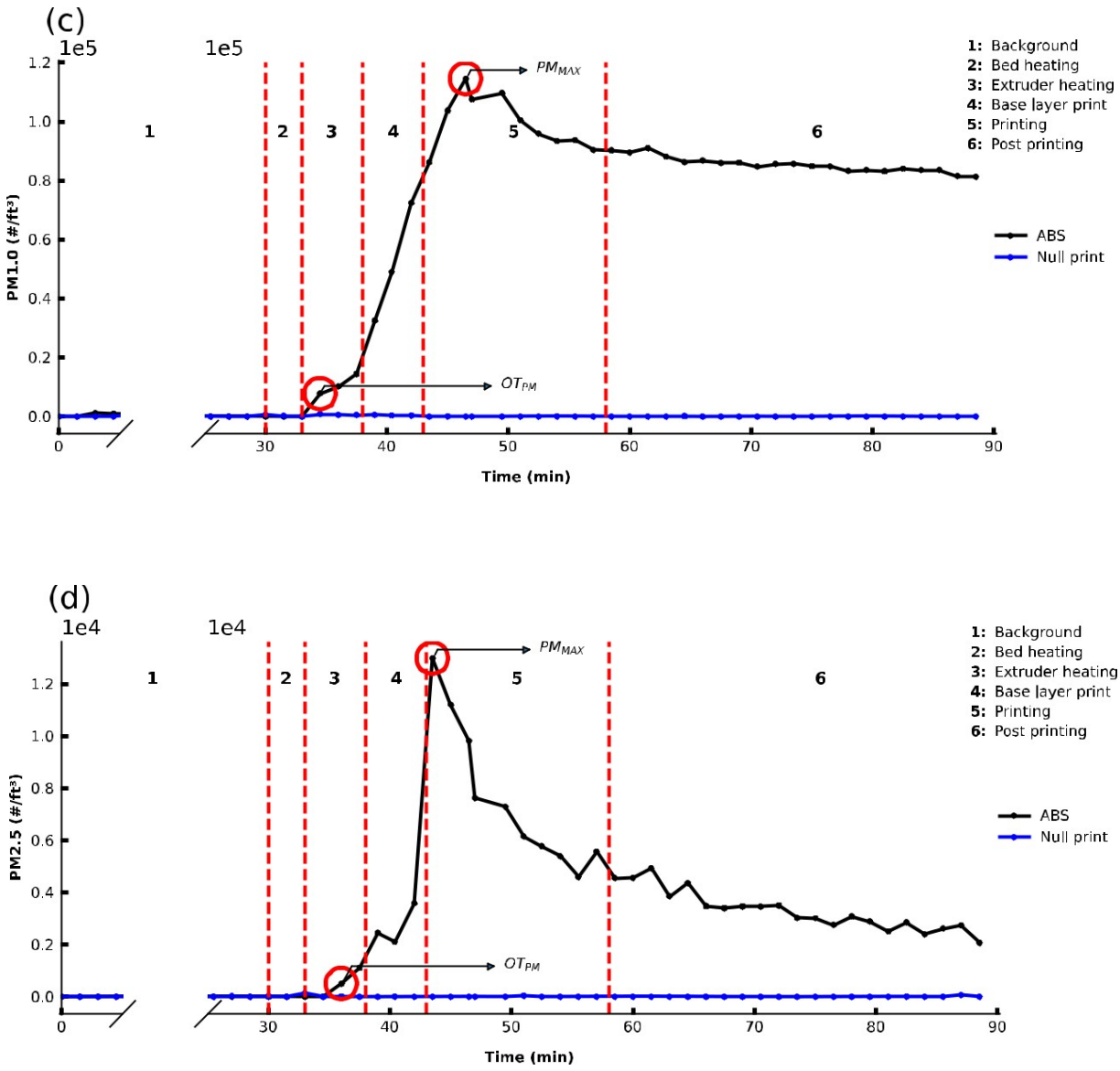

Figure S2. PM emission profiles for (**a**) PM 0.3, (**b**) PM 0.5, (**c**) PM 1.0, (**d**) PM 2.5 over time before, during and after printing of a cube object for ABSB1b (bed plate temperature: 80 °C; extruder temp: 245 °C, 0% fan, 20% infill).